Summary of Experimental Progress

-- the 12th IAEA TM on EPsat Austin, Texas, U.S.A.--

K. Toi

National Institute for Fusion Science,
Toki, Japan

ITER Issues

(A) Mitigation and control of runaway electrons generated by disruption

(B) Good confinement of energetic alphas

(C) Controlled confinement of helium ash generated by slowed-down alphas

Statistics

This TM covers the following 5 categories and experimental presentations are counted to be totally 39.

(a) Alpha particles physics, (b) Transport of energetic particles, (c) Effects of energetic particles in magnetic confinement fusion devices : 5

(d) Collective phenomena: Alfven eigenmodes, EPMs and others : 26

(e) Runaway electrons and disruptions: 1

(f) Diagnostics for energetic particles: 7

I

Classical/Neoclassical Losses of Energetic Ions

- **Losses of energetic ions due to irregularities of magnetic fields (ripple and externally applied magnetic perturbations) must be minimized in ITER.**
- **Reduction of TF field ripple is done by ferittic plates inside the ITER vacuum vessel.**
- **TBM planned to be placed asymmetrically➔ introduce magnetic irregularity ➔ loss of alphas would be slightly enhanced.**

  Experimental test was done in DIII-D (22th IAEA FEC, Deajeon)
- **RMP by ELM control coils for H-mode operation in ITER**

  ➔ enhanced loss of alphas ?

  Experimental test has started on AUG using ELM coils.

Fast Ion Wall Loads in AUG with ELM Coils

In-vessel ELM mitigation coils at AUG

$$\delta = \frac{B_{max} - B_{min}}{B_{max} + B_{min}}$$

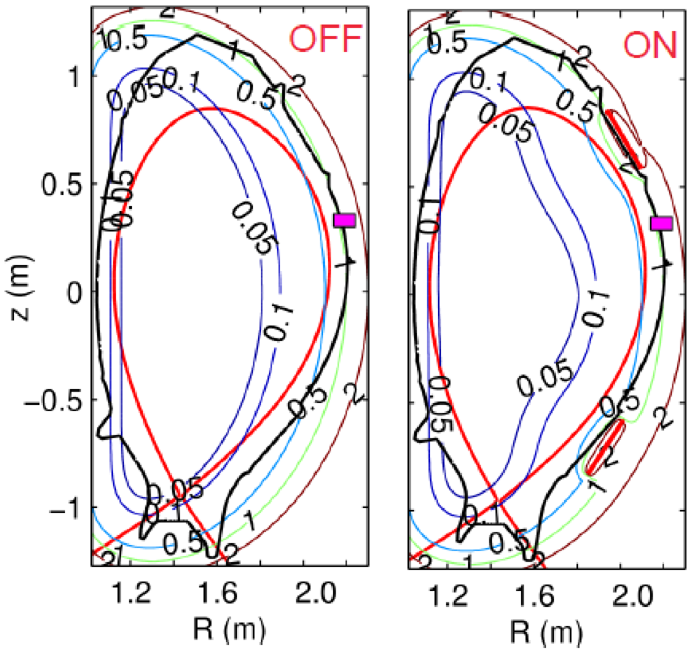

- 8/24 in-vessel saddle coils have been installed in AUG: 4 upper, 4 lower
- I_{coil} = ±0.95 kA ➡ $\boldsymbol{B}_{pert}$ mainly outward (inward) direction

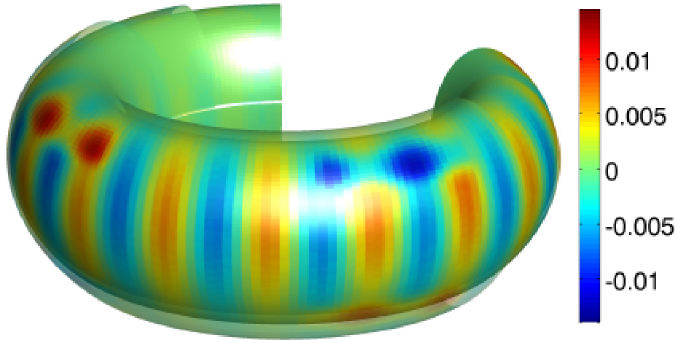

$B_{\perp,pert}$ on ρ = 0.99

[1] W. Suttrop *et. al,* Fus. Eng. Design **84** (2009) 290
[2] W. Suttrop *et al.*, Phys. Rev. Lett. **106** (2011) 225004

Fast Ion Wall Loads in AUG with ELM Coils

Simulation by ASCOT code :

Orbit following Monte Carlo code
(Combined Guiding center + Full orbit code)
3D wall and field to simulate AUG with ELM control coil
200,000 test particles
Bt=1.8T, Ip=0.8MA , Teo=Tio=1.4keV, neo=5~5x1019 m-3

Q5, Q8 perpendicular, Q6 parallel
One at a time, 93 keV and 2.5 MW each
Modelled with ASCOT NBI

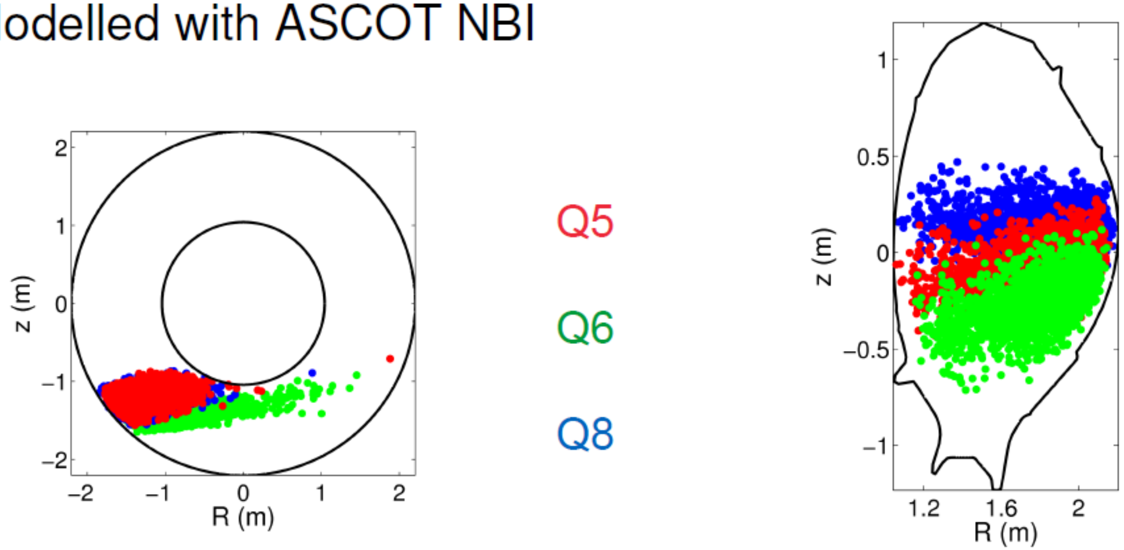

Large wall load from Q6 is predicted by the simulation, i.e, 2% to 8 % enhanced loss by RMP.

Provisional comparison between simulation results and FILD data.

O-15 O. Asunta et al.

Impact of RMP by ELM Coil in ITER 15 MA Scenario

ELM mitigation/control coil (ELMC)

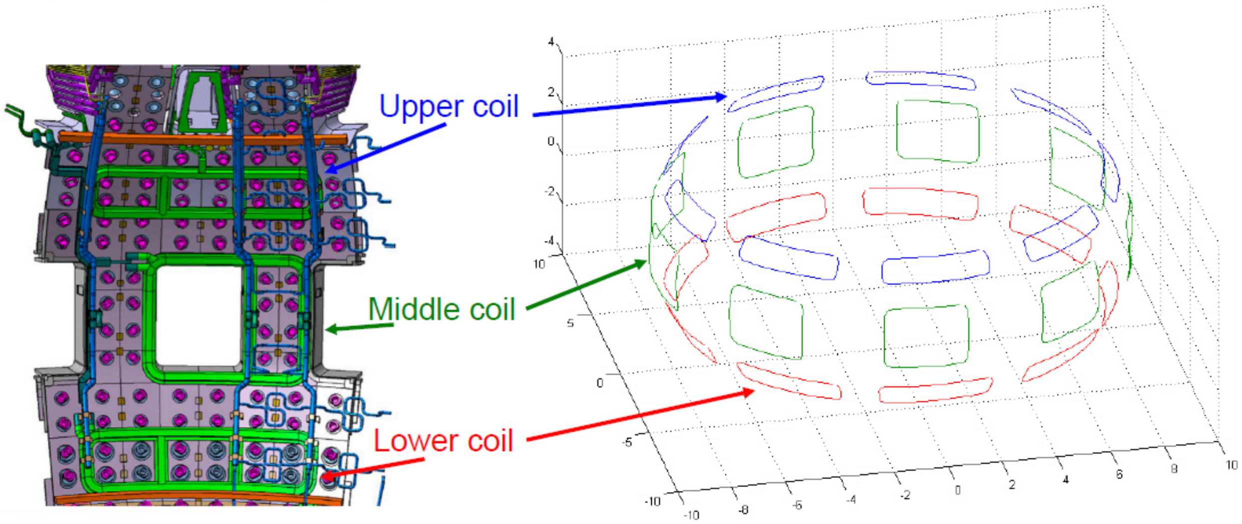

- 3 ELM coils (upper, middle, and lower rows) on each of the 9 vessel sectors which are centered on the toroidal angles, $\phi_{i=\{1,2,..,9\}}$ =30°, 70°, 110°, ..., 350°
- ELMC is modeled as filament loops

n=4 RMP

TFC+FI+Min_n4

Alpha particles

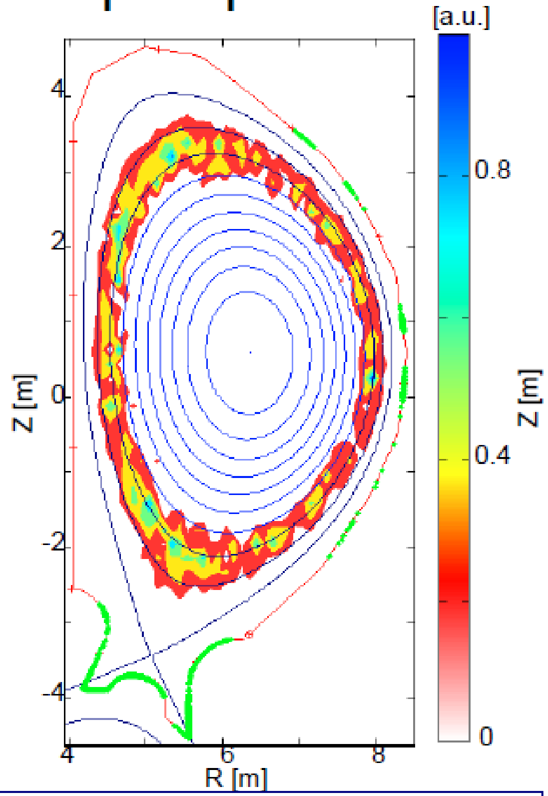

Alpha particles born in the region where ψ_N >0.7 are expelled.

P2-10 K. Shinohara et al.

Results of F3D OFMC calculation

ELMC field increase fast ion loss. NB loss is larger than alpha
Heat load appears in divertor region.

ELMC field is essential for loss

Considered that optimized magnetic field perturbation is effective in deterioration

FI reduce fast ion loss

Fast ion species	Magnetic field	Loss power fraction [%]	Maximum heat load [MW/m^2]
alpha	Case1: TF ripple alone	0.8	0.06
By NB	Case1: TF ripple alone	0.8	0.02
alpha	Case2: TF ripple + FI	0.04	<0.01
By NB	Case2: TF ripple + FI	0.05	<0.01
alpha	Case3: TF ripple + FI + Min_n4	0.95	0.06
By NB	Case3: TF ripple + FI + Min_n4	7.5	0.27
alpha	Case4: TF ripple + FI + Min_n3	1.6	0.06
By NB	Case4: TF ripple + FI + Min_n3	10.0	0.21
alpha	Case5: TF ripple + FI + Max_n4	6.2	0.21
By NB	Case5: TF ripple + FI + Max_n4	26.2	0.36
alpha	Case6: Axisymmetric TF + Min_n4	0.9	0.06
By NB	Case6: Axisymmetric TF + Min_n4	7.0	0.24
By NB	Case7: Axisymmetric TF + (n=4, 30kAt, zero phase difference between upper, middle, lower coils)	0.6	0.03
By NB	Case8: Axisymmetric TF + (n=4, 15kAt)	2.4	0.09

Note: shielding effect of plasmas on field penetration is not considered

Heating Scenarios for Enhanced Ion Tail by ICRF(1)

◆ **Measurement and simulation of ICRF minority-heated fast-ion distribution function on C-Mode**

Comapct neutral particle analyzer (CNPA) has been developed to measure ICRF generated ion tail up to 1.5MeV on C-Mod, where charge exchange with B^{4+} is dominant in the range of E> 0.3MeV.

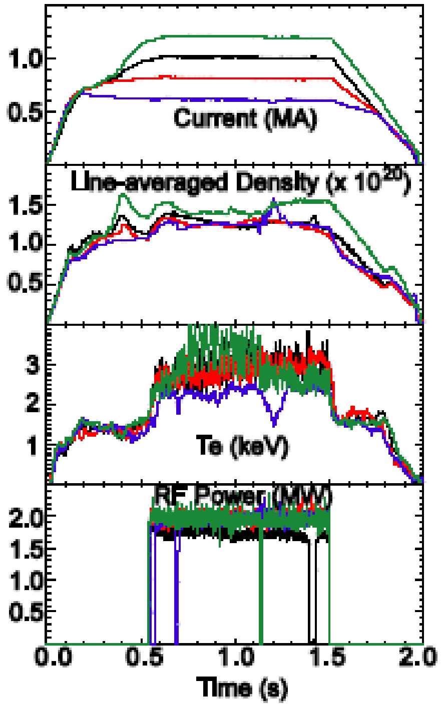

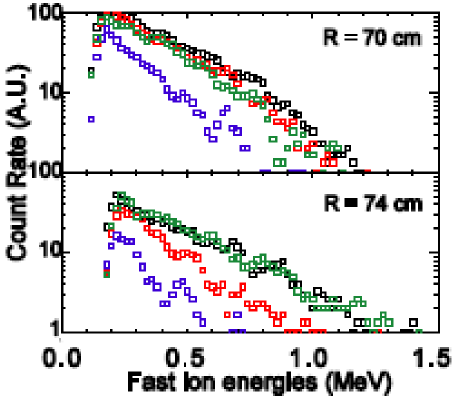

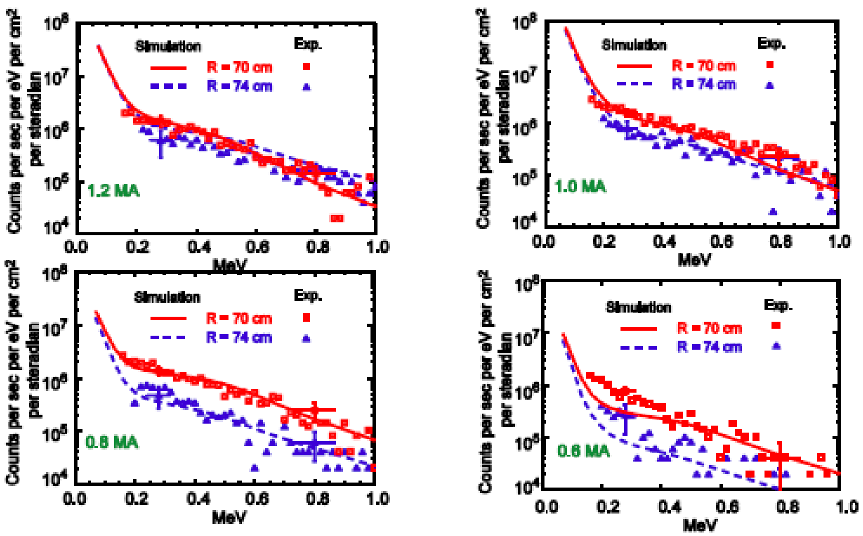

O-27: A. Bader et al.

For discharges with different Ip, simulation with AORSA (solvers for plasma wave field) +CQL3D (solvers for particle motion) agrees well with experiment.

Heating Scenarios for Enhanced Ion Tail by ICRF(2)

- **ICRF heating scenario in burning D-T plasmas**
  (P1-14: Ye.O. Kazkov et al.)
  Direct ion heating is very effective to enhance D-T fusion reactvity. In T-ritch plasma of ~85% , effective ion heating is expected.

- **Energetic ion behaviors during H or He3 minority heating in C-Mod**
  (P2-1: K.T. Liao et al.)
  Fast and thermal minority ion distribution was measured by charge exchange spectroscopy using 50 keV diagnostic beam. Energetic ions in plasma core is measured by CNPA.

II

Energetic Ion Driven Global Modes

AEs and other global modes excited by Energetic Particles

- **Linear mode identification**
- **Stability (Damping rates and Drive)**
- **Nonlinear mode evolution**

Radial transport (redistribution and/or losses) of EPs by energetic ion driven global mode

Radial transport of EPs by micro-turbulence in background plasma

Alfven Eigenmodes in 2D & 3D Plasmas

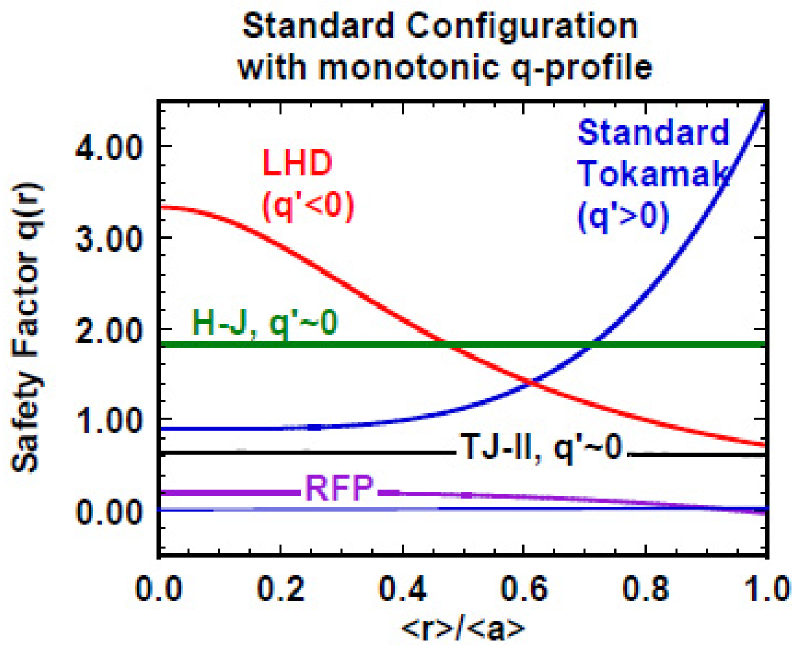

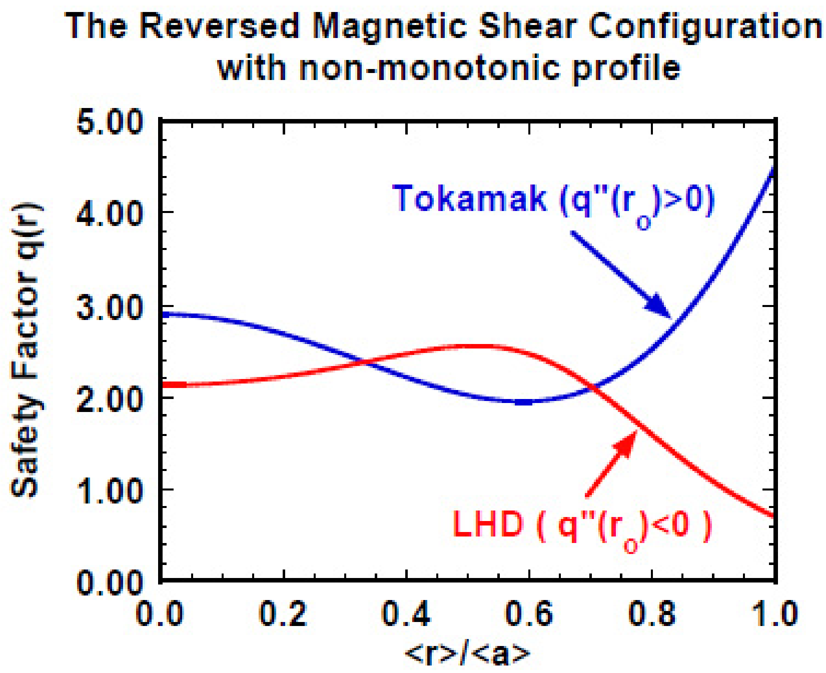

Tokamaks, Spherical tokamaks, Helicals/Stellarators, Reversed field pinch

New comers!

TAE, EAE, NAE exist in both 2D & 3D plasmas.
GAE and RSAE exist in both 2D & 3D plasmas.
HAE and MAE exist only in 3D plasmas.
Non-perturbative modes such as EPM and Fishbones in both 2D & 3D plasmas.

Identifications of Energetic Ion Driven Modes

-- TAEs, RSAEs, BAEs, BAAE, GAM—

2D Measurement of TAE & RSAE Structures in DIII-D

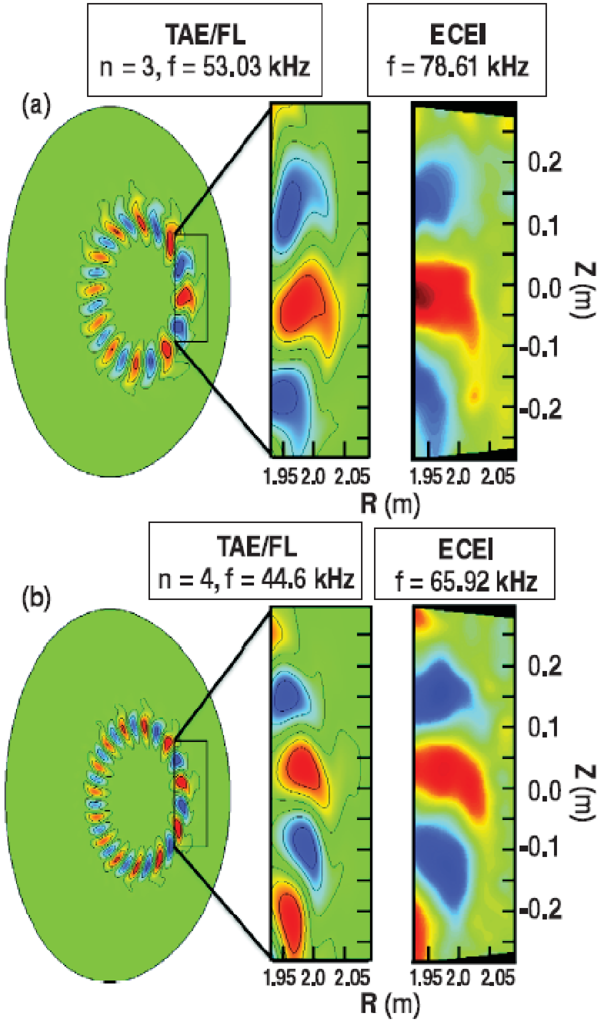

B.J. Tobias et al., PRL(2011)

- **2D measurement of TAE by ECE imaging (ECEI)**
- **Observed twist of eigenfunction in poloidal direction is caused by energetic ion effects.**
- **This result has excellent agreement with the gyro-fluid calculation by TAEFL code (D.A. Spong).**

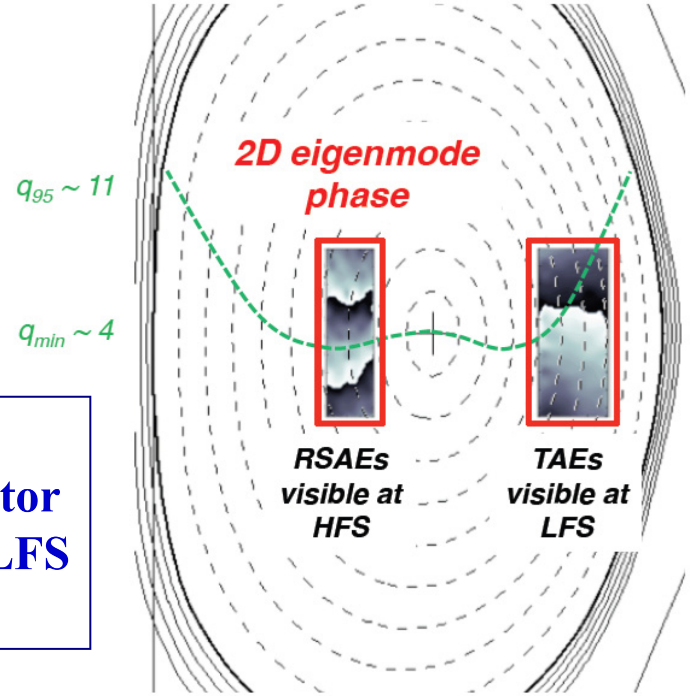

Dual detector Arrays can monitor Simultaneously LFS and HFS.

P2-11 B.J. Tobias et al.

2D Measurement of BAAE (OANBI case)

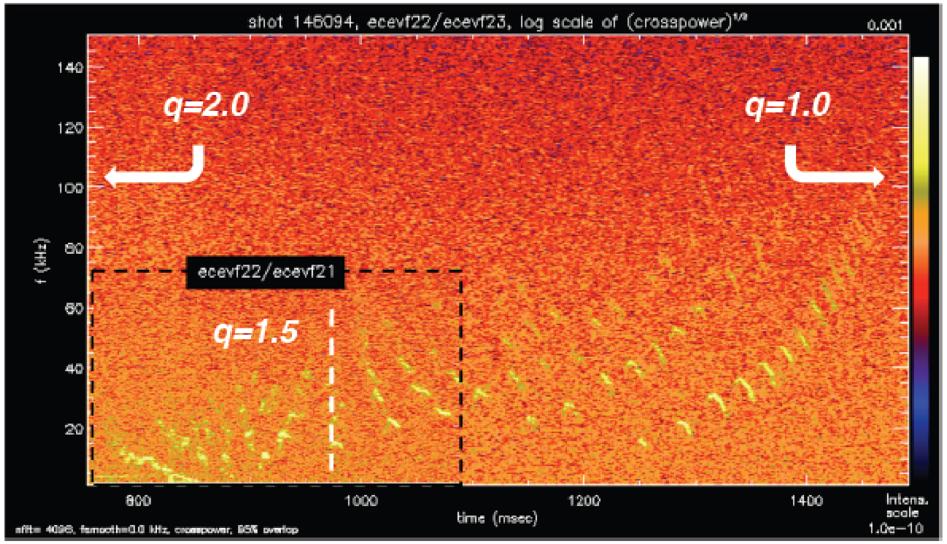

shot 146080
BAAE mode structure

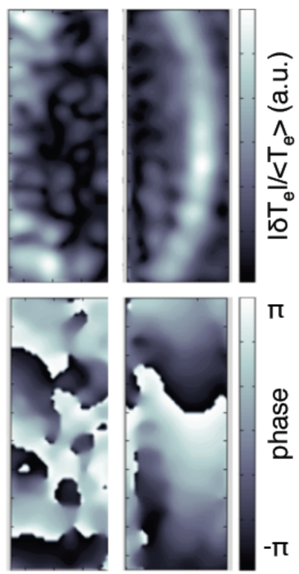

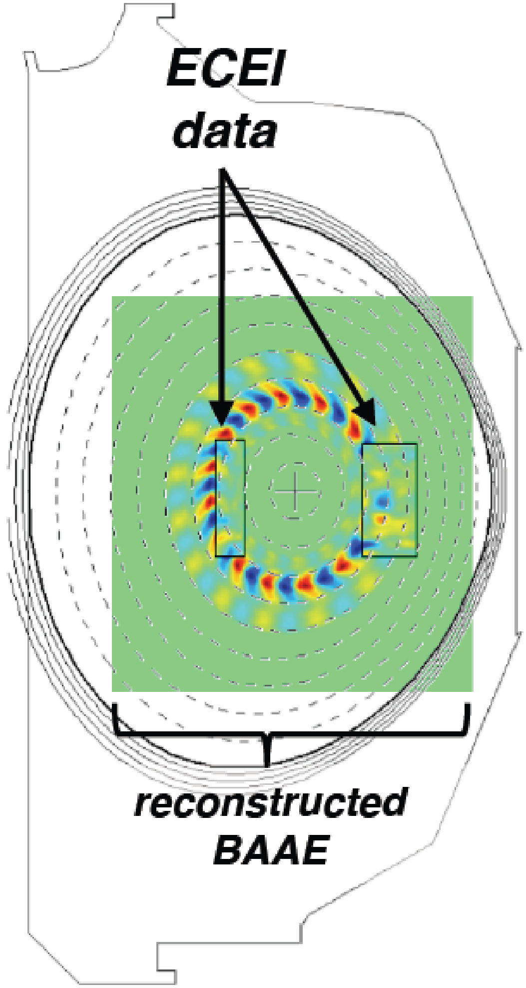

- **ECEI has provided the first 2D images of the BAAE**
  - Highly localized radially about ρ =0.2 ($\leq q_{min}$)
  - Modes rotate in same sense as RSAEs/TAEs (E×B and normal $\omega_{*i,thermal}$ direction)
  - Phase shear curvature is reversed w.r.t. RSAEs/TAEs

P2-11 B.J. Tobias et al.

RSAE and BAE in RS Plasmas of AUG

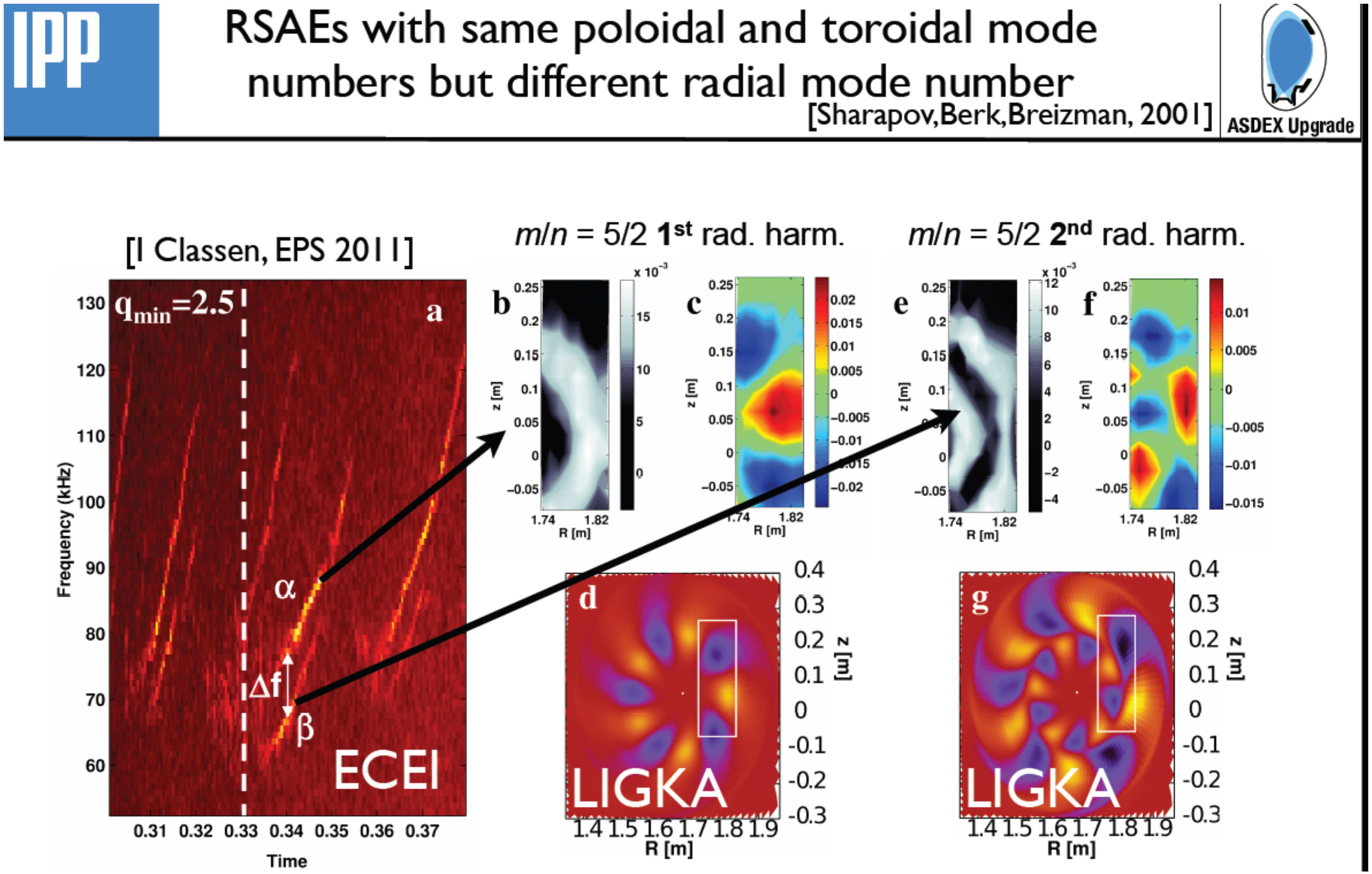

In an RS plasma generated in current ramp up phase in AUG, several interesting modes of which mode frequency is lower than f_{TEA} are detected.

I-5 Ph. Lauber et al.

'extended' Alfvén spectroscopy

frequency difference of radial harmonics of RSAEs gives constraint on curvature of q at q_{min}.
analyse a set of test-profiles: keep q_{min} constant and vary curvature

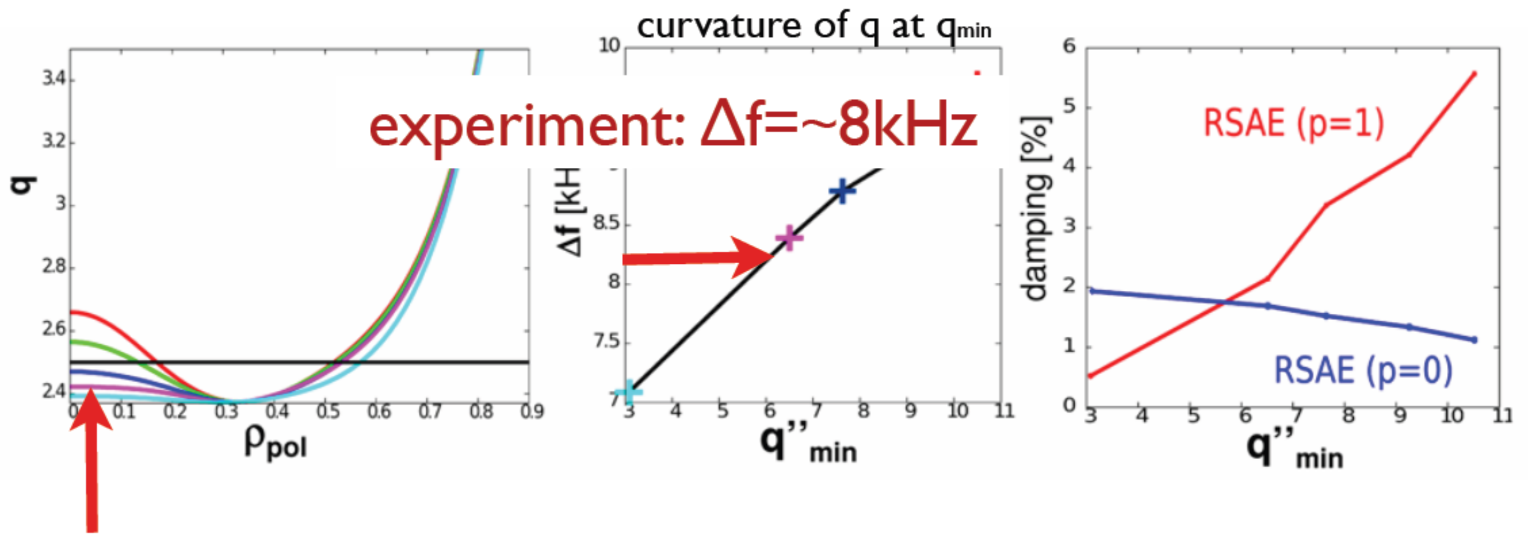

rather flat q-profile is consistent with frequency difference
also radial width of measured modes supports flat q-profile

BAE mode structures, NBI-driven

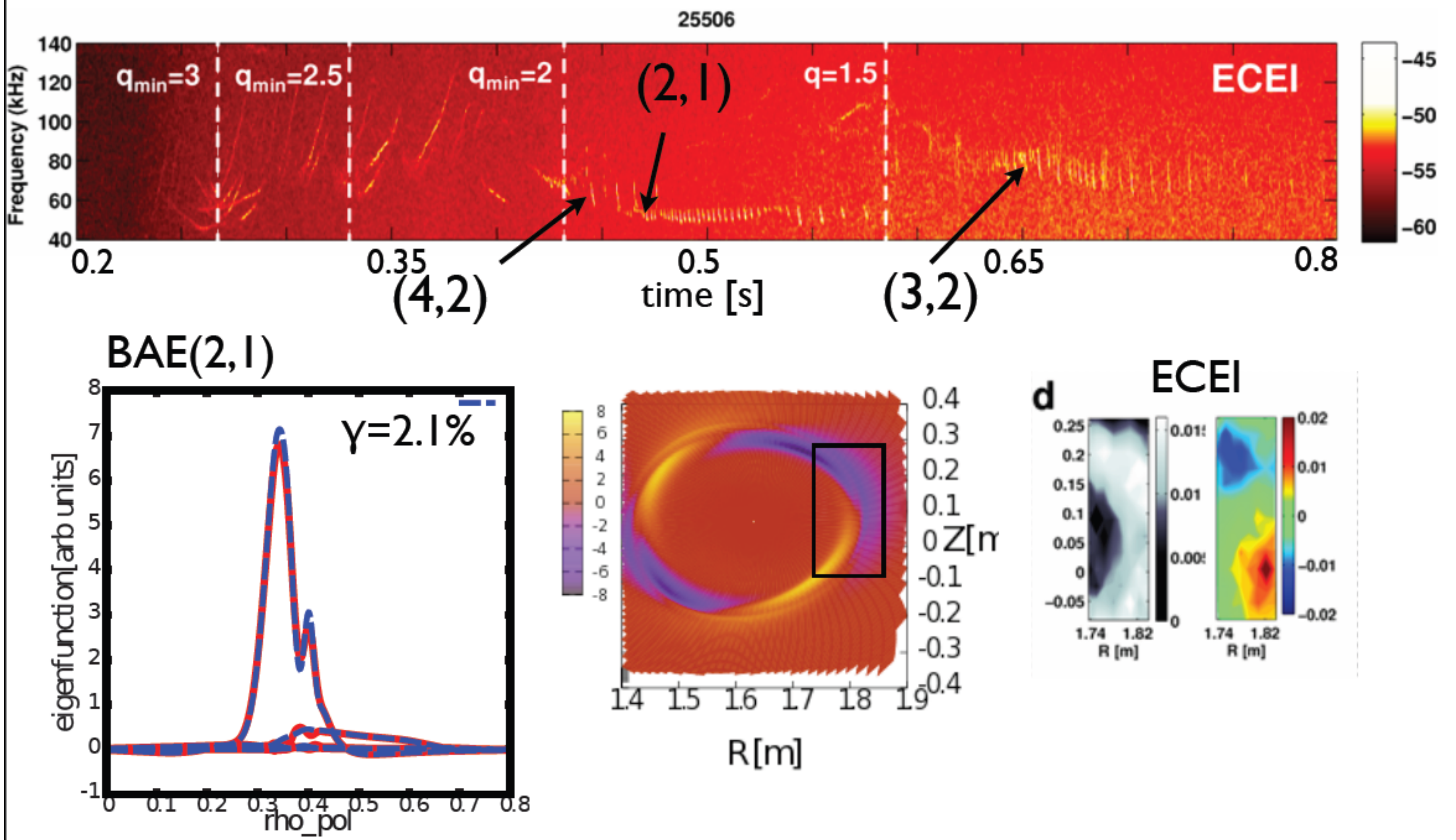

12th IAEA TCM on Energetic Particles, Austin, September 2011

Friday, September 2, 2011

I-5 Ph. Lauber et al.

Alfven/Acoustic Mode Excitation by Off-Axis NBCD

DIII-D

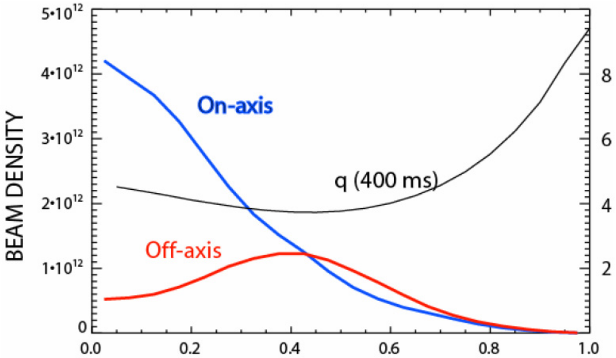

•TAE drive proportional to $\nabla\beta_f$

RSAE

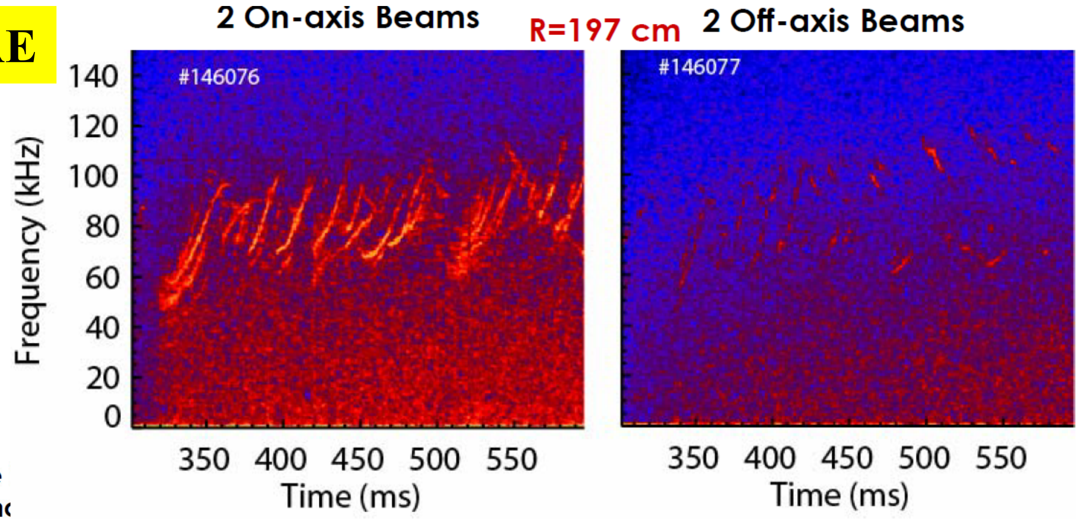

•The stability boundary is higher for off-axis beams.

BAAE

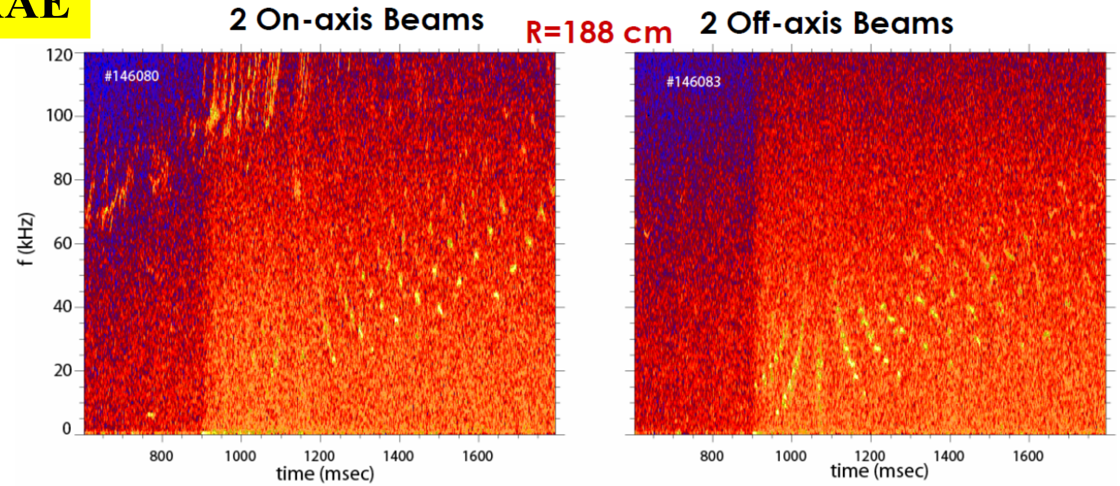

•The frequency pattern in the off-axis case suggests the modes have negative toroidal mode numbers

O-9 W.W. Heidbrink et al.

Energetic Ion Driven GAM (EGAM) in DIII-D

Recipe for E-GAM Excitation in DIII-D: Counter Tangential Beam Injection into High q_{min} Plasma

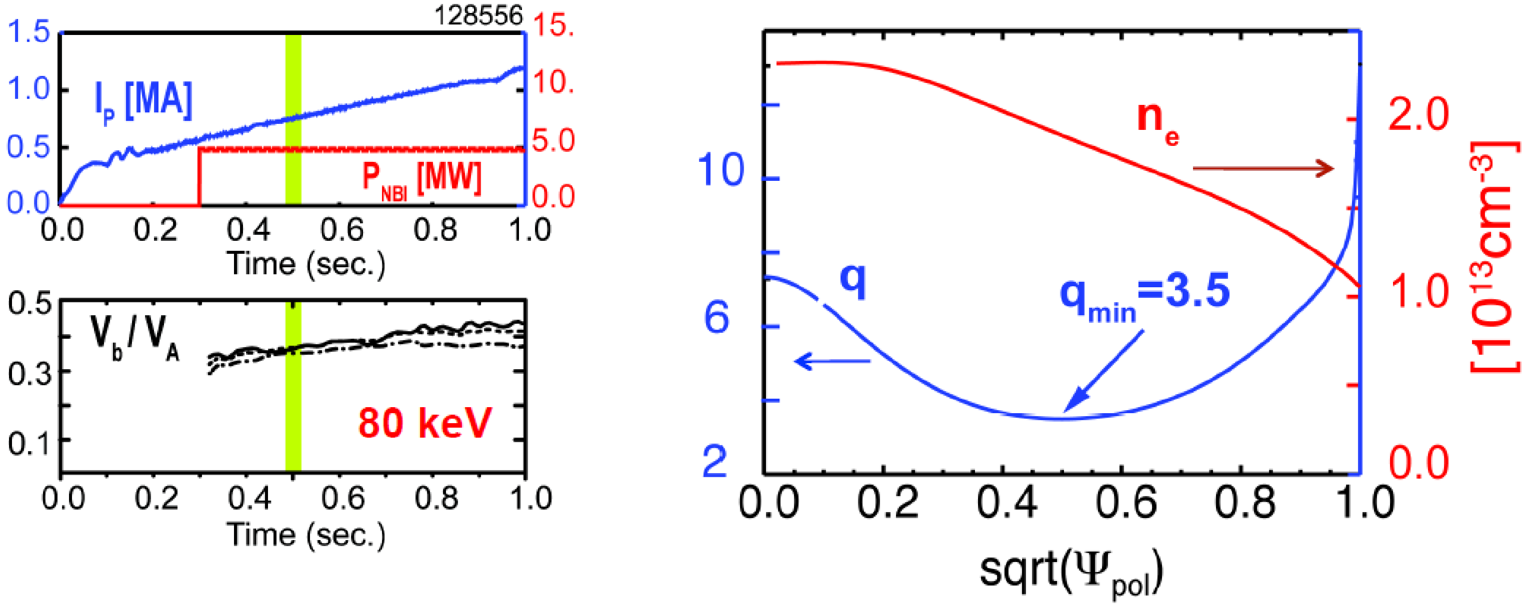

- q_{min}> 3 T_i, T_e< 2 keV, typically. Why?
- 80 keV bounce frequency ≈ GAM frequency at high q in DIII-D
- Ion Landau damping minimized at high-q through sideband resonance
- Note: co beams can drive modes, but typically much weaker, shorter

Strong Outward Radial Propagation of E-GAM Observed in Simulation and BES Measurement

Fu, Hybrid simulation

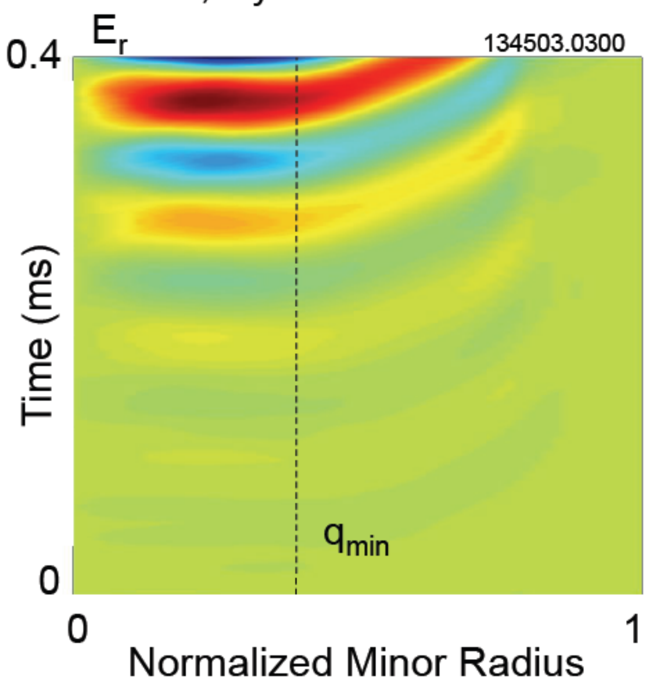

BES, DIII-D

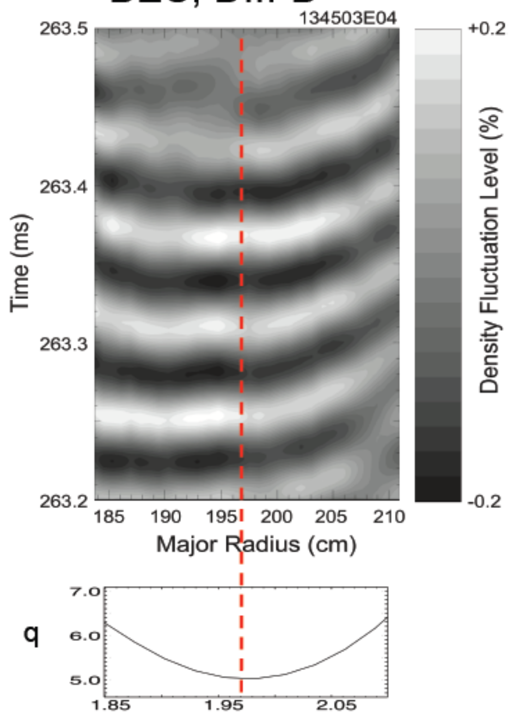

- Directional sensitivity of mode excitation confirmed from Hybrid simulation, orbit analysis and resonance condition

  - prediction of large losses over a broad energy range observed

- Theoretical prediction of nonlinear structure of second harmonic validated using BES, can be used to infer E_r

SPIRAL Code Simulations Are in Good Agreement with of Fast Ion Loss Detector For Pitch and Energy of Loss

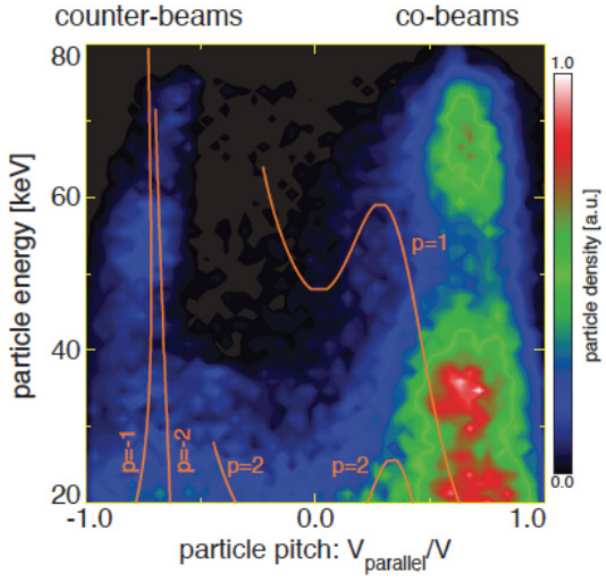

FILD1: Pace, Fisher

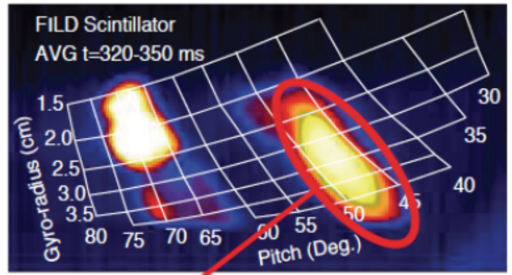

- First-orbit losses from:
  - 210L third-energy fraction
  - 210R half-energy fraction
  - 210L full-energy fraction
- First-orbit losses from:
  - 210R third-energy fraction
  - 210R half-energy fraction
- EGAM induced losses

• Note: No E-GAM losses observed for co-injected particles

SPIRAL: Kramer

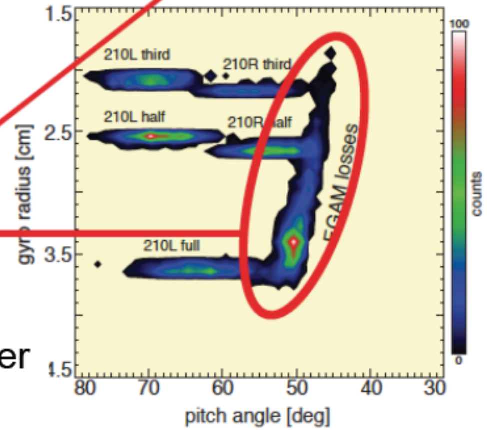

O-2 R. Nazikian et al.

Up-sweeping n=0 modes associated with neutral flux increase were observed for low density LHD plasmas.

- The typical initial frequencies are 50 -70kHz and their frequencies chirp-up during their mode activity activities.
- No significant increase of Hα-signals were observed.
- Typical estimated slowing-down time is ~8[s] at the core.

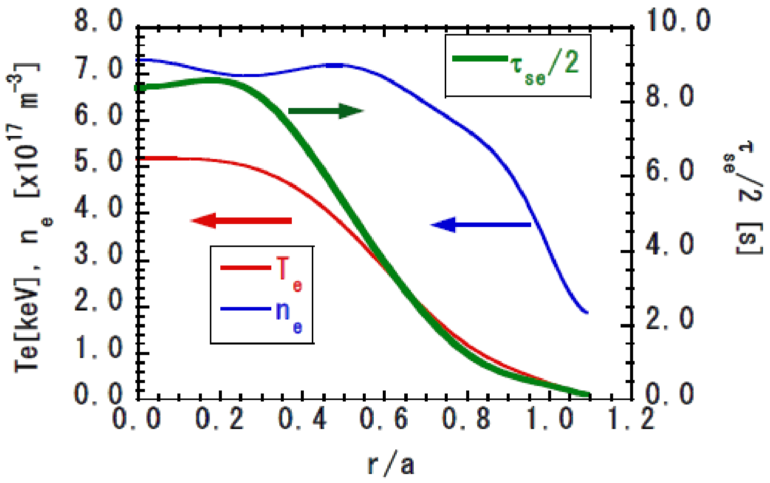

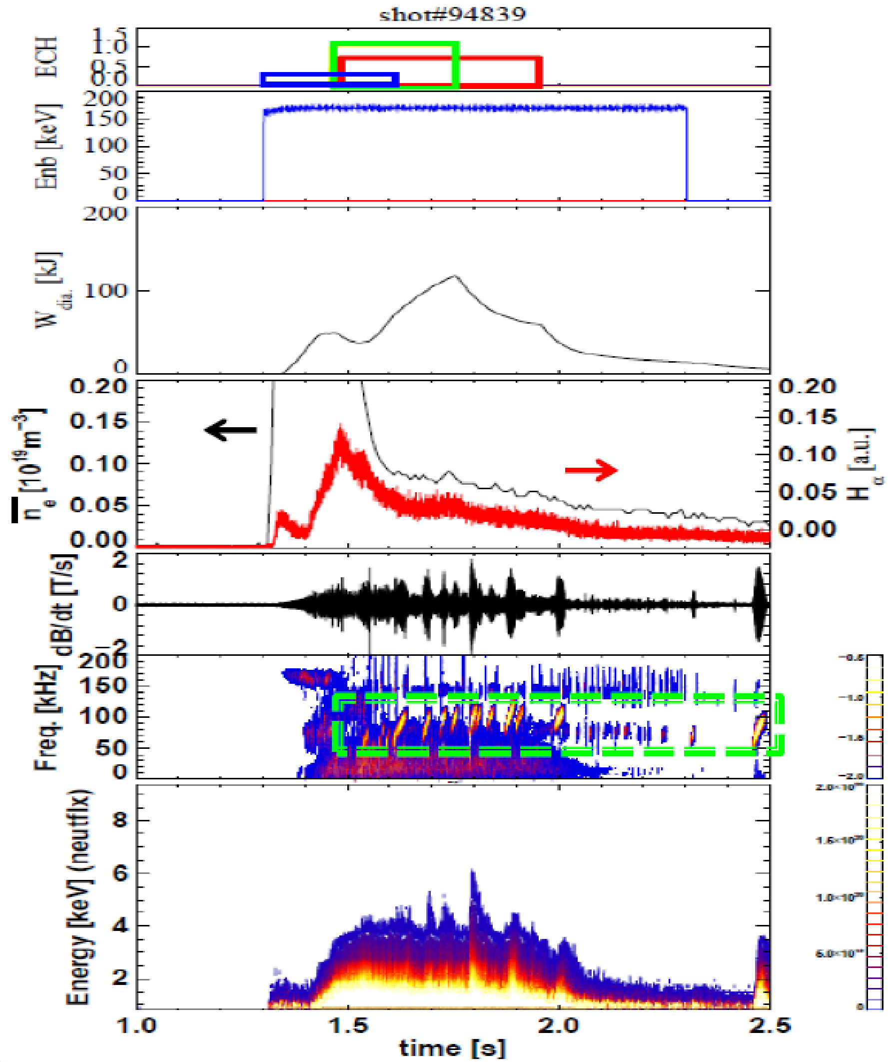

O-3 M. Osakabe et al.

Temporal behavior of the mode and neutral flux indicates either anomalous heating or radial transport of bulk ions by the mode activity.

- The mode grows very quickly at its initial phase (γ_{eff}=~4.6x10^3[s^{-1}]).

- The ion temperature starts to increase when the mode amplitude reaches a certain value (~2x10^{-2} [a.u.]), and the effective growth rate of the mode decreases (γ_{eff}=~2.3x10^2 [s^{-1}]), simultaneously.

- When the mode frequency reaches to a certain frequency close to the orbital frequency of the energetic particle produced by the NB, the mode amplitude starts to decrease gradually (γ_{eff}=~ −69 [s^{-1}]) .

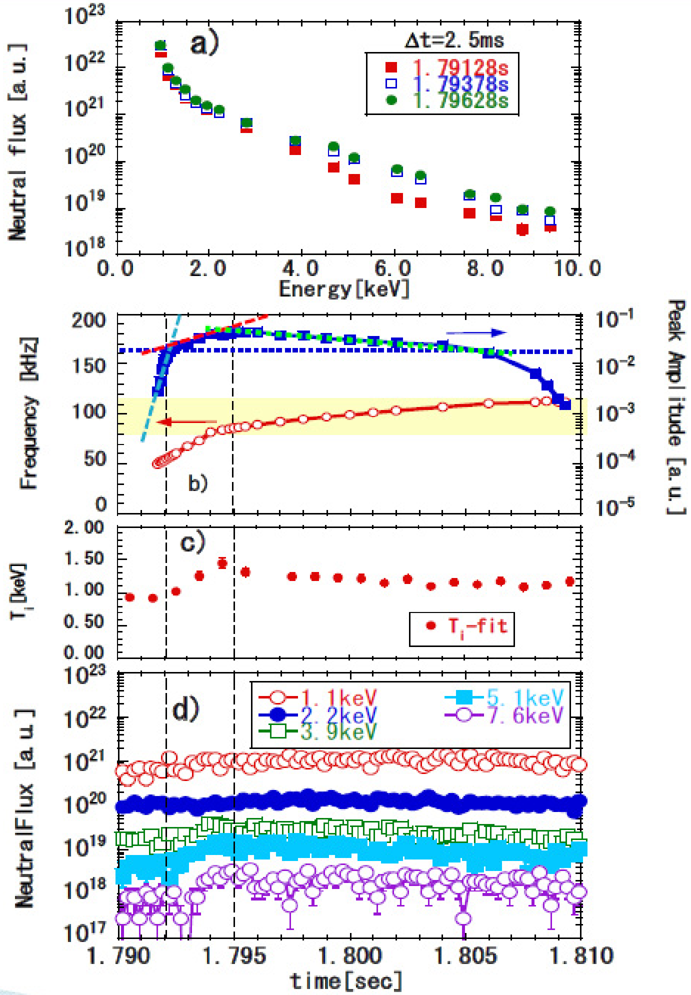

O-3 M. Osakabe et al.

Observation of Two Types of Energetic Ion Driven GAM on LHD

(Type I) GAM excited quasi-stationary in reversed shear plasmas by EPs

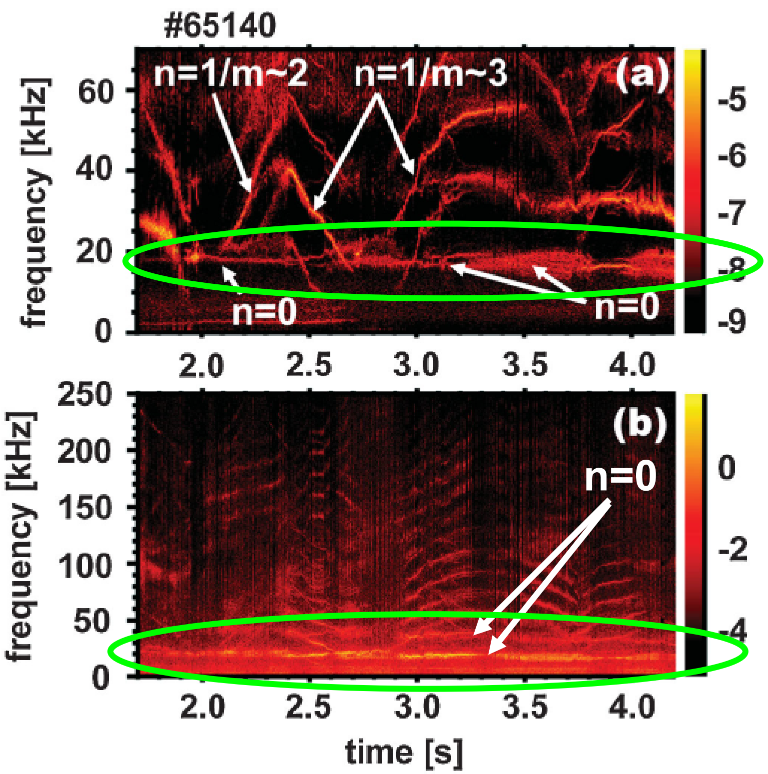

K. Toi et al, PRL(2010)

Nonlinear evolutions: pitchfork splitting, mostly up-ward frequency chirping

This GAM may be controllable and sustainable.

(Type II) This GAM is excited just after the switch-on of NBIs

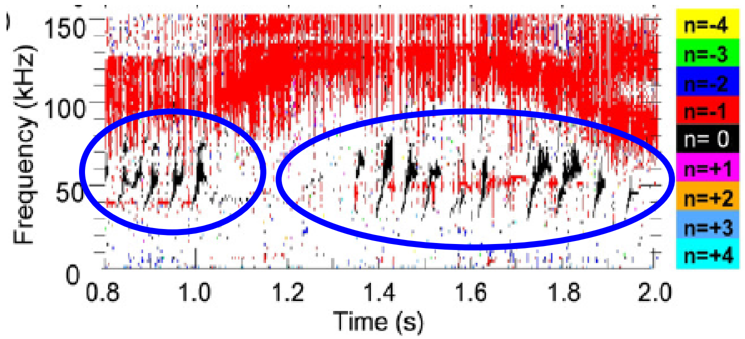

T. Ido et al., NF(2011)

This is excited **transiently (just after NBI switch on)** in very low density range (<n_e> < 0.2×10^{19} m^{-3}).

O-4 K. Toi et al.

Potential and density Fluctuations (by HIBP)

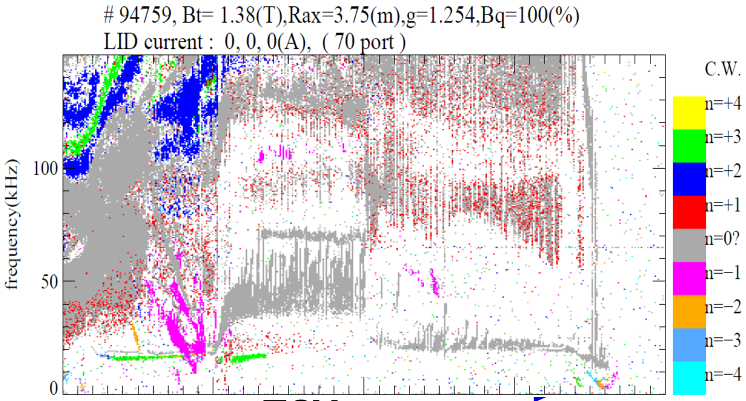

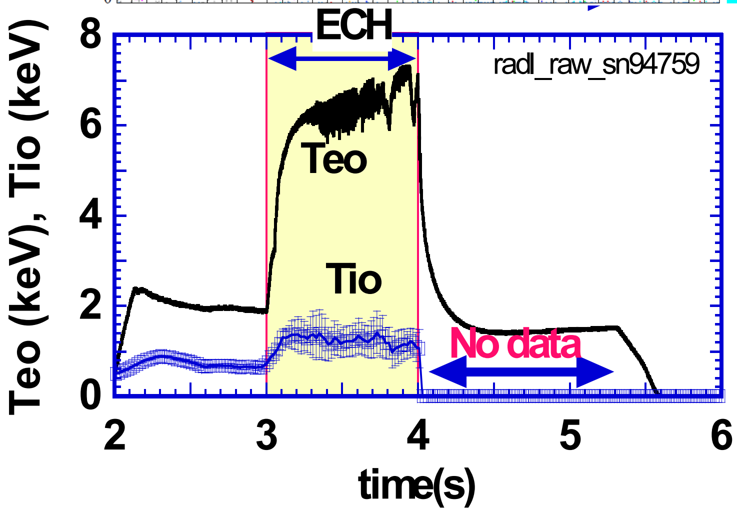

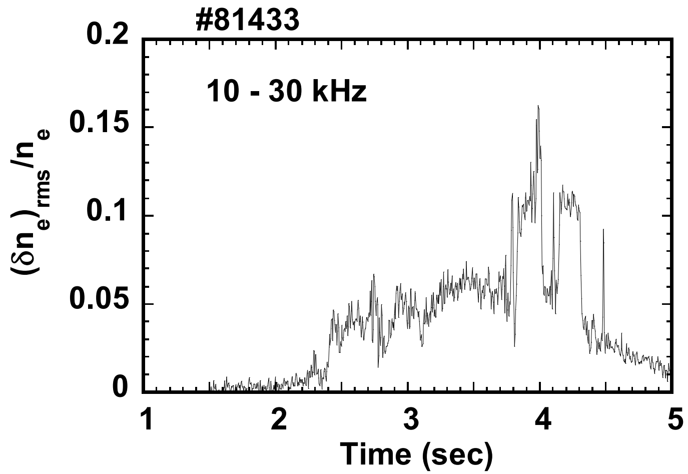

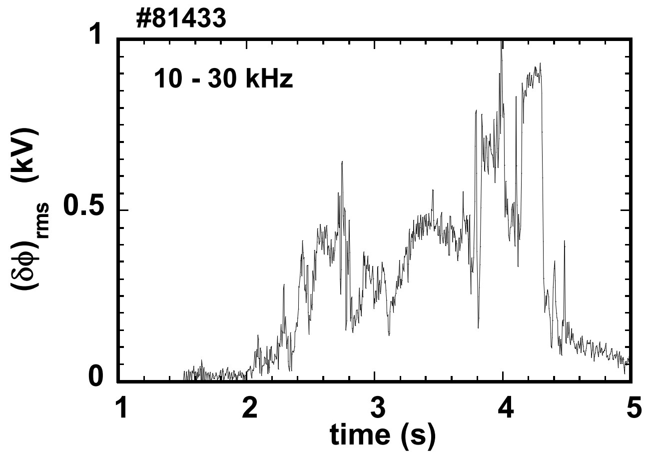

The GAM frequency rises when ECH is applied.

Amplitudes of potential and density fluctuations induced by GAM gradually increase with the decrease in the rotational transform.

These fluctuation amplitudes are very large near the GAM center:

$(\delta n_e)_{rms}/n_e$~up to 15 %, $(\delta\phi)_{rms}/Te$ ~ up to 70%

O-4 K. Toi et al.

Measurement of Damping Rate of TAEs
--Alfvén Eigenmode Active Diagnostics--

Aim: address physics of mode damping, identify modes most prone to instability in different burning plasma scenarios, and parameters to control stability

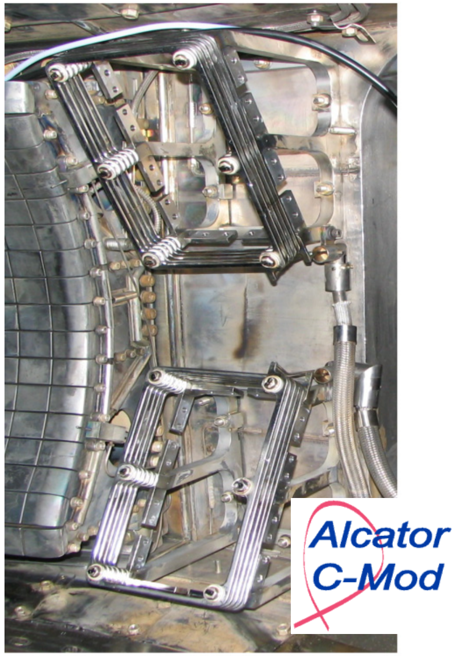

high field & density, $T_e \sim T_i$

EFDA EUROPEAN FUSION DEVELOPMENT AGREEMENT JET

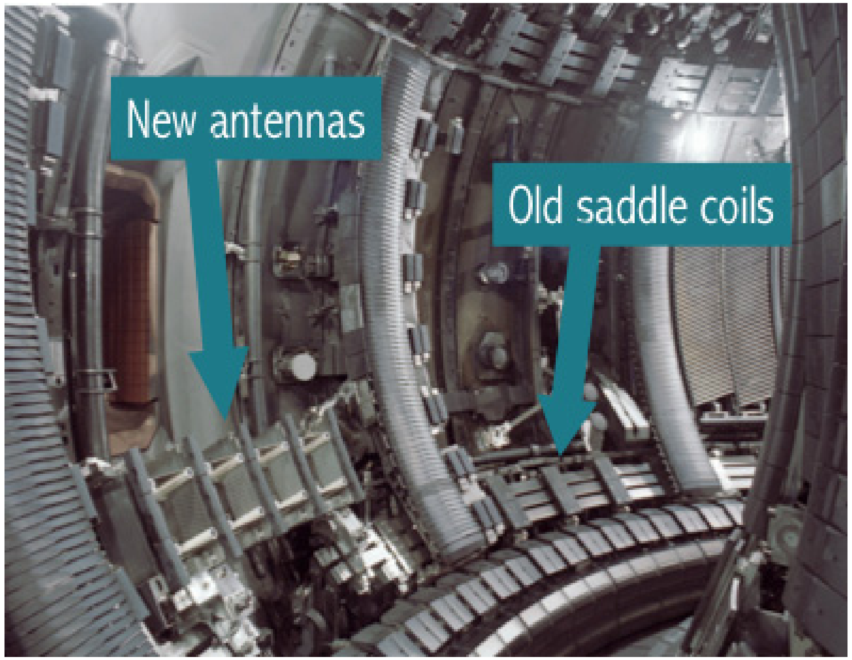

ITER-relevance for size and shape scaling, scenarios

MAST

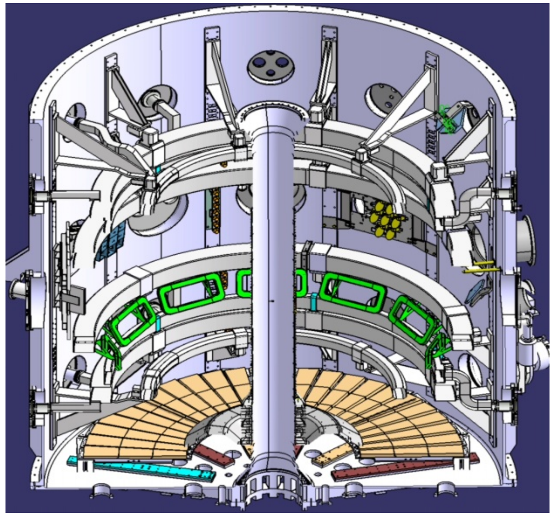

tight aspect ratio, broad range of β

O-10 D. Testa, A. Fasoli et al.

Ex. of γ/ω measurements for n=7 TAE

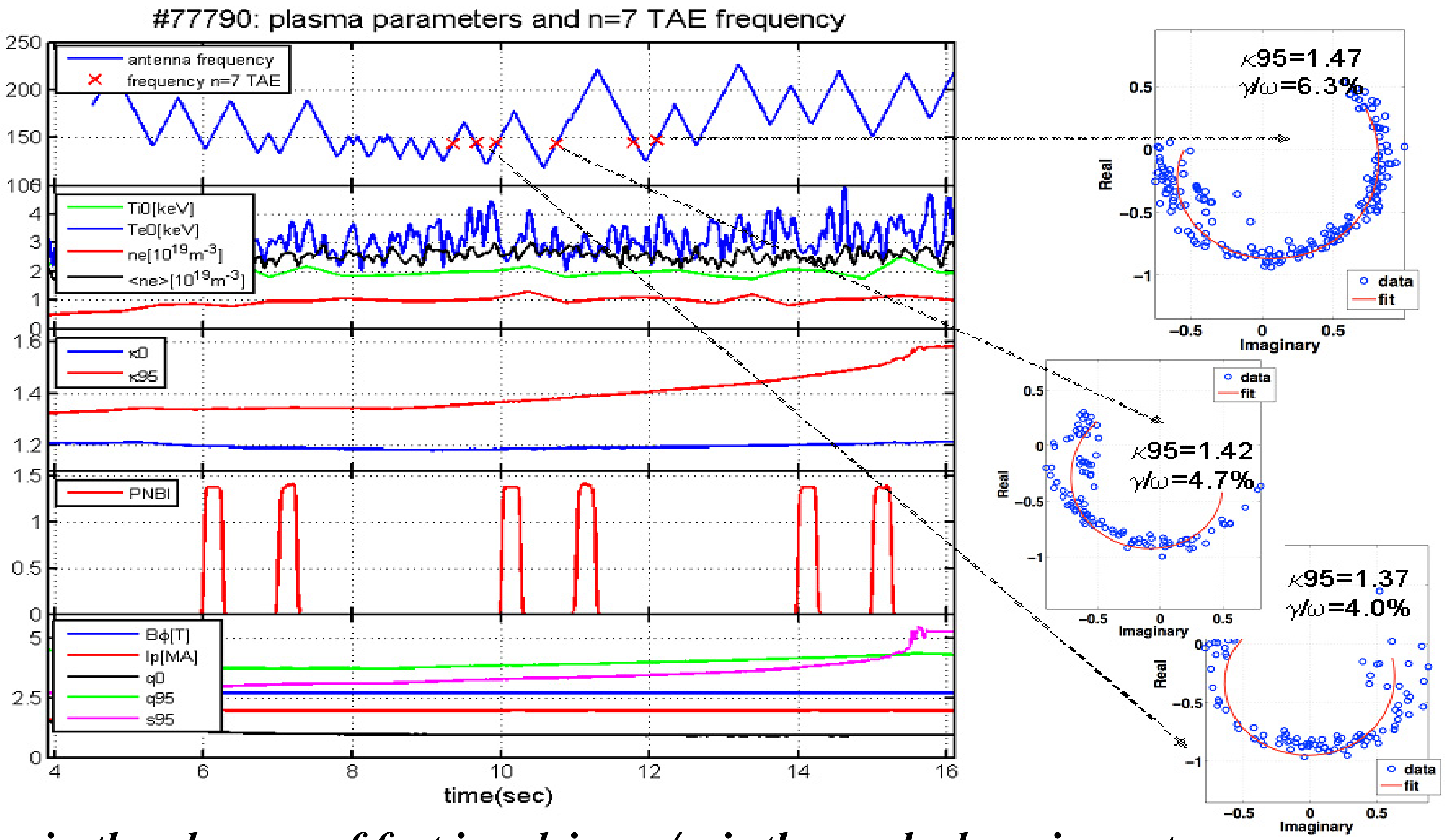

Note: in the absence of fast ion drive, g/w is the mode damping rate

Antenna configuration to drive odd modes (3<|n|<11) n=3 mode dominates.
➔ Dependence of γ/ω on κ_{95} and q_o for n=3 TAE

plasma shape effect for n=3 TAEs: measurements vs. modeling

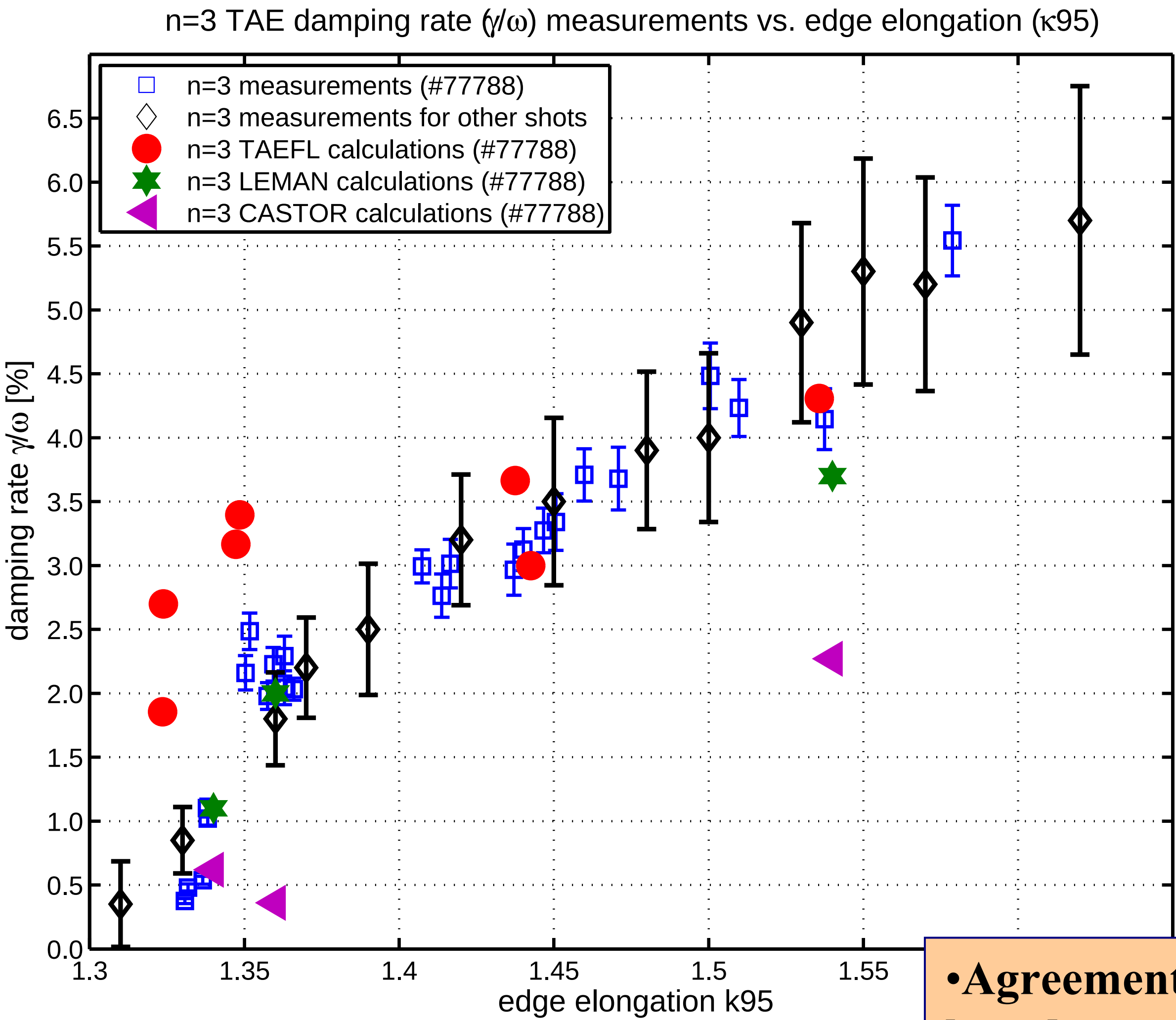

- **LEMan**: **gyro-kinetic approach** ➔ good agreement with data
- **CASTOR**: fluid approach ➔ large discrepancies with data
- **TAEFL**: γ/ω extrapolated back from marginal stability threshold for fast-ion driven modes ➔ good agreement with data, very important to test validity of the modeling approach

•Agreement with numerical codes based on gyro-kinetic or gyro-fluid models has reached quantitative level.

O-10 D. Testa, A. Fasoli et al.

Excitation of Alfvenic and Acoustic Modes by Energetic Electrons

Alvenic and acoustic global modes can be destabilized through wave-particle resonance interaction which depends on particles speed but not on particle mass.

Charactersitic orbit size and gyro-radous is small.

$(\rho_{he}/a \sim 0.005 << (\rho_{\alpha}/a)_{ITER} \sim 0.03 << (\rho_{hi}/a)_{JET} \sim 0.3)$

➔ Energetic electron study may bridge the gap in orbit width and gyro-radius

- **O-14(FTU & Tore Supra_el-fishbone), O-20(LHD, el-AEs), P2-5(TJ-II, el-driven mode),**

Electron Fishbones in LH Plasmas of FTU

e-fishbones in FTU tokamak

In LHCD discharges two regimes of e-fishbones were observed according to the LH power:

- An almost steady state (fixed point) at moderated values of LH power (1st branch)
- A regular bursting behavior (limit cycle) at high LH power (2nd branch)

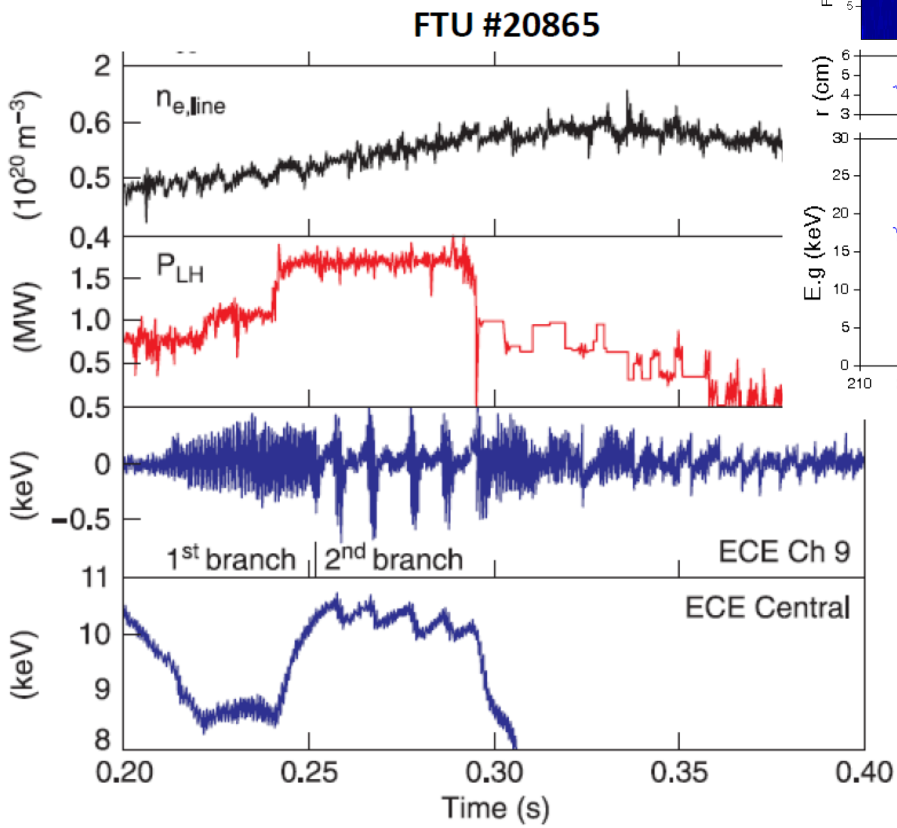

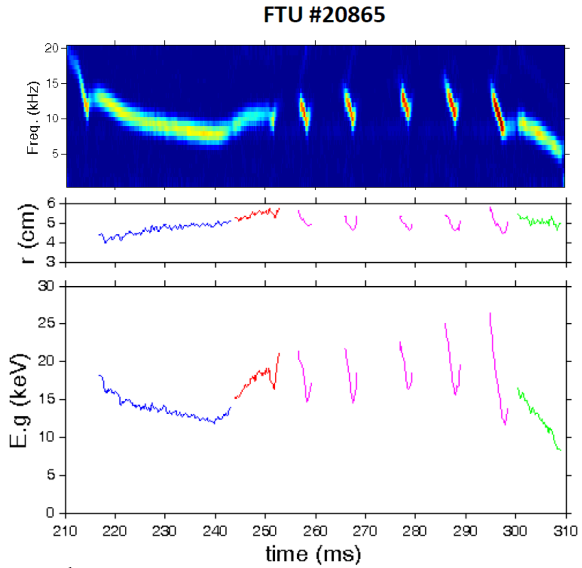

[F.Zonca, Nucl. Fusion 2007]

O-14 Z.O. Guimaraes-Filho et al.

Electron Fishbones in LH Plasmas of FTU

e-fishbones in Tore Supra

- At moderated Lower Hybrid power, 1MW, and low density, n_0~$2.5x10^{19}m^{-3}$, MHD modes identified as precessional e-fishbones may be destabilized
- Frequency jumps between modes with different structures are observed

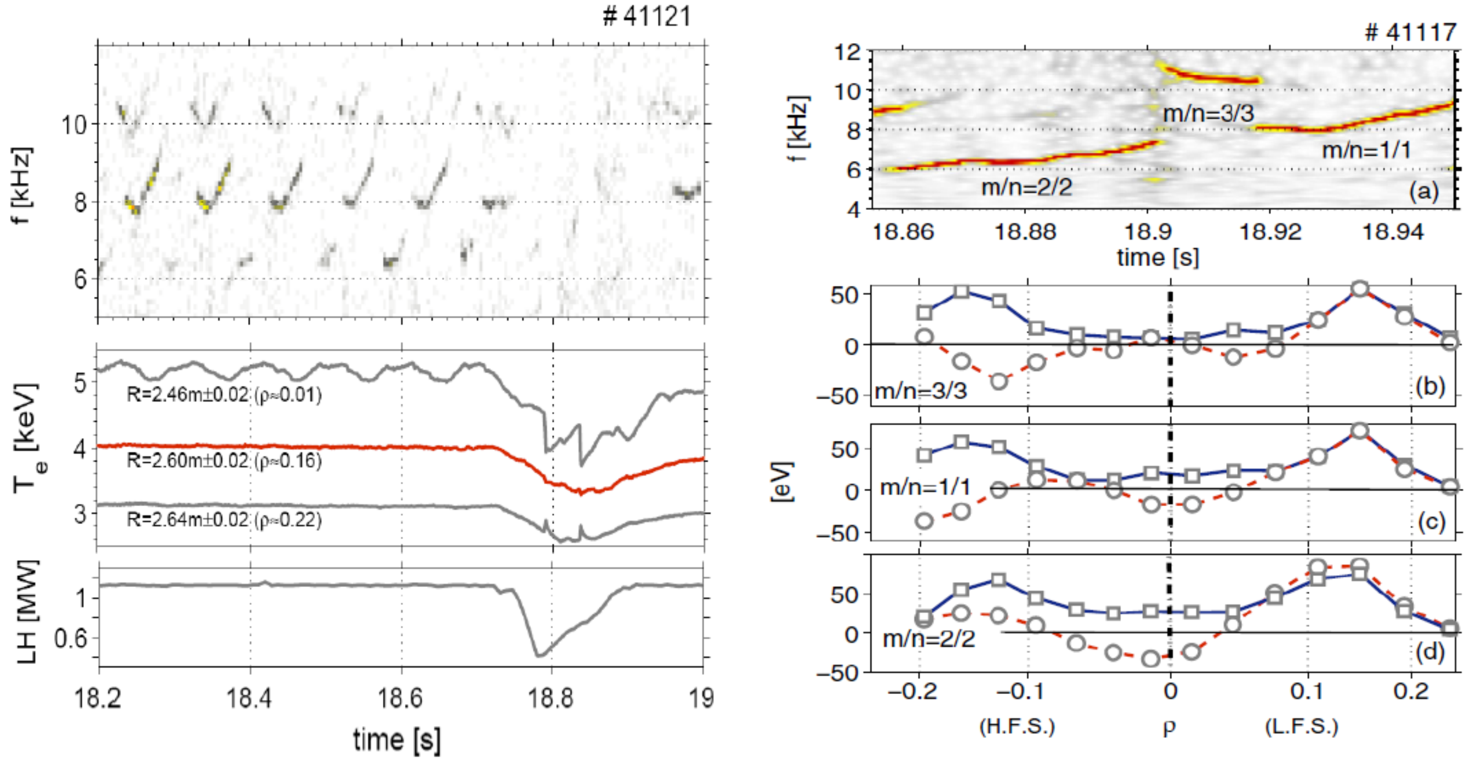

[A.Macor, PRL 2009]

O-14 Z.O. Guimaraes-Filho et al.

Global Modes Excited by Energetic Electrons on LHD

Frequency of magnetic fluctuation varies according to ECRH turn-on/off

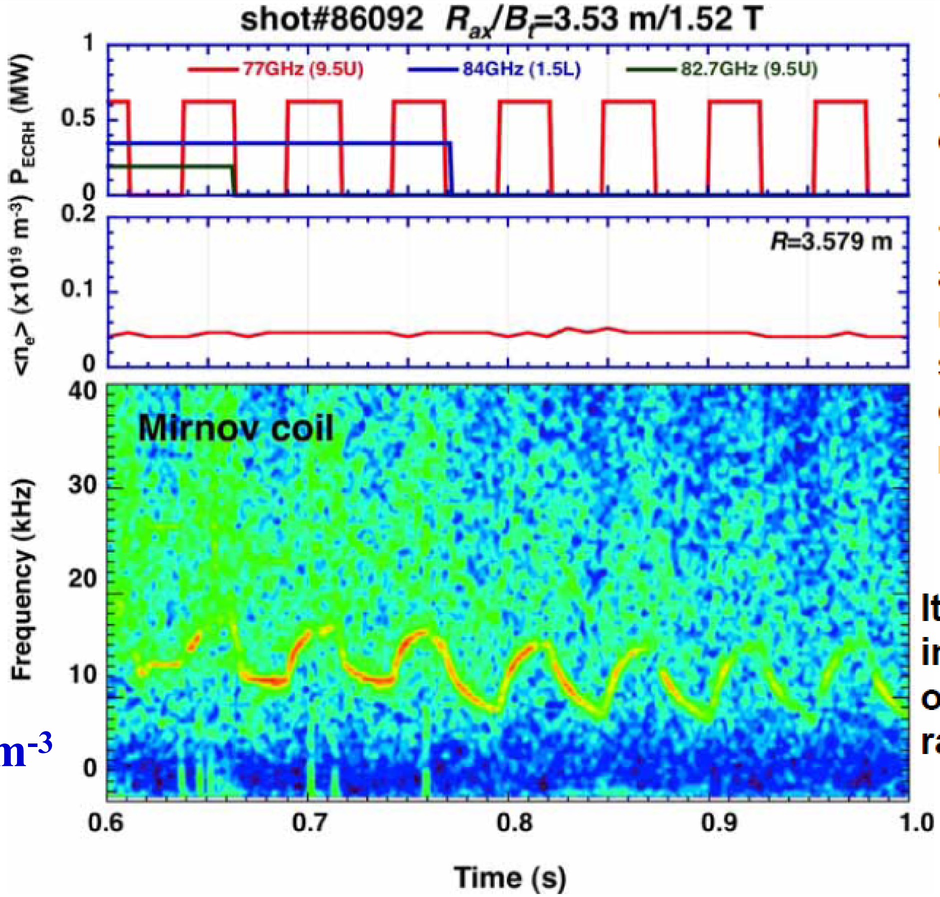

• Electron density is constant during ECRH modulation.

• MP frequency goes down after ECRH turn-off and goes up following ECRH turn-on, suggesting that the frequency change is associated with plasma temperature.

Te>>Ti
Te=10keV
Ti=1keV
$<n_e><0.2\times10^{19}$ m^{-3}
T_{e_tail} ~150 keV

$<n_e>>0.2\times10^{19}$ m^{-3}
:no mode exciation

It looks that the mode excited in 2nd harmonic ECRH plasmas of LHD has an acoustic nature rather than Alfvénic.

O-20 M. Isobe et al.

Global Modes Excited by Energetic Electrons on LHD

Rapid jump of potential to positive at plasma core while bursting Mirnov activities are present

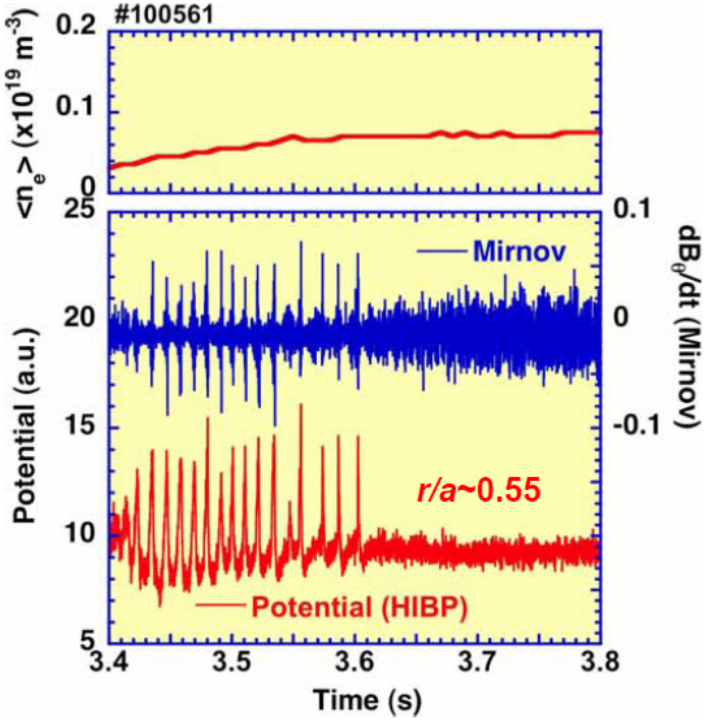

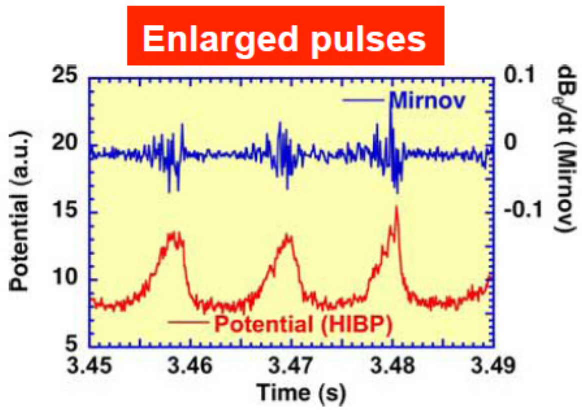

- Potential changes to positive as magnetic fluctuation grows
- Note that fluctuation on potential has not been visible.

O-20
M. Isobe et al.

Pulsatile potential change to positive is probably due to rapid expulsion or radial transport of suprathermal electron

Spanish Heliac T-JII

In TJ-II Heliac (CEAMAT, Spain), global modes Are excited by intense ECH, [P2-5: K. Nagaoka et al.]

Contributions from New Groups to this IAEA TM
Reversed field pinch & Shearless stellarator

Fast Ions are Barely Studied in RFP Concept

MST

- **Fast ion confinement and transport in Reversed Field Pinch (RFP) devices could be quite different from in Tokamaks.**
  - $B_t \sim B_p$, ρ_{fi}/a: 0.1~0.25 → large prompt loss
  - Large magnetic fluctuations, stochastic magnetic field
    → could lead to rapid diffusion of charge particles
  - $V_{fast\text{-}ion} > V_{Alfvén}$ → fast ions could drive Alfvén instabilities

- **The newly installed 1 MW neutral beam injector on MST provides a good test-bed for fast ion study in RFPs.**
  - Interplay between magnetic fluctuations and fast ion confinement
  - Fast ion driven instabilities
  - Control of MHD dynamo and tearing modes?
  - Plasma beta limit?

NBI: tangential injection
E=25keV (positive ion source)
1MW, 20 ms pulse

O-19 D. Liu et al.

NBI Induces Bursting Modes

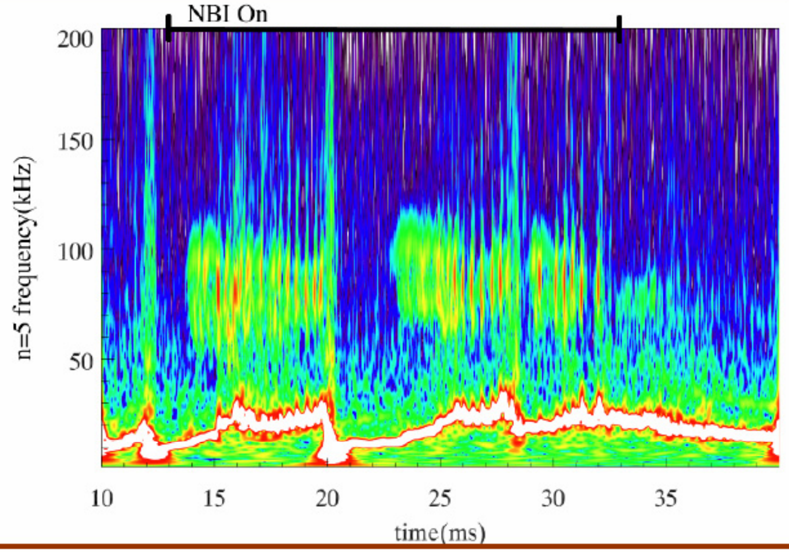

$F=B_\varphi(a)/<B_\varphi>= 0$ (or q (a)=0)
I_p=300kA
$n_e=0.7\times10^{13}cm^{-3}$

- NBI induced bursting magnetic fluctuations have been detected on magnetic coils in F= 0 (or q(a)=0) plasmas with co-NBI, not in any F<0 plasmas.
- Frequencies are in the range of 60~150kHZ with n=4 or n=5, m=1, much less than the predicted TAE frequency (~300kHz)
- The strongest coherence activity scales inversely with density, but does not scale with magnetic field strength.
- The mode is not identified yet, could be EPM….

Fast ions in MST behave roughly classically in spite of stochastic magnetic field. NBI induces bursting modes at frequencies of 60-150kHz that scales with density, not magnetic field.

O-19 D. Liu et al.

Studies of AEs in HJ with low magnetic shear

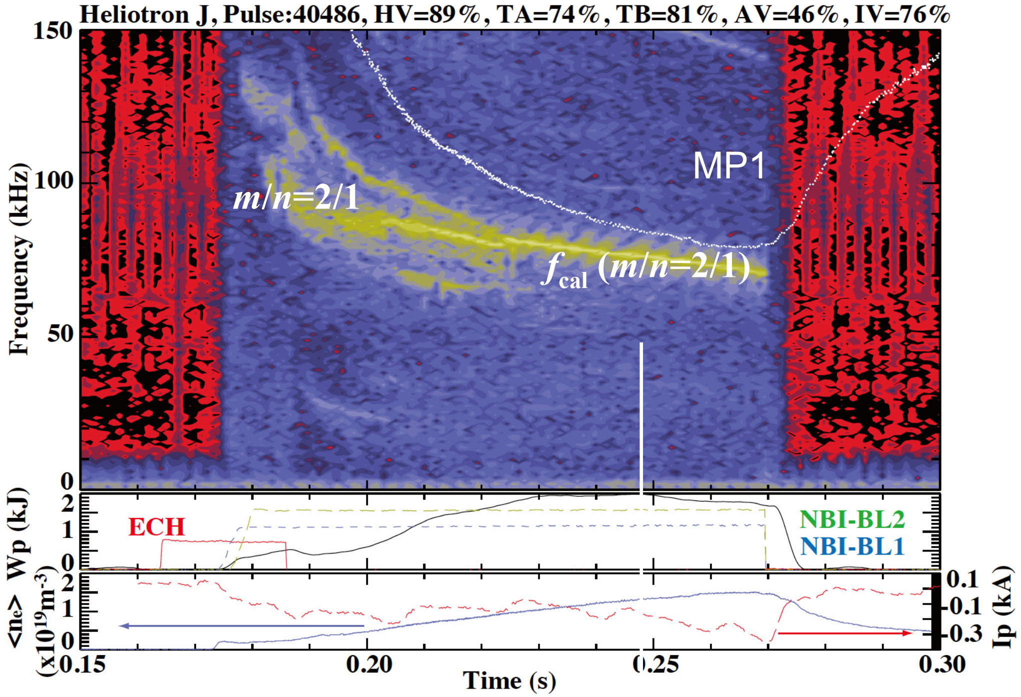

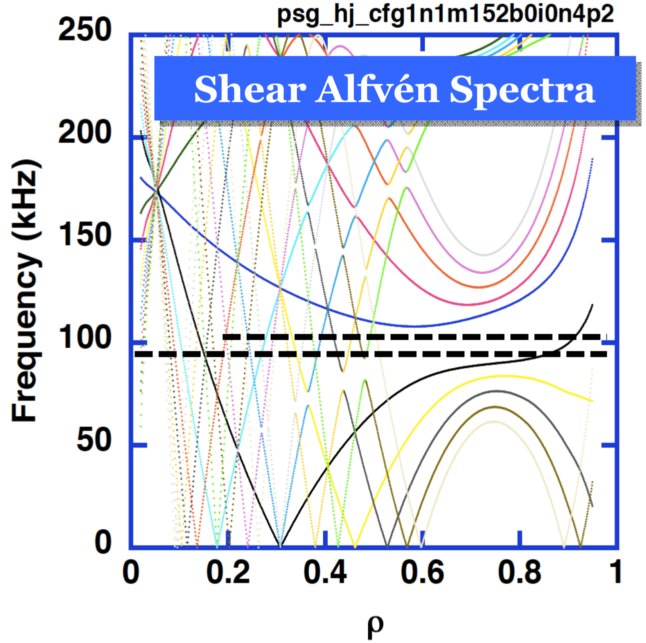

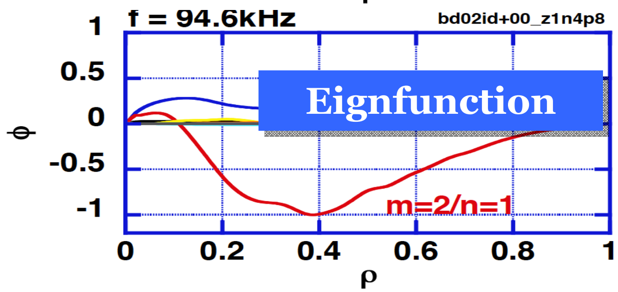

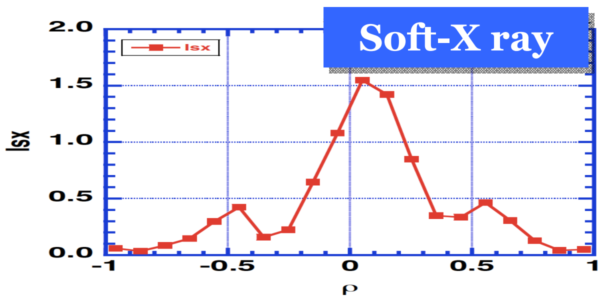

- ✓ Heliotron J : **low magnetic shear** ,
  + magnetic well for MHD stability.
- ✓ The observed modes during NBI are identified as **GAEs** by the comparison between exp. results and shear Alfvén spectra in 3D magnetic configuration.
- ✓ In the range of 0.45 < i/2p < 0.65, GAEs are dominant in *f* < 500 kHz. HAE frequency is *f* > 1MHz.

P2-18 S. Yamamoto et al.

Nonlinear Evolution of TAEs

- **Steady state evolution, periodic (pitchfork split), chaotic v.s. Bursting: This is controlled through competition between electron drag and velocity diffusion (pitch angle scattering).**

NONLINEAR NBI-DRIVEN ALFVÉN EIGENMODES ON MAST: HOOK FREQUENCY

This physics are More general, bacause These kind phenomena Are not sensitively affected By a system, i.e., magnetic configurations.

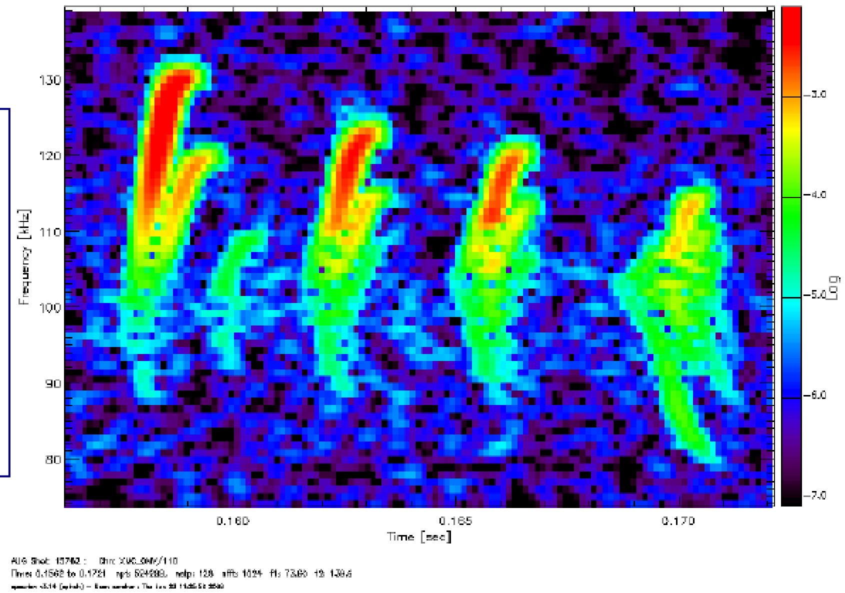

These modes are seen at ratio of $\Delta\Omega_{Diff}/\Delta\Omega_{Drag} \approx 0.5$, in line with the stronger competition between the drag acting to deepen the hole and diffusion that acts to destroy the hole

Nonlinear Evolution of TAEs

In MAST, electron drag always prevails the diffusion.

➔ always, bursting with rapid frequency chirping?

STEADY-STATE TAE: POSSIBLE OBSERVATION OF STEADY-STATE BGK MODE SIMILAR TO M.LLILLEY's MODELLING

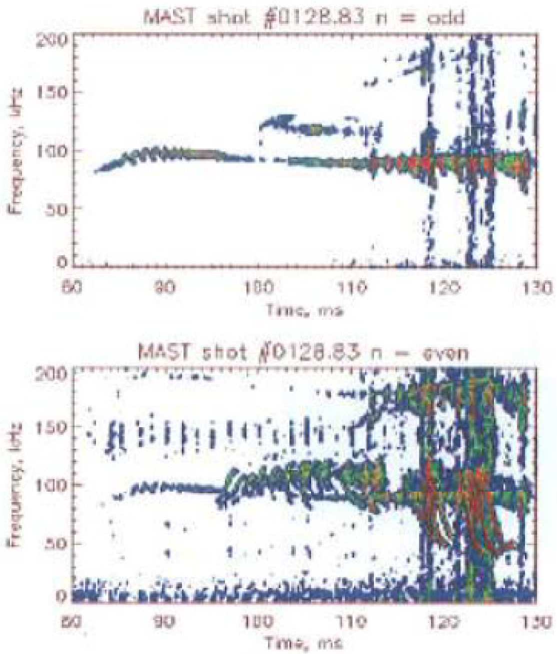

TAE excited in MAST discharge #12883 during NBI power increase

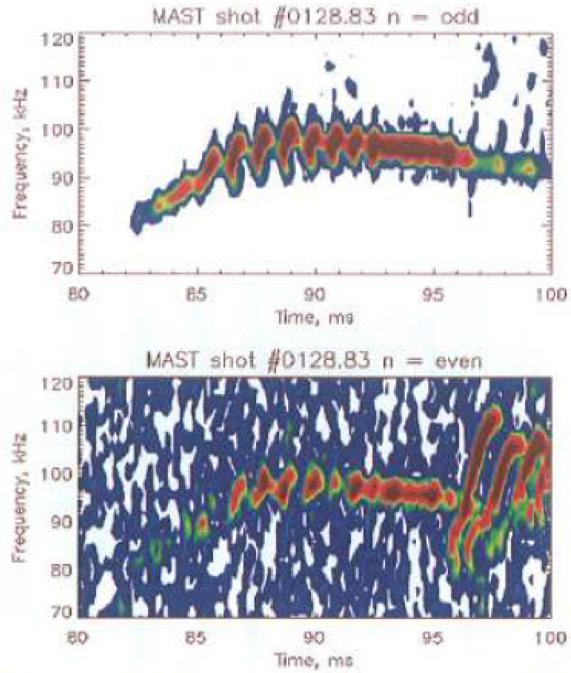

Zoom of the spectrogram in the early phase, from 80 to 100 msec

ITPA Joint experiments are going on.

IIII

Radial transport of EPs by energetic ion driven global modes

- **Velocity-space resolved (pitch angle and energy) diagnostics for confined and lost energetic ions are crucially important to clarify energetic ion transport mechanisms.**

  FIDA (fast ion CX spectroscopy) ;

  FILD or SLIP (lost fast ion probe)

- **Experimental results from**

  Tokmaks: DIII-D(I-6, P1-18),

  NSTX(I-3, O-1, O-12, P1-7, P1-18)

  Helicals/stellarators: LHD (I-7)

Energetic ion redistribution by sawteeth in DIII-D

Sawteeth strongly couple to ICRF-accelerated trapped ions

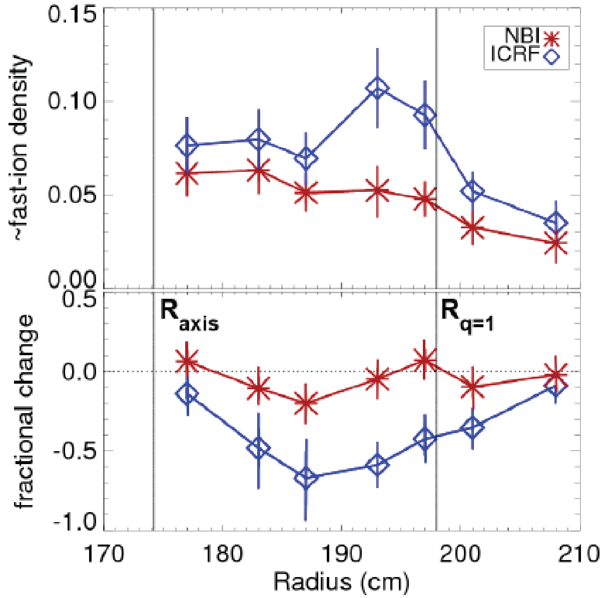

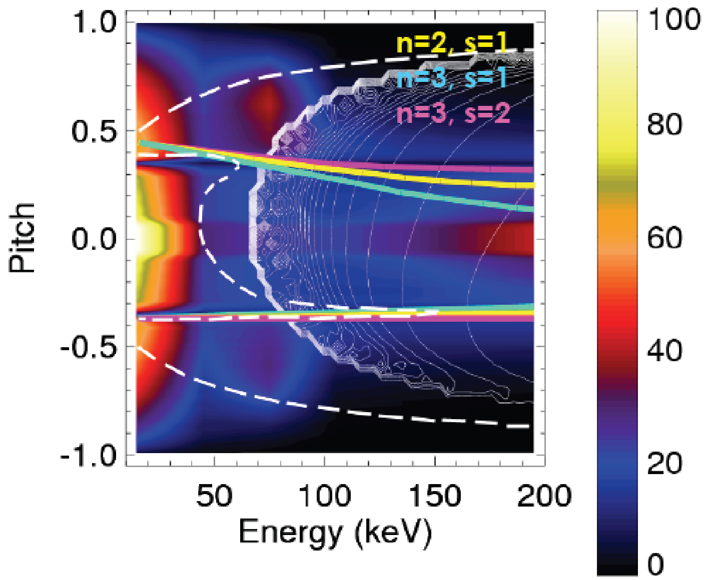

$$n\omega_{pr} = s\omega_b$$

- Observed enhanced transport of trapped ions during ICRF due to bounce/precession resonance

Moderate energy fast ions: transport by flux attachment
High energy ions: resonatce interaction

I-6 C.M. Muscatello et al.

Energetic ion losses by fishbones in DIII-D

Off-axis fishbones observed to expel fast ions due to precession resonance

- 7 independent fast-ion loss detectors observe beacon-like losses
- Fishbones interact with deeply trapped via precession resonance

$$\omega = \omega_{pr}$$

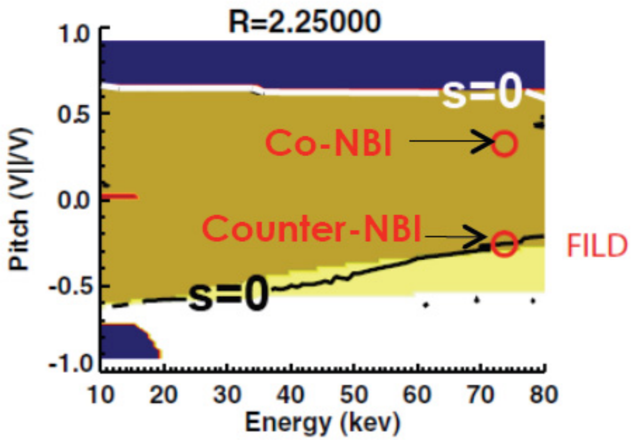

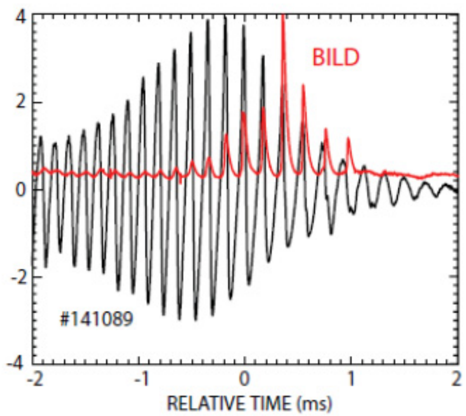

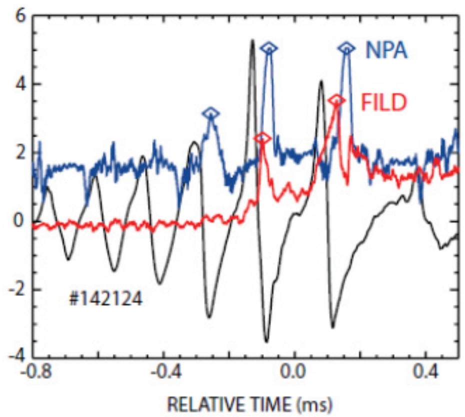

Fishbones: resonant kicks into loss boundaries

I-6 C.M. Muscatello et al.

Coherent losses by TAEs & RSAEs in DIII-D

Coherent loss measurements during strong AE activity

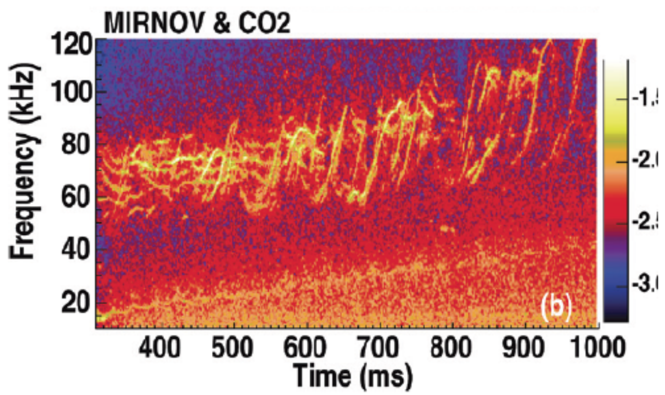

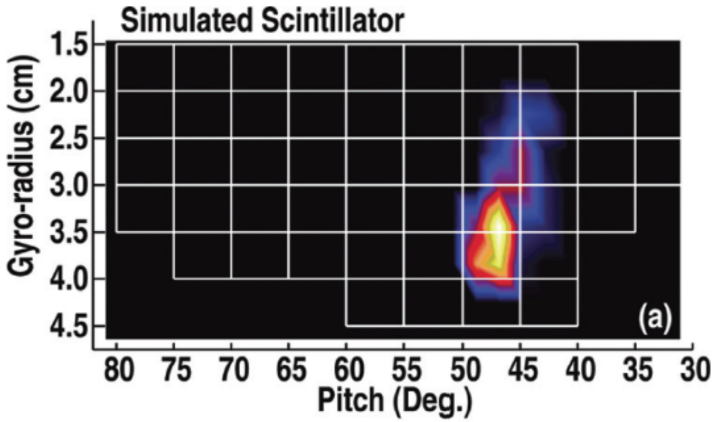

- Fast-ion loss detector measures signal coherent with TAEs and RSAEs
- Modeled losses reproduces measured signal with approximately correct energy band and pitch

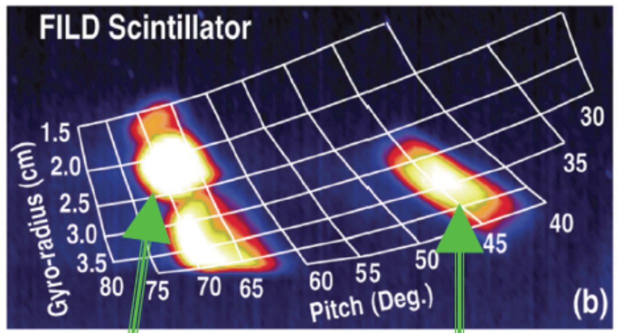

NBI prompt losses

AE-induced losses

TAEs/RSAEs: resonant kicks into loss boundaries

Coherent losses by TAEs, RSAEs & EGAM on DIII-D

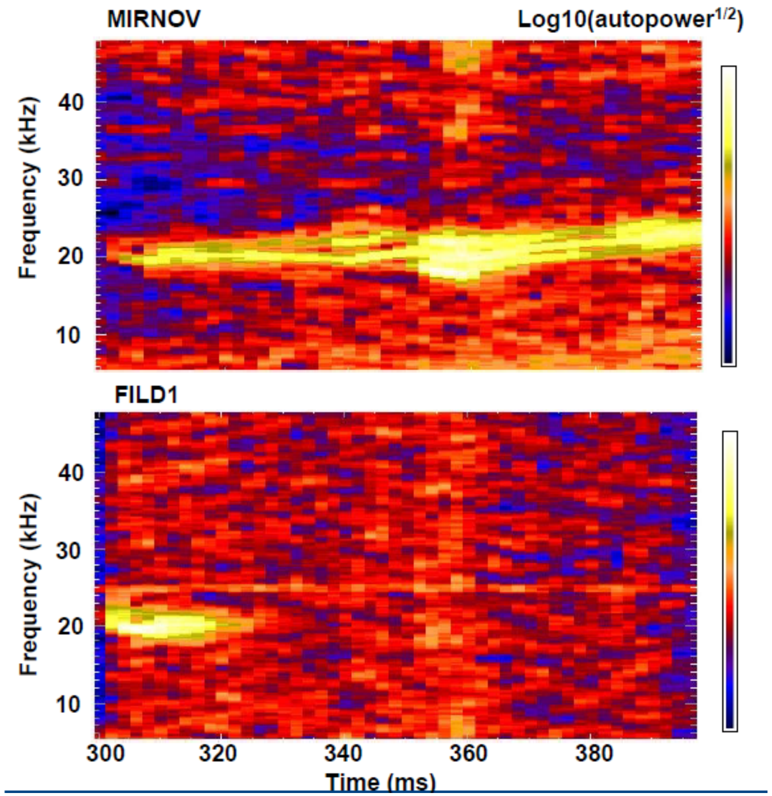

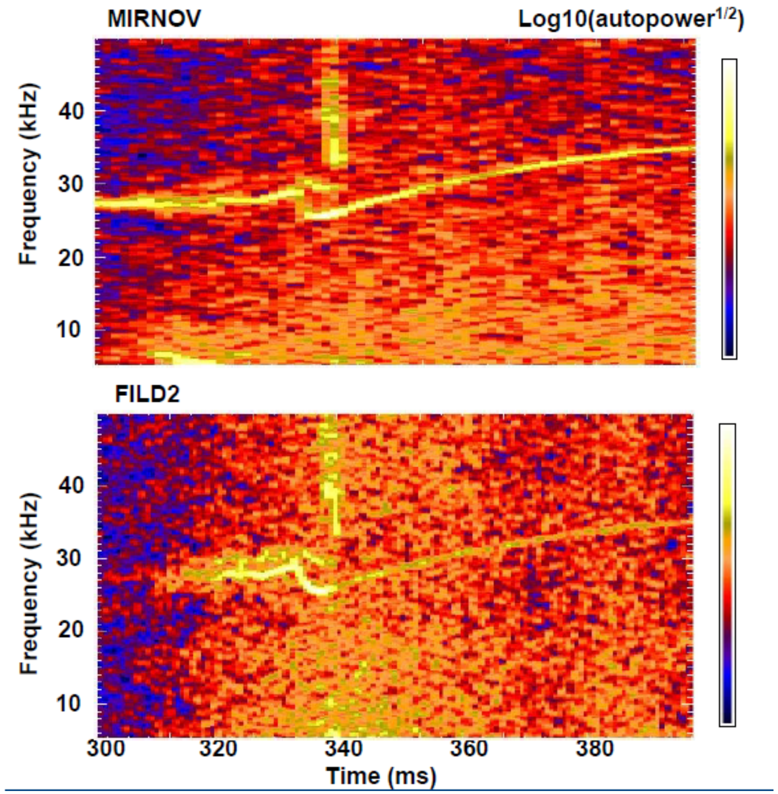

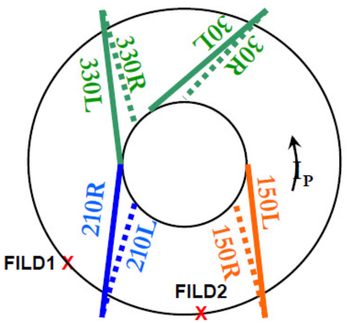

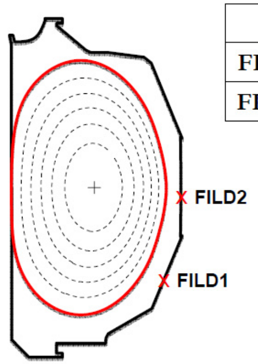

	r_L (cm)	α (°)
FILD1	1.5-5.0	30-75
FILD2	2.5-8.0	35-85

- Generally, FILD1 has stronger signal in oval shape plasmas while FILD2 is more suitable in circular shape plasmas.

Coherent losses by TEAs, RSAEs are detected by two FILDs. The loss by EGAM excited by counter NBI is also observed.

P1-3 X. Chen et al.

Energetic ion losses by EGAM in DIII-D
-- SPIRAL Simulation --

- SPIRAL successfully reproduced the experimental results from FILD
  we can use it now to look into details of the EGAM−particle interaction
- Coherent losses are found in the simulations when particle are loaded uniformly in energy between 20 and 80 keV and pitch between −1 and 1 at R,Z=(2.0,0.0)m

Experiment

pitch and gyro−radius resolved FILD losses

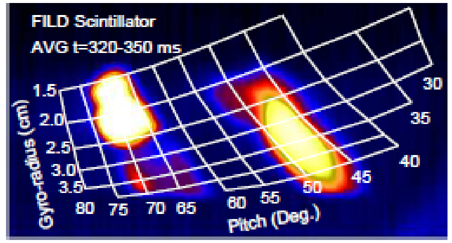

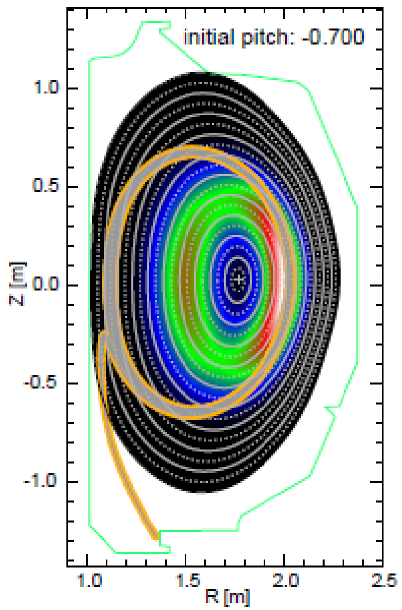

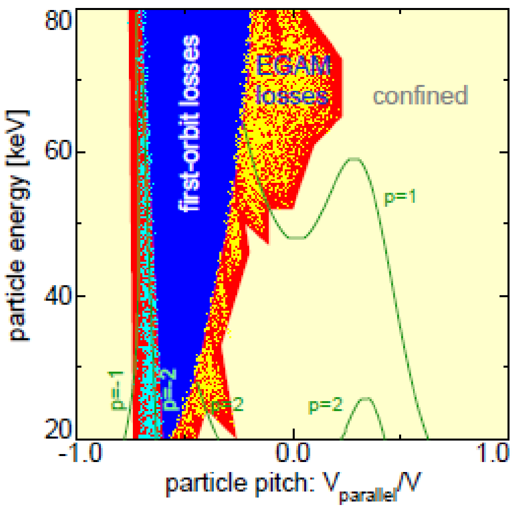

blue dots: lost particles that give >1% of its energy to the mode

yellow dots: lost particles that gain >1% of its energy from the mode

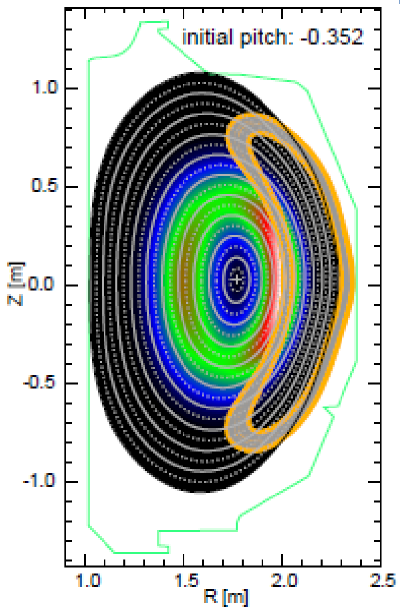

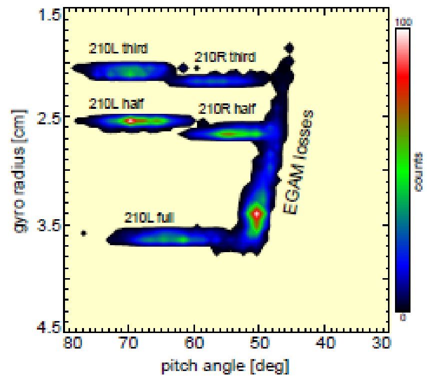

SPIRAL simul.

SPIRAL code is also successfully applied to NSTX data.

P1-18 G.J. Kramer et al.

Energetic ion losses by TAE Avalanche in NSTX L-Mode Plasmas

TAEs with low-intermediate toroidal mode number (*n*=2→7) are observed, with dominant *n*=2-4 modes

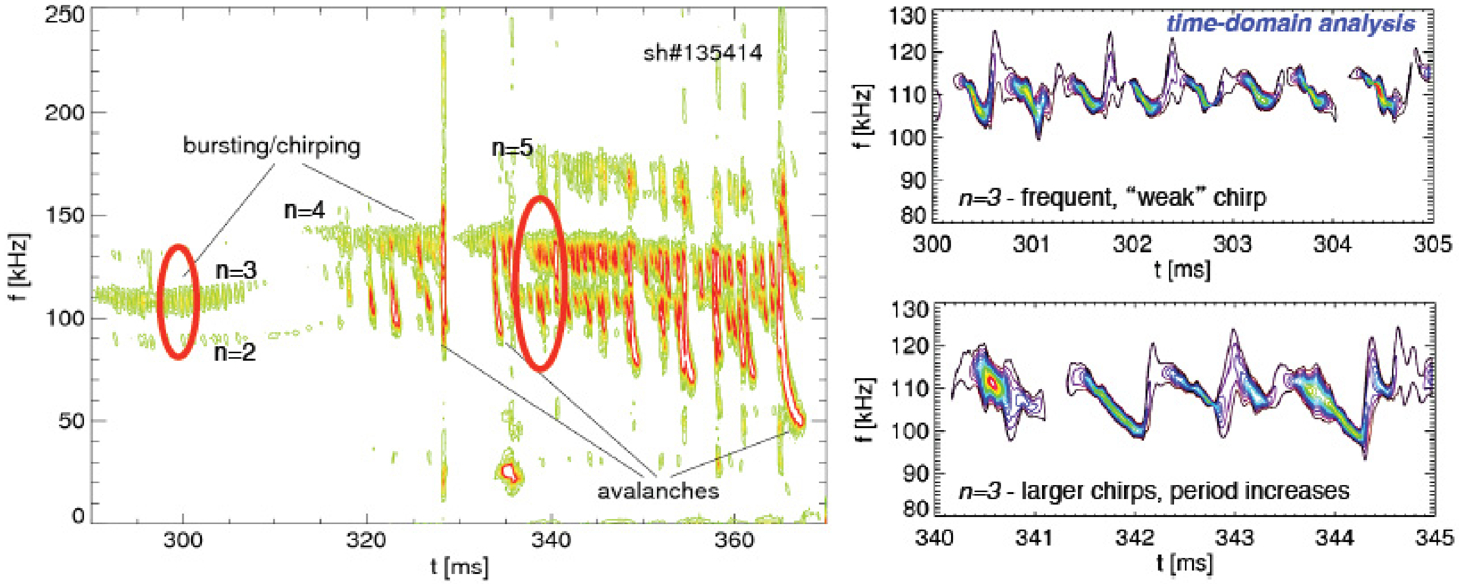

- Burst separation 0.5 – 2 ms
  - No systematic variation with n_e, T_e, P_{NB}, …
  - Frequency evolution does not follow unique patter (e.g. $t^{-1/2}$, linear, exponential)
- Usually, each mode chirps independently of the others...
- ... but, eventually, *avalanches* occur:
  - Drop in neutron rate, FIDA

A burst in which several TAEs of differing n occur is termed an "avalanche".

I-3 M. Podesta et al.

Energetic ion losses by TAE Avalanche in NSTX L-Mode Plasmas

Mode structure maintains its shape even during strong, *multi-step* avalanches

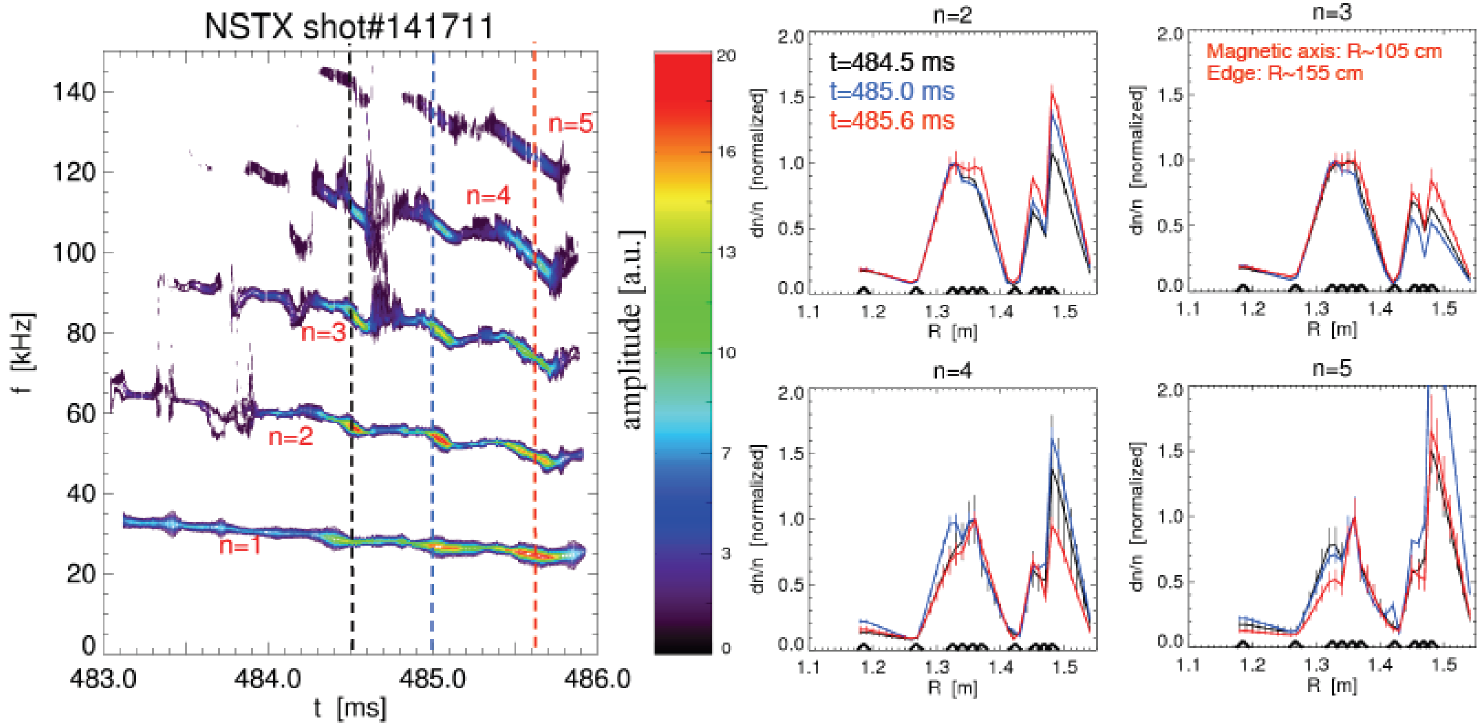

- Re-scaled dn/n shown (compare radial structure, not amplitude)
- Outward propagation of *unstable front* during burst not observed
  - Broad mode structure, ~ minor radius
  - Incomplete transition TAE → EPM?

Zonca et al., NF 2005

???

I-3 M. Podesta et al.

Energetic ion losses by TAE Avalanche in NSTX

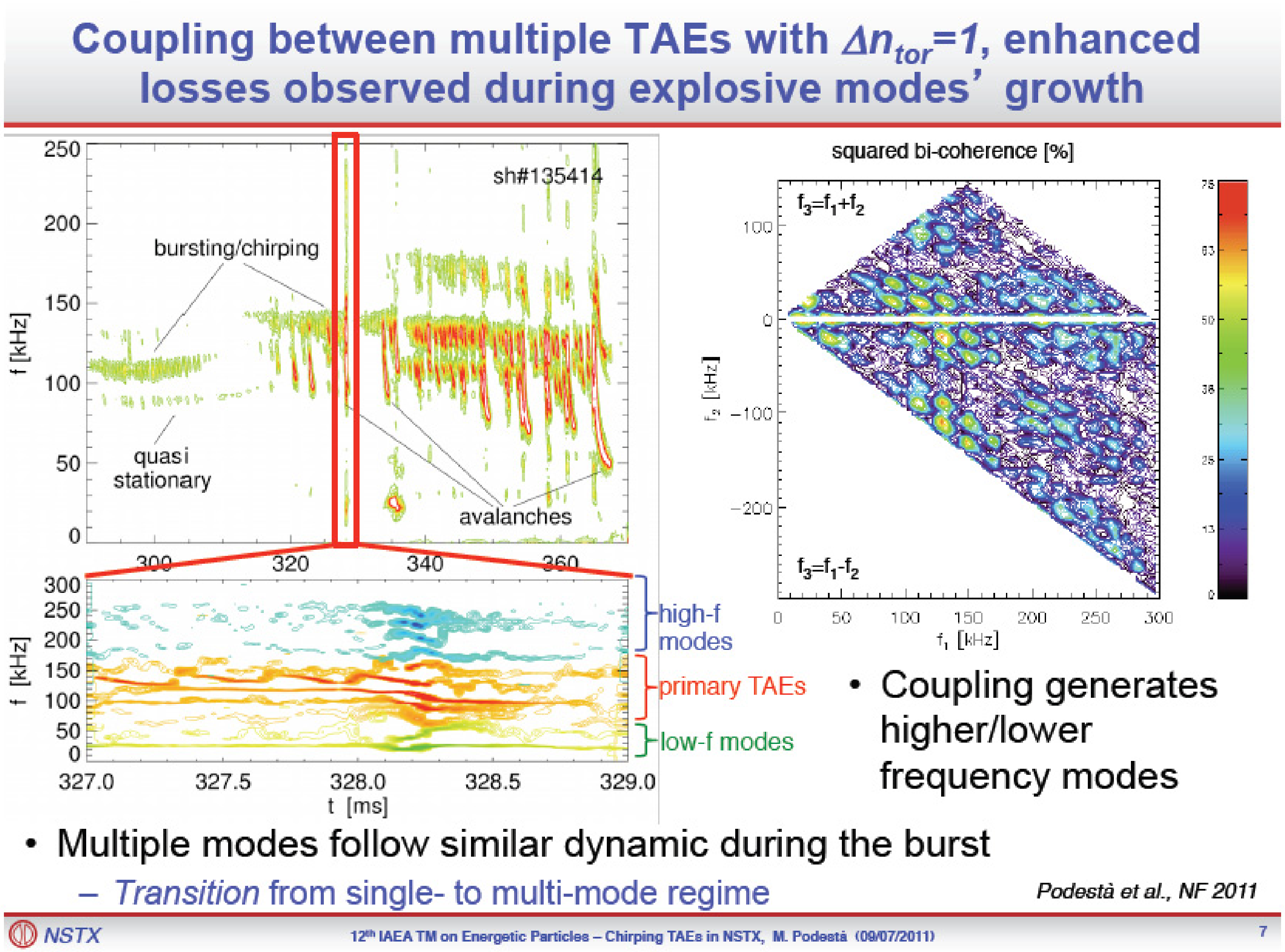

???

I-3 M. Podesta et al.

TAE avalanche in NSTX H-mode

ORBIT simulations predict losses in good agreement with observed neutron rate drop

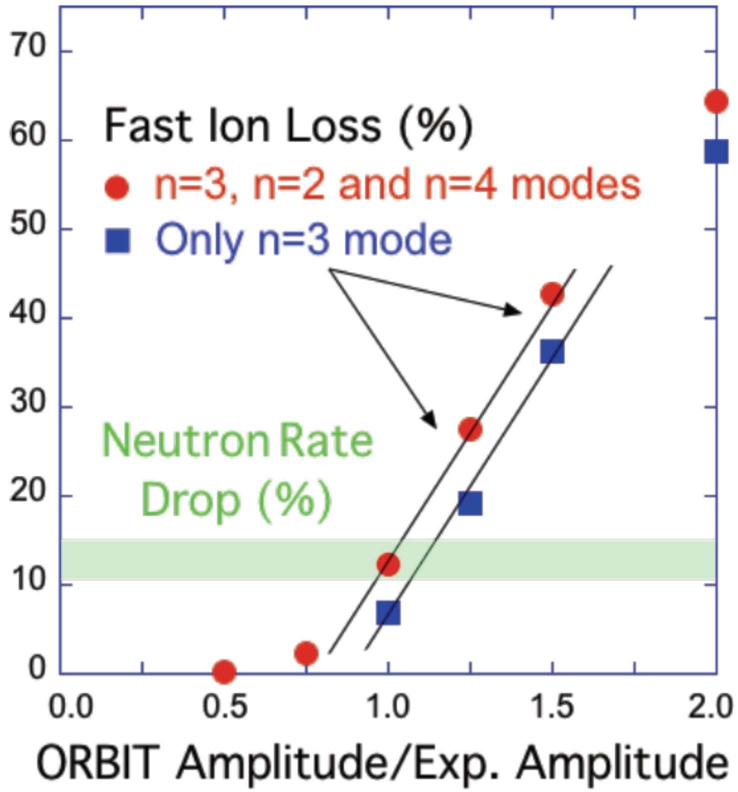

- *ORBIT simulation is done for 1ms burst at 0.285s.*
- *Mode amplitude, frequency evolution in ORBIT are from experimental measurements.*
- *Mode structure from NOVA.*
- *Initial fast ion distribution is from unperturbed TRANSP calculation – not necessarily self-consistent.*
- *Losses are strongly non-linear with mode amplitude – as expected for avalanche.*

Energetic Ion Losses by TAE Avalanche in NSTX

Test whether code-modeled stochastic domain presence coincides with lost pitch angle ranges

- Stochastic maps shown on following slides for 4 pitch angles marked (4 μ values)

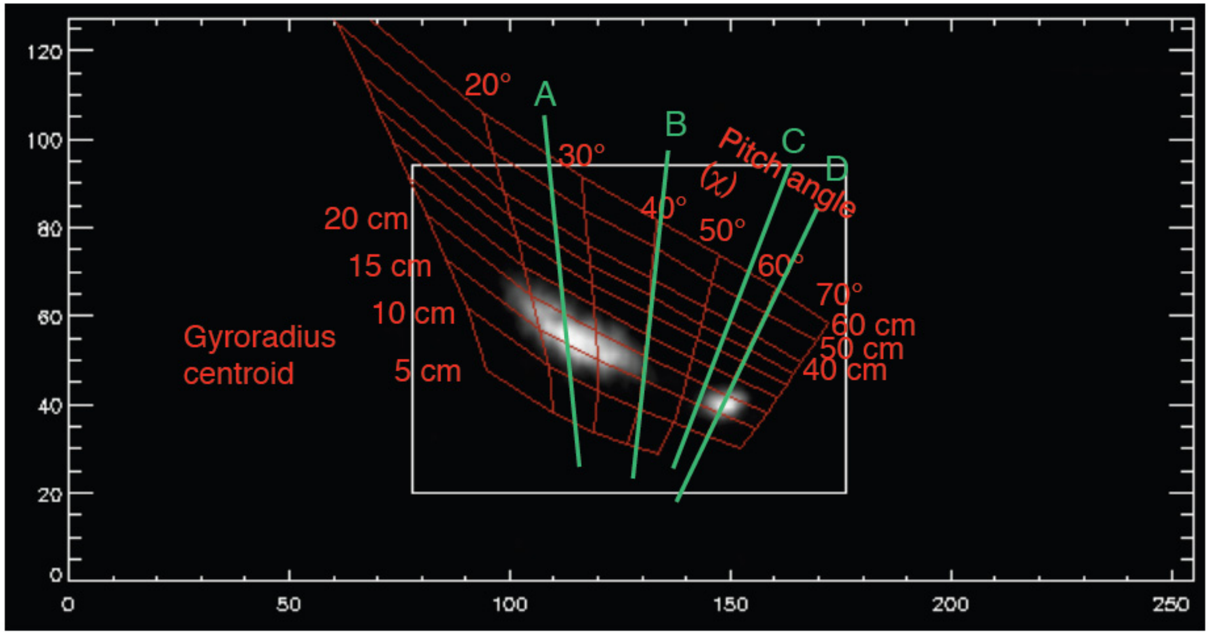

Losses appear at a given pitch angle only if (1)Beam deposited in stochastic region, and (2) Stochasticity expands all the way to the loss boundary along the line of transport.

O-1 D.S. Darrow et al.

Energetic ion losses by Low f-Modes in NSTX

In NSTX H-mode early kink (n=1,2) is accompained by n_{FIDA} depletion and CAE destabilization

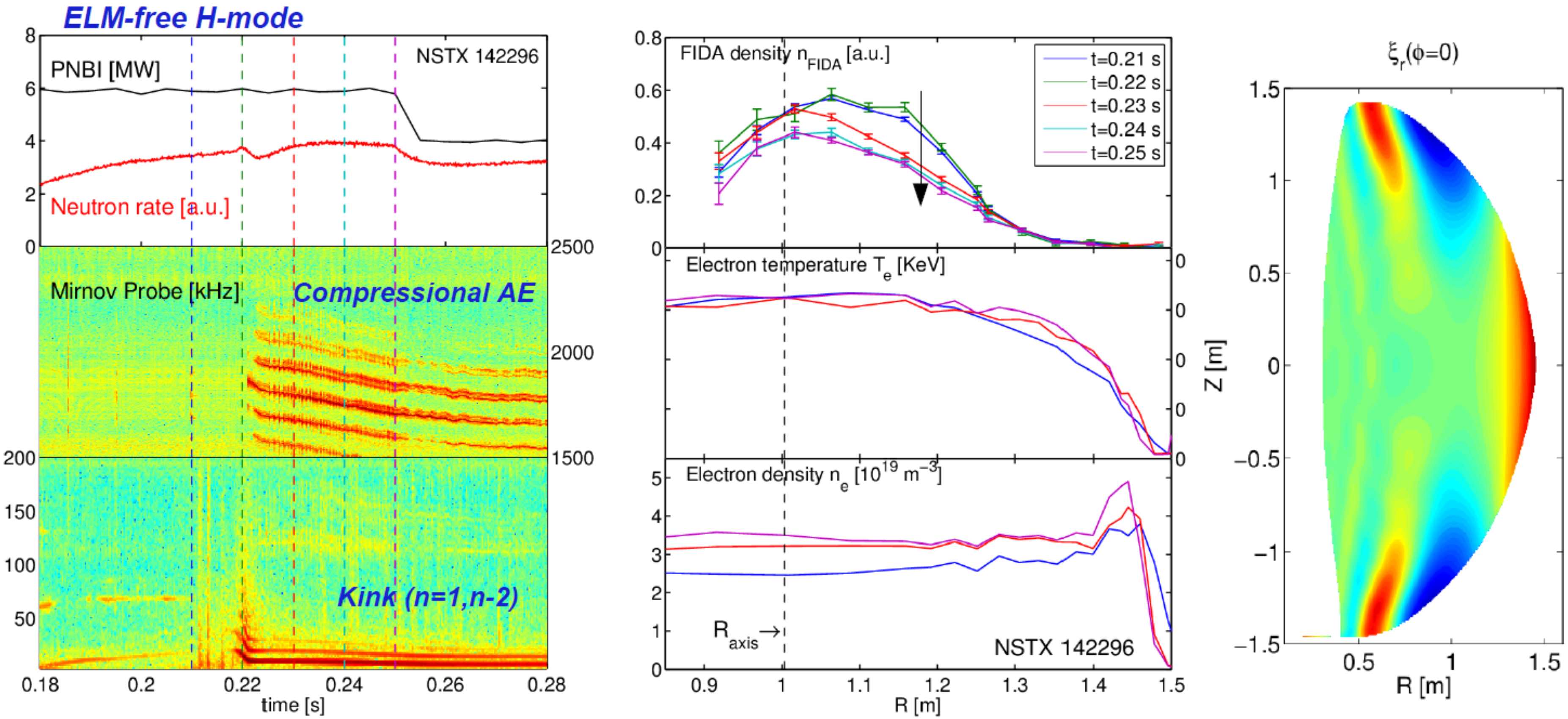

???

O-12 A. Bortolon et al.

Energetic ion losses by Low f-Modes in NSTX

- Kink effect from differential distribution $\Delta F = F_{kink} - F_{equi}$

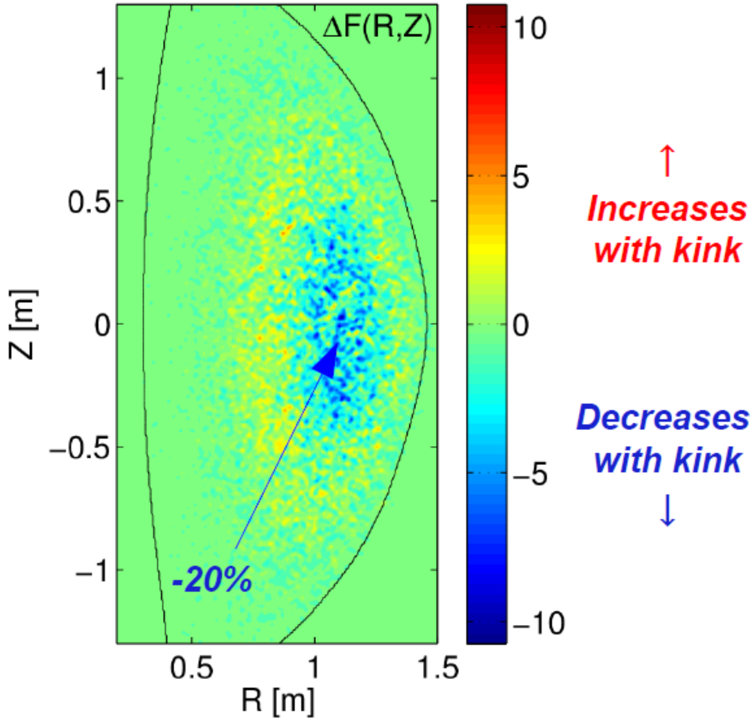

- Redistribution of core confined particles towards the edge

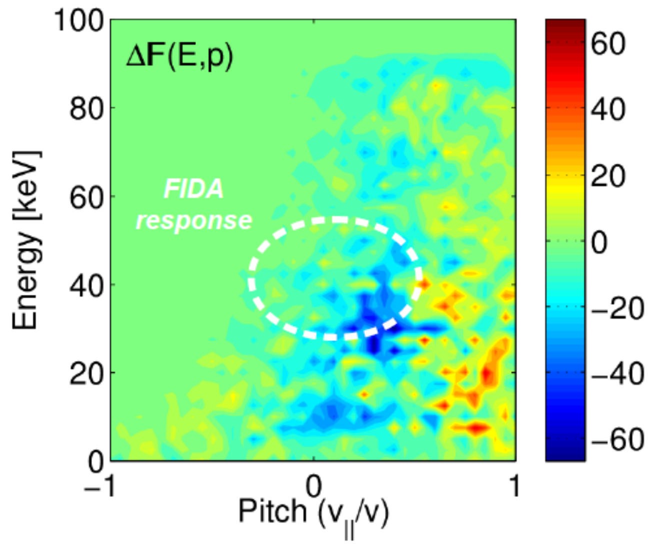

- Slowing down distribution shifts towards $v_{||} / v = 1$
- Net decrease in the region of maximal FIDA response

Full Orbit simulation with SPIRAL code indicate Redistribution in *real* and *velocity* space (3% losses)

O-12 A. Bortolon et al.

Energetic ion losses by AEs on AUG

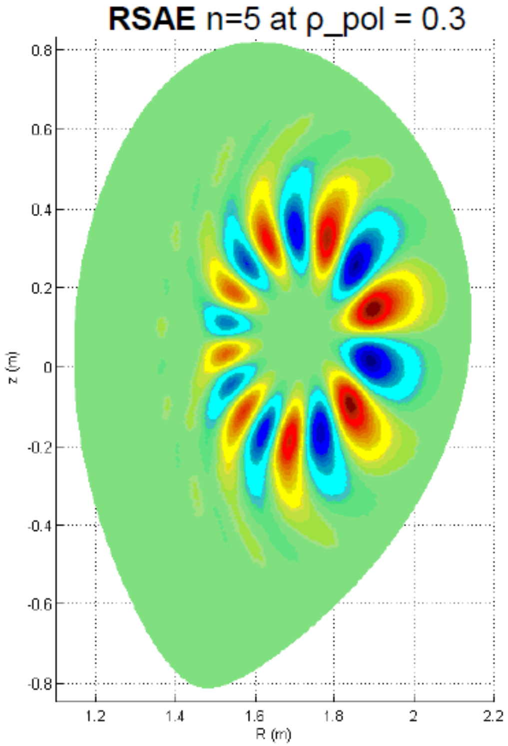

Redistribution / Loss Due To NBI Driven Alfven Eigenmodes

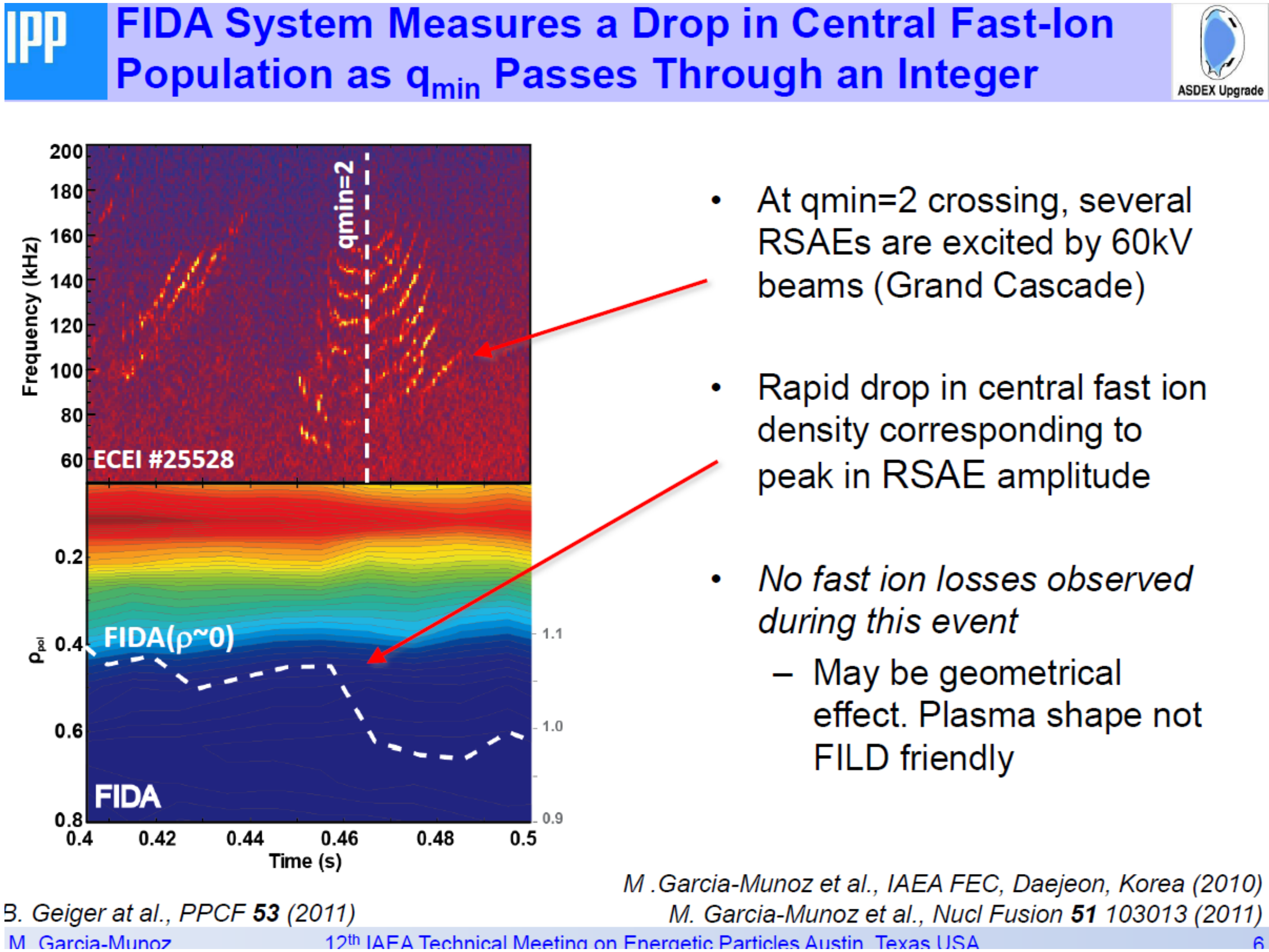

O-11 M. Garcia-Munoz et al.

Energetic ion losses by AEs on AUG

TAEs Observed to Cause Fast Ion Loss

ASDEX Upgrade

$\Omega_{n,p} \sim \omega_{MHD} - n\cdot\omega_{tor} - p\cdot\omega_{pol}$

Resonances n=1-5, p=1-4

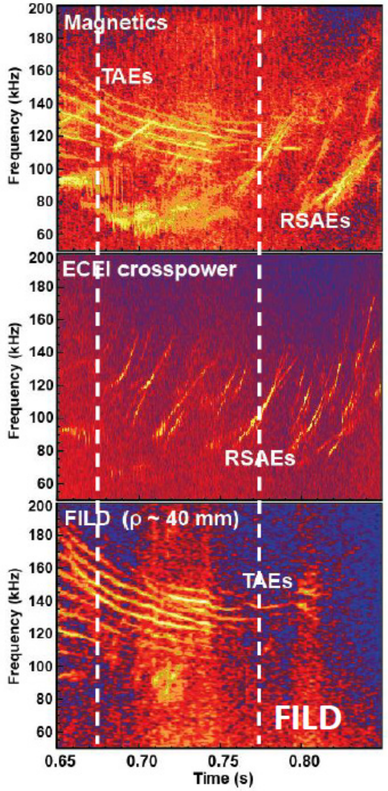

FILD SCINTILLATOR

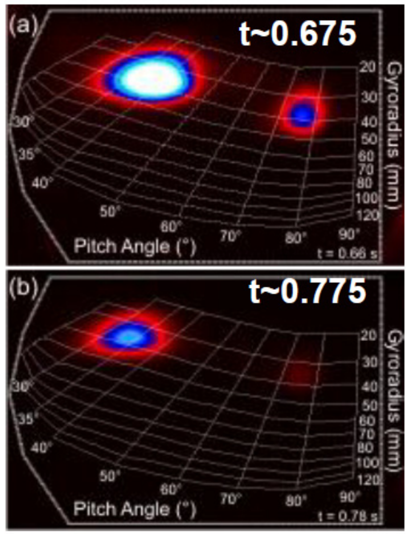

- FILD spectrogram shows clear coherent losses from beam driven TAEs
- FILD Scintillator indicates TAE induced losses appear near gyro-radius corresponding to injection energy

M .Garcia-Munoz et al., IAEA FEC, Daejeon, Korea (2010)
*M. Garcia-Munoz et al., Nucl Fusion **51** 103013 (2011)*

Wave-Particle Resonances are in Phase-Space Region Corresponding to Passing-Ions

➡ Larger Fast-Ion Losses

Energetic ion losses by ELMs on AUG

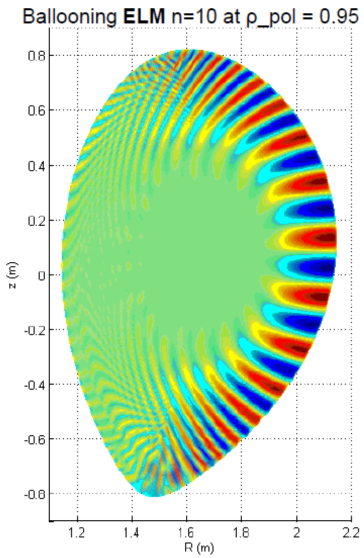

Role of Fast-Ions in ELM Cycle. Especially In The Presence Of Other Core Modes

Fast-Ions Seem To Contribute To ELM Stability

ASDEX Upgrade

Low-freq pedestal fluct. prior ELM crash leads to an increasing fast-ion loss flux which seems to contribute to the ELM triggering

- Frequent, small ELMs are often accompanied by large fluxes of fast-ion losses during and pre-ELM crash

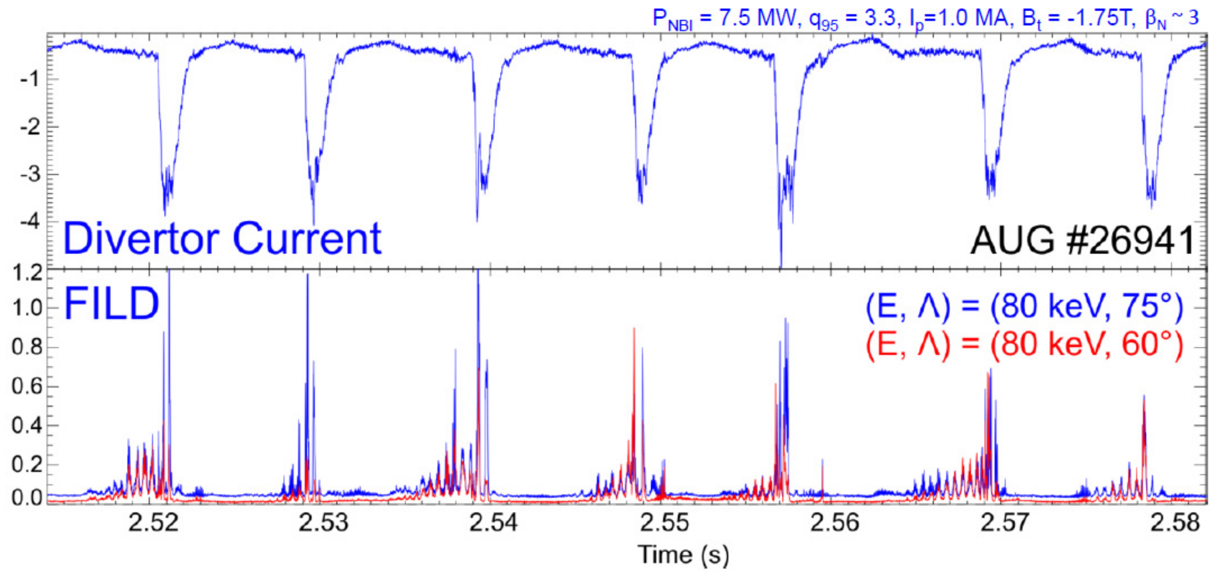

Pre-ELM Divertor current (ELM Monitor) Rise Correlated with FILD

Deeply trapped particles are strongly affected. Several loss mechanisms are present.

O-11 M. Garcia-Munoz et al.

Drops in neutron emission by FB

JET discharge 69100

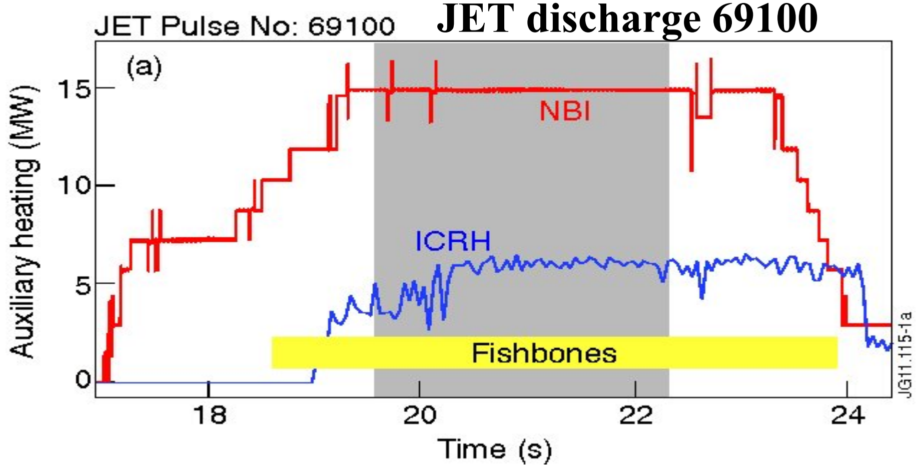

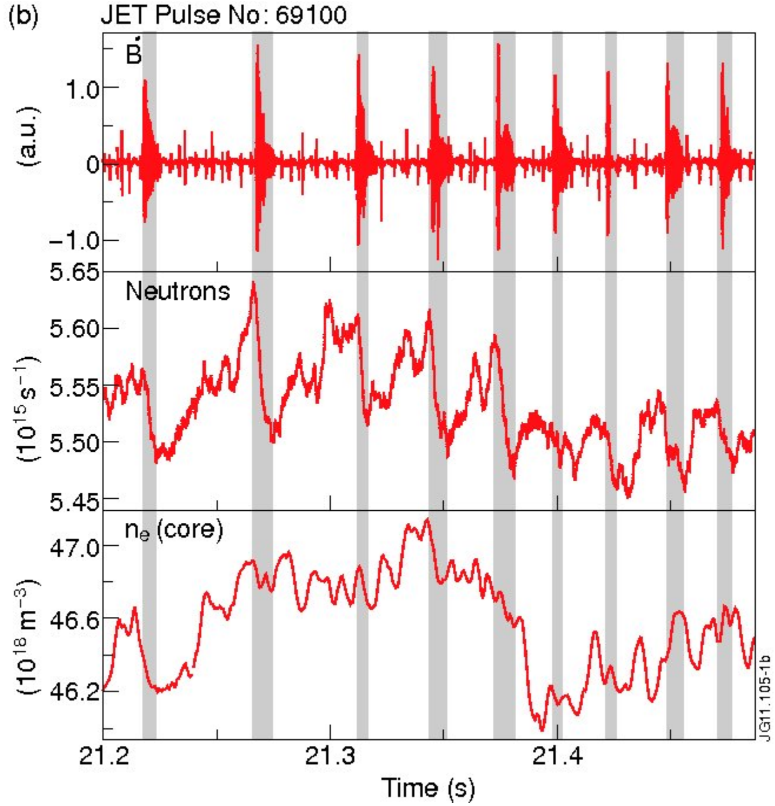

B=2.7T, I=1.2MA, q95=6.5, β_N=2.6, β_{pol}=1.8, δ ~ 0.4, n_e/n_{GW}=0.77, 15 MW NBI, 6 MW RF (H-minority)

- NPAs and gamma ray spectrometers show negligible second harmonic D acceleration (in agreement with PION and SELFO)
- 95% of neutrons originate from beam-target or beam-beam (TRANSP)
- Timing of FB occurrence and RF-free reference discharge show that FBs destabilised by NBI
- One of the ^{235}U fission chambers connected to fast DAQ, measures fast drops in neutron rate correlated with the FBs

O-18 Perez von Thun et al.

Drops in neutron emission by FB

- Neutron drops simulated for a set of runs with varying fishbone amplitude (using ASCOT-HAGIS-MISHKA)
- Experimental measurements evaluated for an ensemble of 40 fishbones (t=19.6-22.3 s)

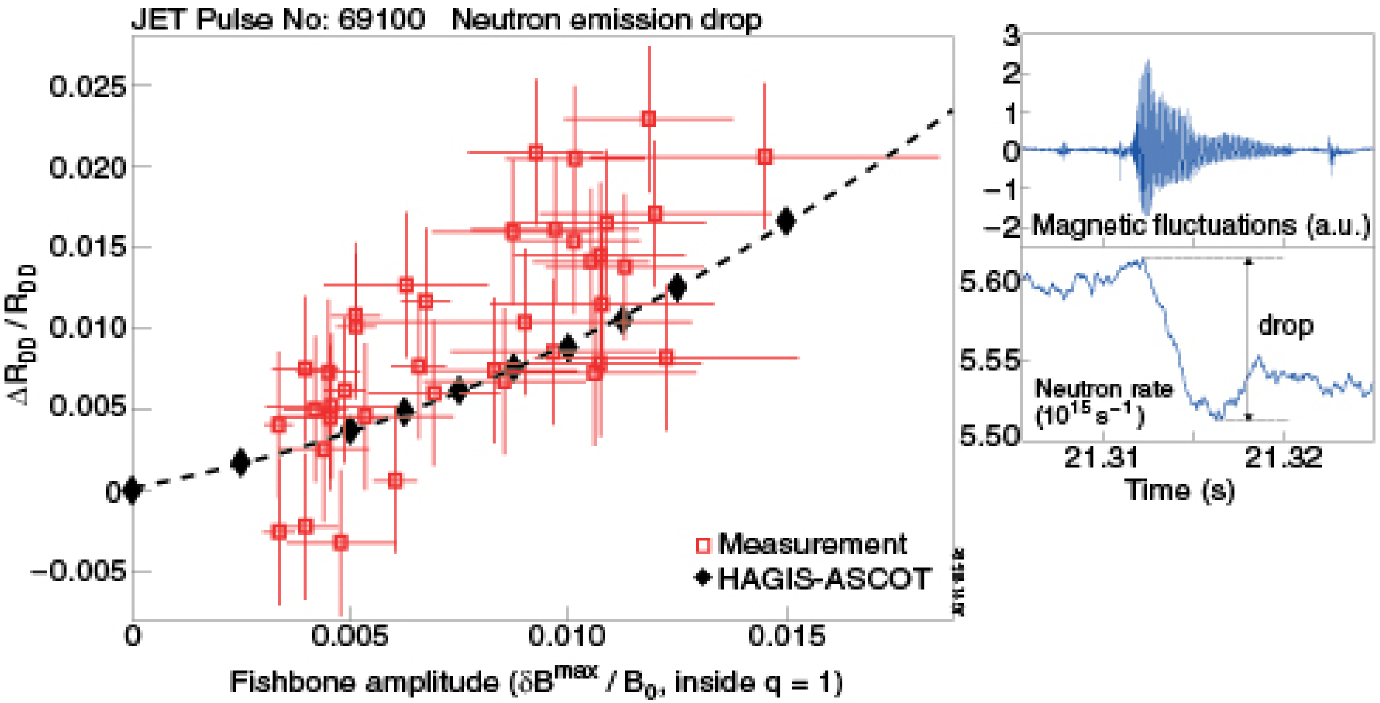

Drop quantification

- **For this range of amplitudes simulations predict drops of order 0.5-1.5%. Quadratic dependence on FB amplitude (diffusive-type transport)**
- **To within a factor 2 measured drops are consistent with simulations.**

O-18 Perez von Thun et al.

Energetic ion losses by AEs in LHD

To clarify dominant mechanism of losses induced by TAEs is also very important on the Large Helical Device (LHD). In LHD, a large Shafranov shift increases by increased plasma beta, generating magnetic well. On the other hand, large shafranov shift tends to increase energetic ion losses. Moreover, the energetic ion losses increase, having stronger dependence for $(b_{\theta TAE}/Bt)^s$, that is, s=1 to 2, and >2.

Guiding center Monte Calro code: DELTA 5D in LHD plasma

Full orbit code: in the vacuum (from the lost ion probe head to plasma surface)

Connection of a fast ion orbit at LCFS: smooth orbit connection=> lost to the detector

I-7 K. Ogawa et al

Energetic ion losses by AEs in LHD

Image of scintillator plate

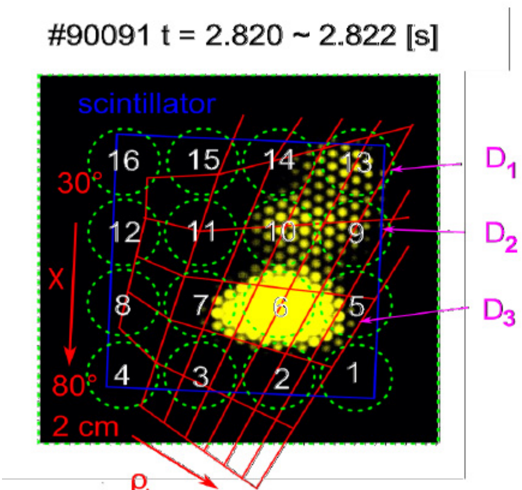

Time trace of TAE2, RIC and Γ_SLIP(#90091)

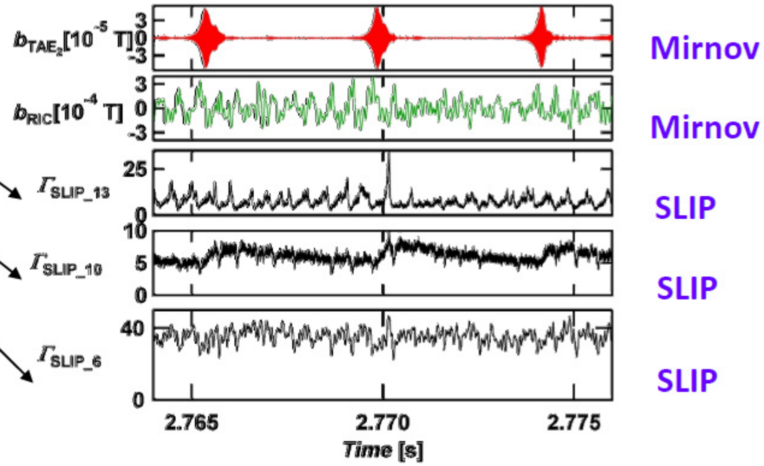

TAE induced loss dependence on Mirnov fluctuation amplitude

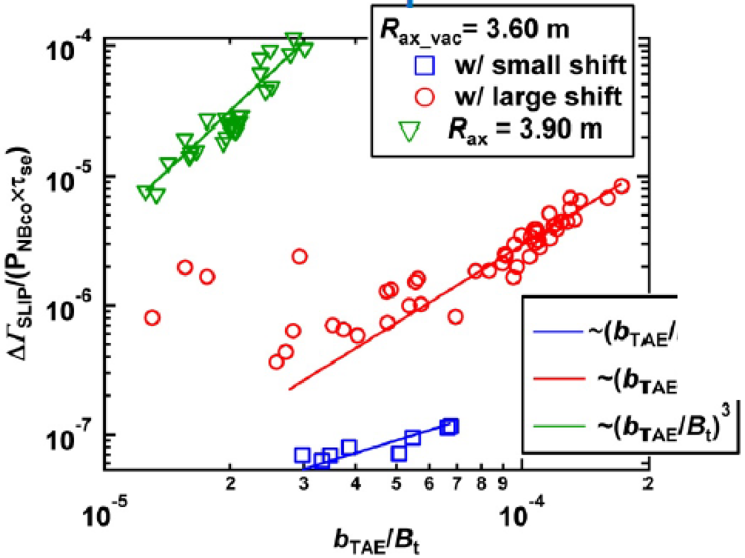

Eigenfunction of TAE in each configuration

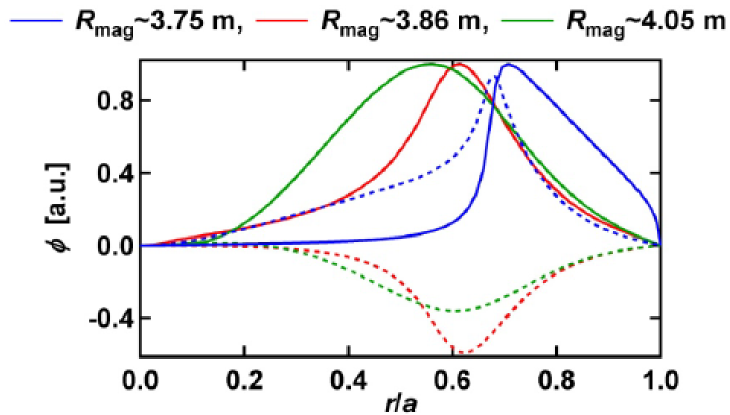

I-7 K. Ogawa et al

Energetic ion losses by AEs in LHD

Calculation result

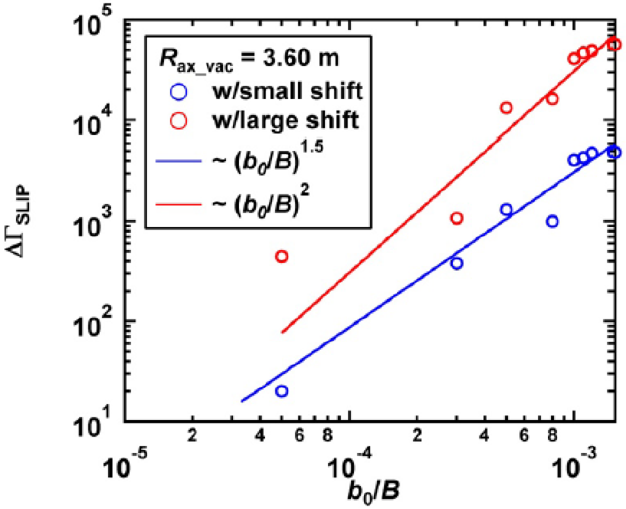

Experimental result

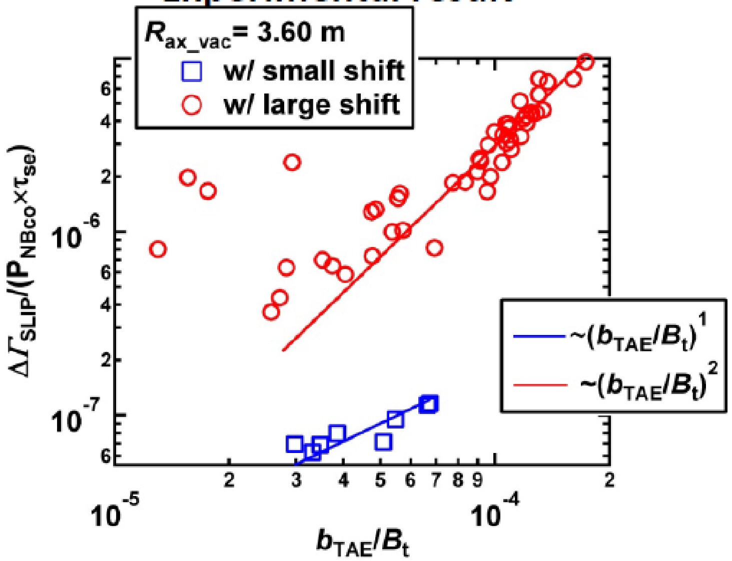

- Loss flux dependence on fluctuation amplitude.
  - b_0 indicate the fluctuation amplitude at peak position in a plasma
- Relation between b_0 and b_{TAE} observed in experiment have a certain relationship in each configuration.
  - b_0 have same connection with b_{TAE}.
- Loss flux dependence on fluctuation amplitude have some relation as that of at LCFS.
- Loss flux dependence on fluctuation amplitude is similar as observed in experiments on R_{mag} of 3.75 m and 3.86 m.

I-7 K. Ogawa et al

A Unknown Interesting Phenomenon in NSXT

- **At a certain condition where high frequency mode GAEs are excited and low frequency modes such as NTM are suppressed in H-mode, the charge exchange flux close to the injection energy is strongly enhanced (by a factor of ~4). This is called High Energy Feature (HEF).**

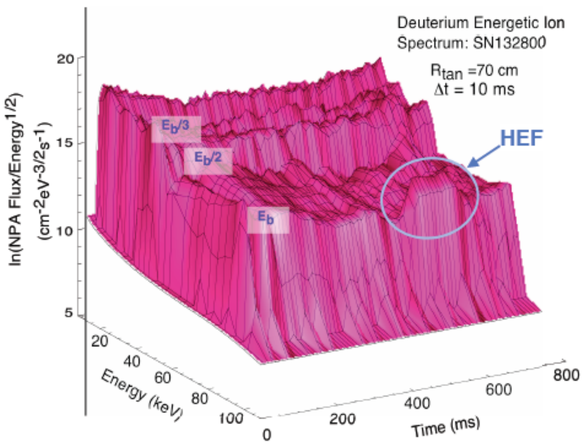

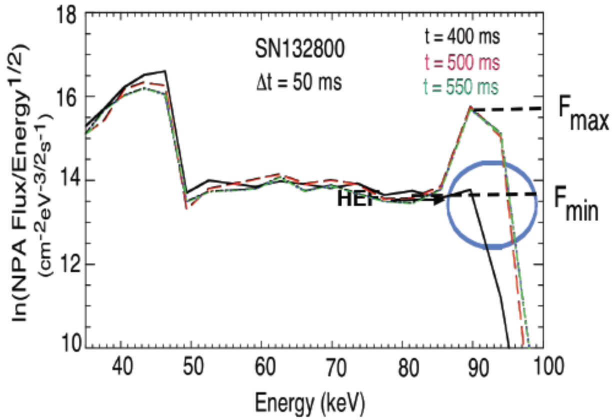

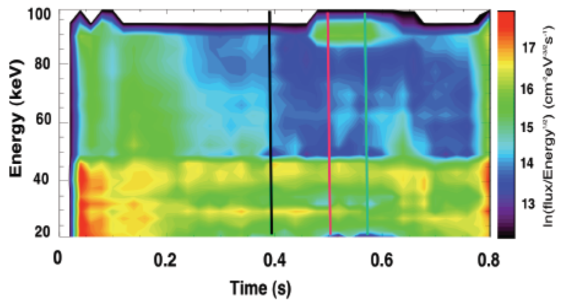

- **The NPA charge exchange spectrum exhibits enhanced signal only near E ~ E_b (e.g. never at $E_b/2$ or $E_b/3$).**
- **HEF can be characterized by peak-to-base flux ratio H = F_{max}/F_{min} ~ 10.**
- **Lack of evolution of a slowing-down distribution below the HEF is a common (and not understood) feature.**

GAE may play a role in triggering HEF
(P1-15 Y. Kolesnichenko, this conf)

P1-16 S. S. Medlly et al

Integrated Approach to Predict AE Stability and Induced Energetic Ion Losses in DIII-D & ITER

- **Stability analysis of AEs (TAEs, RSAEs) using NOVA-K code using experimentally obtained profile data and calculated fast ion distribution function.**
- **Fast ion losses calculated by ORBIT and SPIRAL codes.**

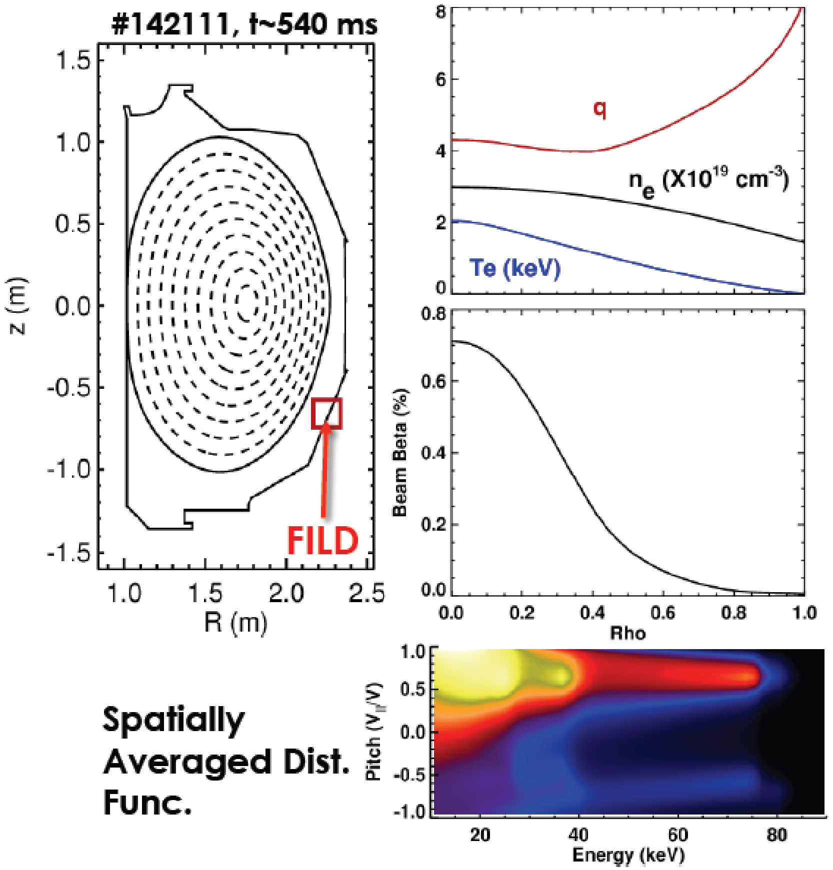

- Oval chosen to accommodate up/down symmetric equil. codes
- High q-min during current ramp
- Beam pressure profile obtained by subtracting thermal pressure from MSE constrained equilibrium pressure
- Pitch angle distribution obtained from TRANSP – primarily co-injection

P2-12 M.A. Van Zeeland et al

Integrated Approach to Predict AE Stability and Induced Energetic Ion Losses in DIII-D & ITER

- **Stability analysis of AEs (TAEs, RSAEs) using NOVA-K code using experimentally obtained profile data and calculated fast ion distribution function.**
- **Fast ion losses calculated by ORBIT and SPIRAL codes.**

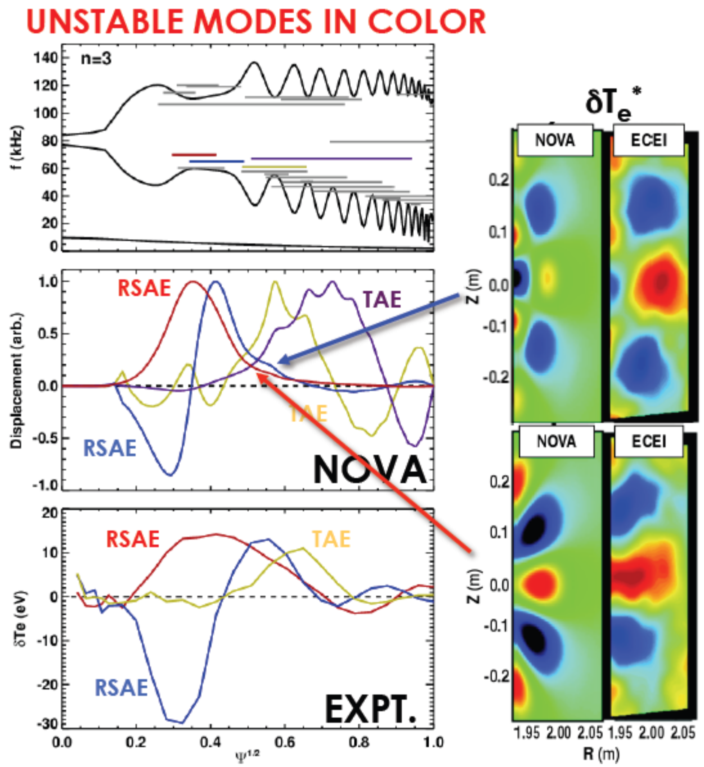

- Continuum and modes are calculated with NOVA for range of q_{min} (frequency variation aids mode identification)
- NOVA-K calculates stability in presence of beam ions
- ECE, ECEI, magnetics, BES, etc. all used to identify eigenmode
  - Radial, toroidal, poloidal structure, frequency variation with qmin, etc.
- Several n=3 modes are identified experimentally in agreement with NOVA-K
- TAEFL also finds similar modes unstable*

*B.J. Tobias, et.al. , PRL 106, 075003 (2011)

Searching of unstable TAEs and RSAEs
Check of experimental data

P2-12 M.A. Van Zeeland et al

Integrated Approach to Predict AE Stability and Induced Energetic Ion Losses in DIII-D & ITER

Measured Modes Correspond Well with Modes Predicted to be Unstable by NOVA-K (n=1-6)

Freq. (kHz)	Type	Drive	Damping	Drive-Damping	OBSERVED
n=1					
Modes Tested = 19					
56.26	RSAE	0.162	-0.007	0.154	NO
59.7	TAE	0.021	-0.003	0.017	YES
n=2					
Modes Tested = 27					
57.23	RSAE	0.133	-0.027	0.106	YES
62.43	RSAE	0.105	-0.011	0.094	YES
59.98	TAE	0.053	-0.011	0.042	NO
54.63	TAE	0.042	-0.037	0.005	NO
70.83	TAE	0.005	-0.003	0.001	NO
n=3					
Modes Tested = 28					
64.92	RSAE	0.101	-0.011	0.089	YES
69.75	RSAE	0.064	-0.003	0.061	YES
61.11	TAE	0.049	-0.029	0.019	YES
67.04	TAE	0.017	-0.011	0.005	NO
n=4					
Modes Tested = 31					
76	RSAE	0.052	-0.002	0.05	YES
71.7	RSAE	0.056	-0.008	0.048	NO
68.49	RSAE	0.061	-0.02	0.041	NO
71.76	TAE	0.022	-0.011	0.01	YES
n=5					
Modes Tested = 38					
79.71	RSAE	0.056	-0.003	0.053	YES
75.48	RSAE	0.053	-0.007	0.046	NO
72.54	RSAE	0.051	-0.01	0.041	NO
n=6					
Modes Tested = 46					
82.8	RSAE	0.033	-0.009	0.024	YES
76.97	RSAE	0.03	-0.018	0.011	NO
74.4	RSAE	0.031	-0.029	0.002	NO

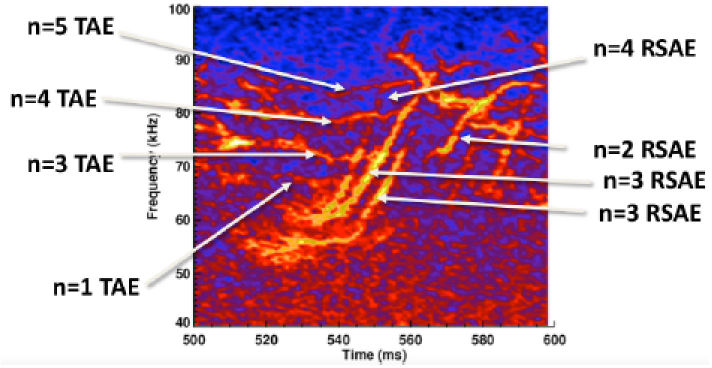

- Stability for hundreds of AEs calculated
- *Most unstable mode observed experimentally in all cases except n=1*
- Low-n more unstable as observed experimentally
- RSAEs typically most unstable
  - Radial harmonic RSAEs also unstable
  - Fundamental is most unstable - as in expt.
- Dominant damping mechanisms are e- collisional, e- landau, and radiative

P2-12 M.A. Van Zeeland et al

Integrated Approach to Predict AE Stability and Induced Energetic Ion Losses in DIII-D & ITER

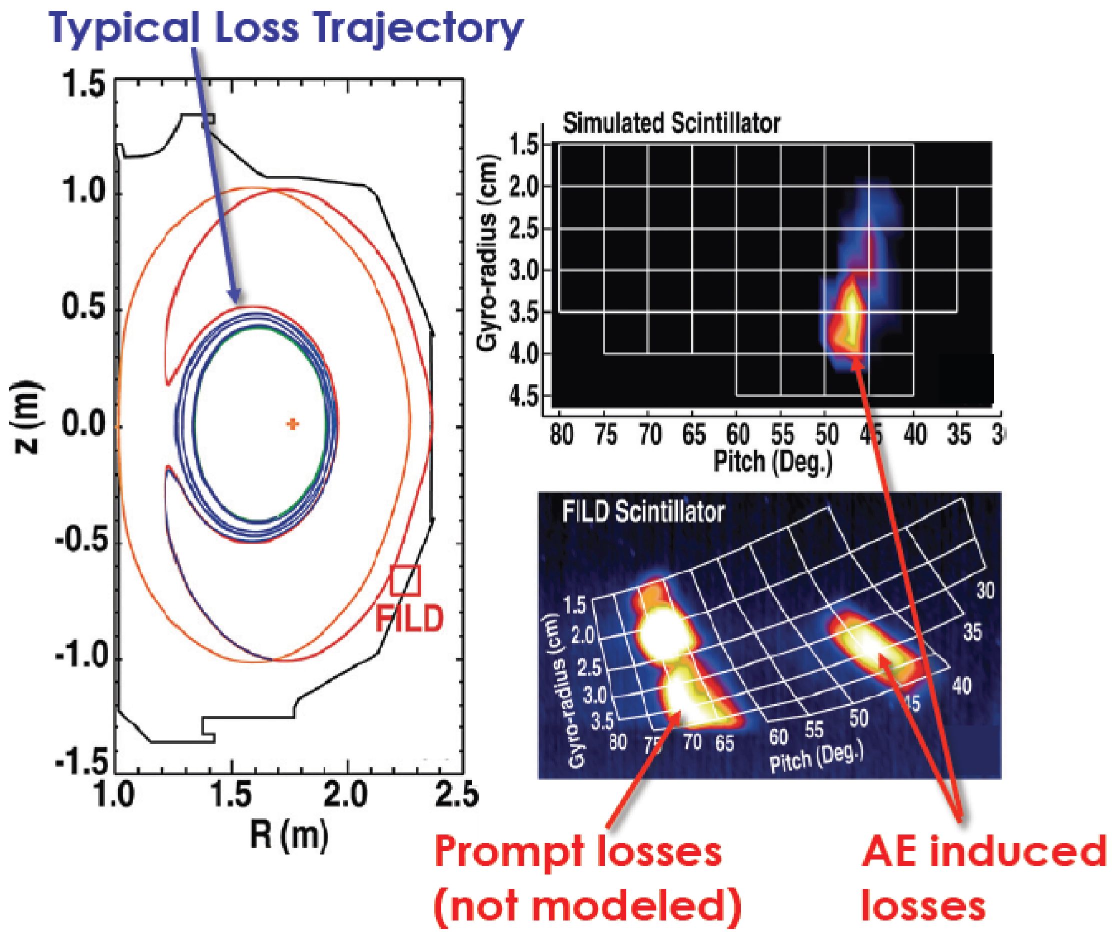

- Loss simulations follow particles from TRANSP distribution function in presence of NOVA eigenmodes
  - Amplitudes obtained from experiment
- Losses at FILD peak near injection energy (80 keV)
- Most common loss mechanism observed is transition of counter passing particles to trapped lost orbit

M.A. Van Zeeland, et al., Phys. Plasmas, 18, 056114(2011)

This approach works very well for DIII-D data.
This was applied to ITER-ISO 8MA scenario
➔ n=5 & 6 RSAE, n=6 TAEs

P2-12 M.A. Van Zeeland et al

Radial transport of EPs by Micro-Turbulence

- **Impact of micro-turbulence in background plasma on energetic articles.**

  First recognition: deficit of energetic ions in plasma core (AUG, DIII-D)

  ➔ Study of this topic in a plasma with off-NBCD on DIII-D

  (ITER relevant: to realize broad current density profile for improved global stability)

  O-9 (DIII-D)

Basic study of microturbulence induced energetic ion transport using a simple tokamak with vertical field and linier device

O-24 (TOPEX)

O-25 (LAPD)

Effects of Micro-Turbulence on EP transport
- Off axis current drive in DIII-D -

1. Are there significant deviations from classical behavior in low-temperature quiet plasmas?
2. Does plasma microturbulencecause additional fast-ion transport?
3. What is the effect of off-axis beam injection on Alfvén eigenmode stability? (*This is shown above*)

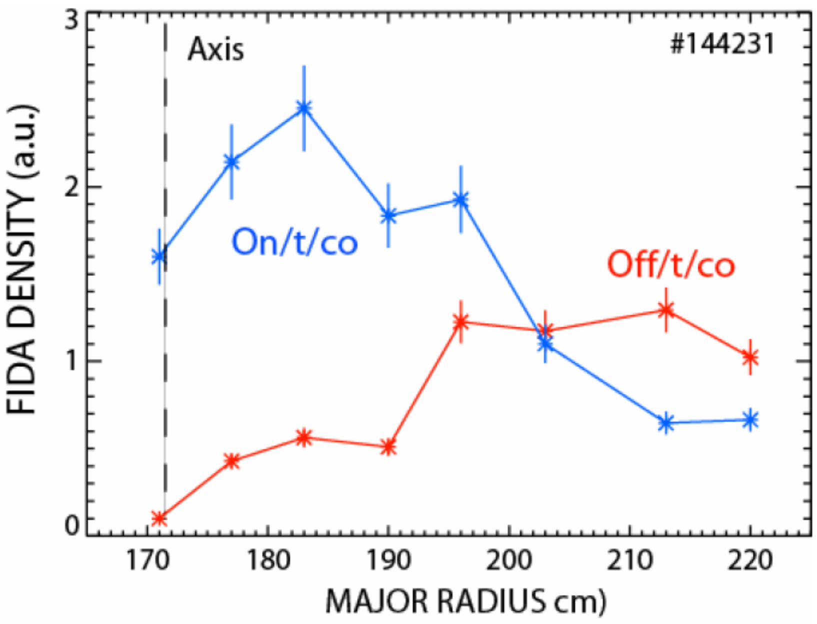

Tangential FIDA data

O-9 W.W. Heidbrink et al.

Effects of Micro-Turbulence on EP transport

Preliminary Analysis: No evidence of enhanced transport at higher T or β in new experiments

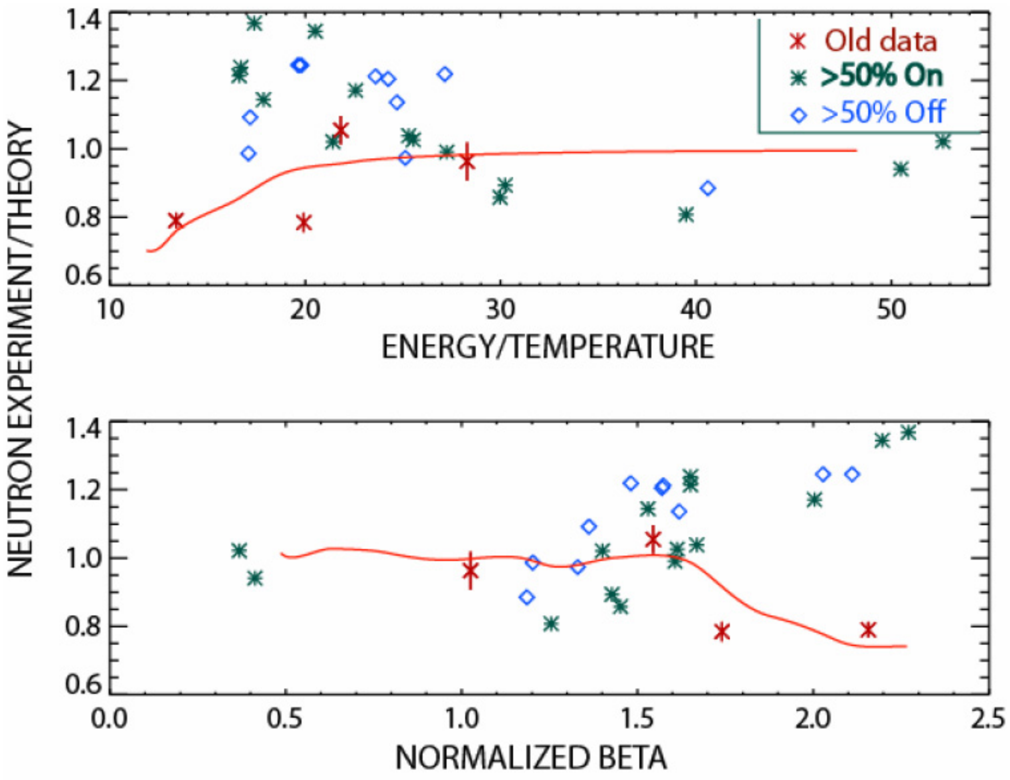

- Off-axis beam ions are as well confined as On-axis
- Detailed comparison with gyrokinetic simulations in progress

Effects of Micro-Turbulence on EP transport
-- Experiment in TORPEX --

The TORPEX device

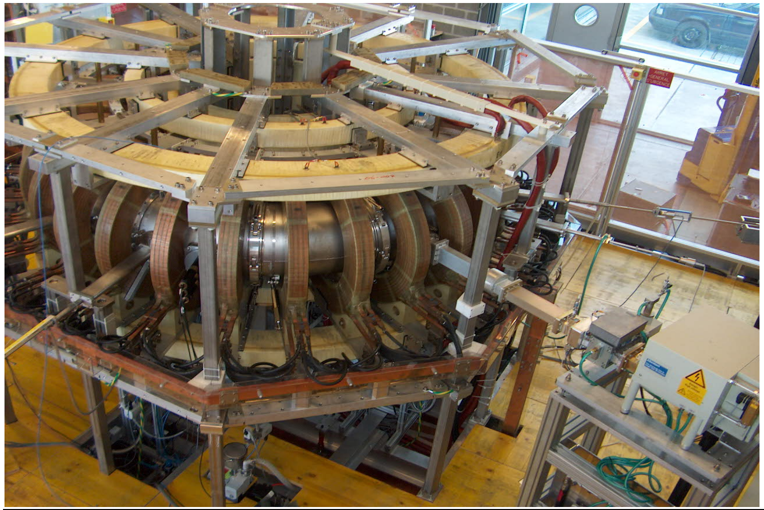

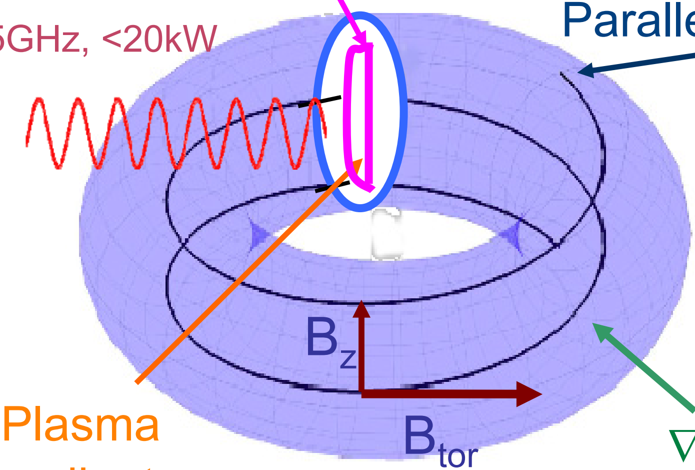

- Open field lines - no plasma current
- Plasma production by EC waves
- Extensive diagnostic coverage (electrostatic, magnetic, fast camera)
- □B, curvature, pressure gradients

H_2, D, He, Ne, Ar plasmas

R = 1 m; a= 0.2 m

B_t = 76 mT; B_z= 0 - 6 mT

T_e = 2 – 20 eV

n_e = 0.1 – 5 x 10^{16} m^{-3}

O-24 A. Fasoli et al.

Fast ion current profile – theory vs. experiment,

Theory

Without plasma

With plasma

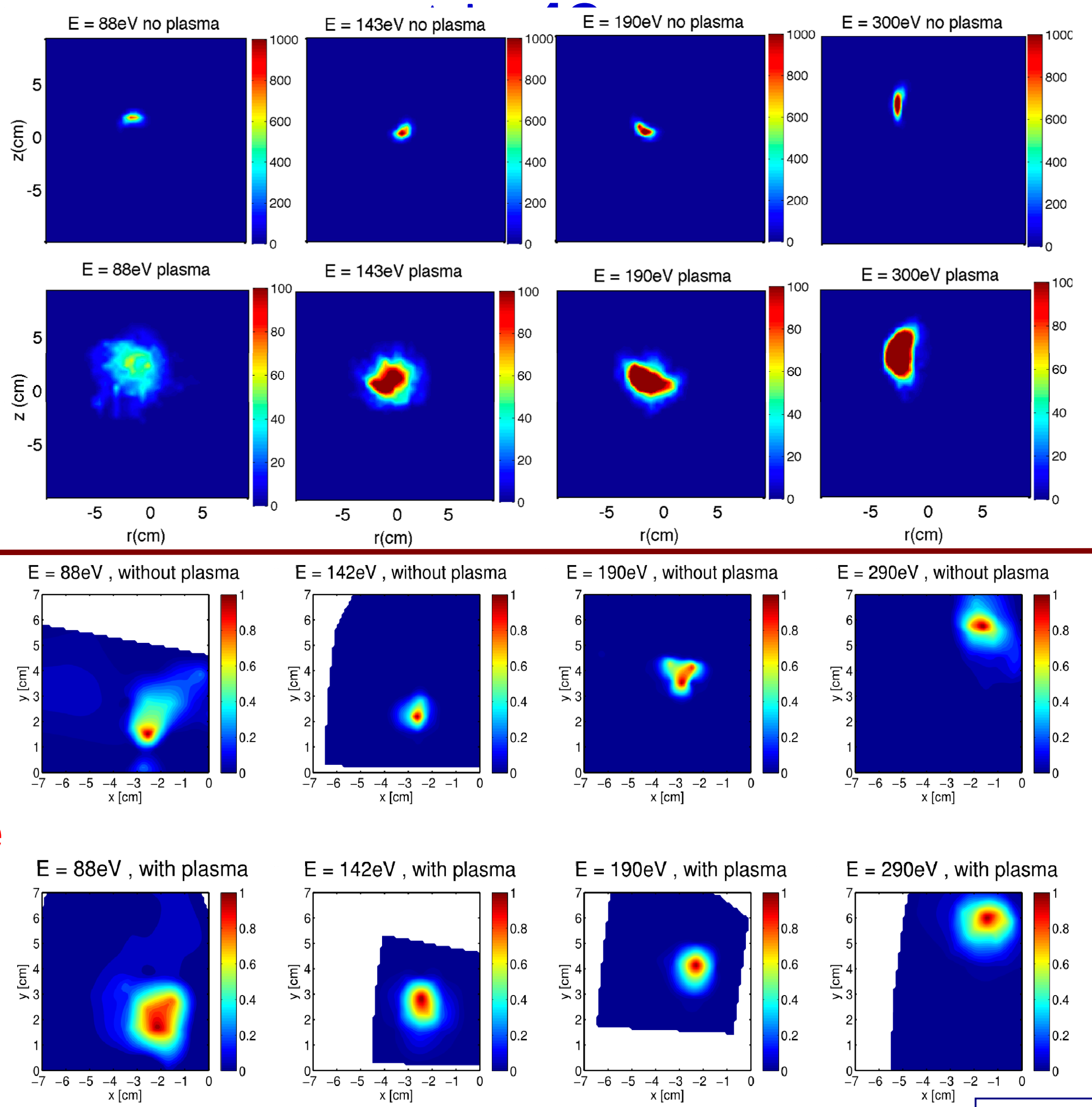

Experiment

Without plasma

With plasma

Effects of Micro-Turbulence on EP transport
-- Experiment in LAPD --

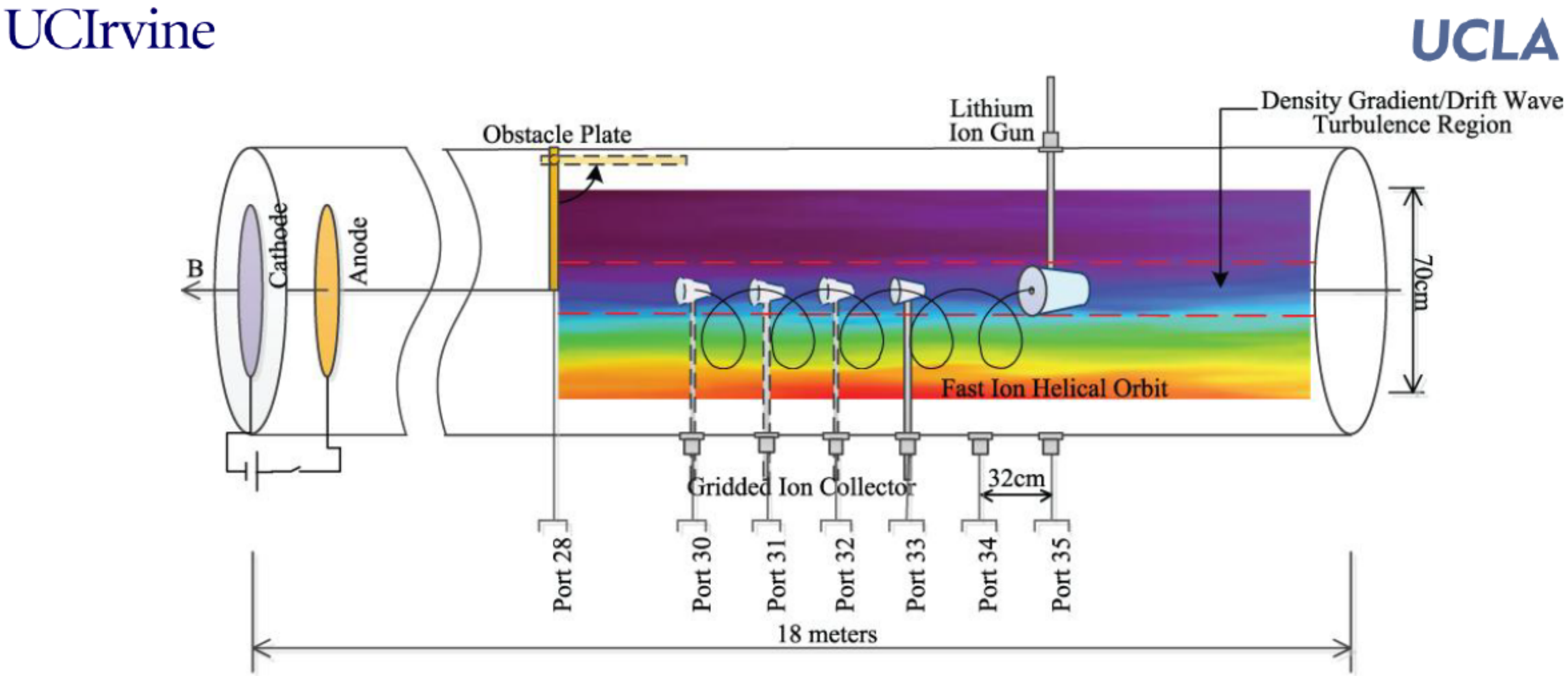

O-25 S. Zhou et al.

Effects of Micro-Turbulence on EP transport

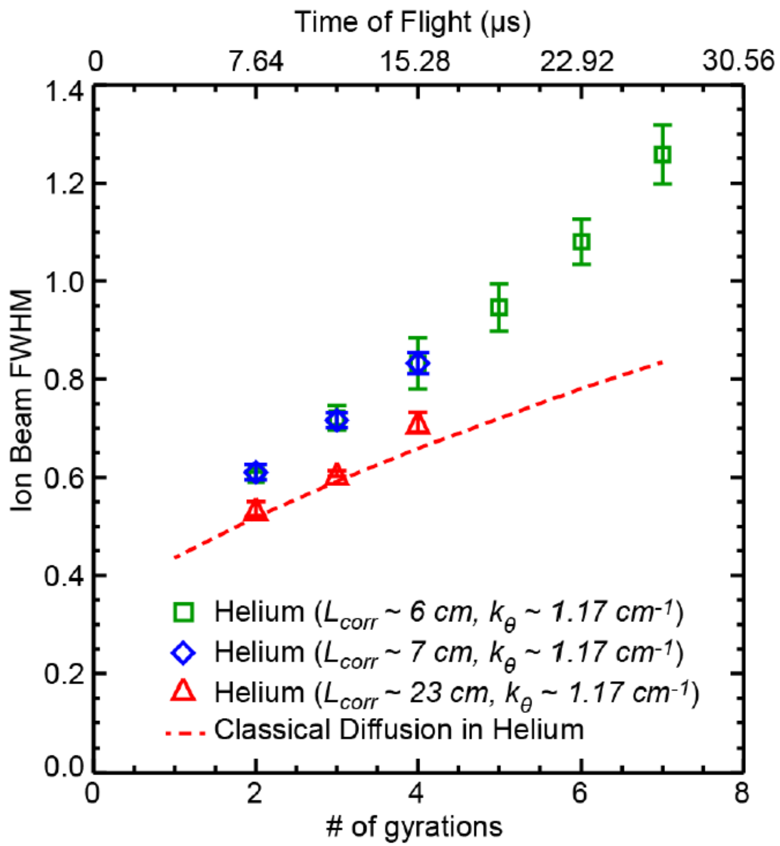

Drift waves induced by an annular obstacle placed perpendicular to the Axial magnetic field enhance radial diffusion of fast ions.
Obit averaging effect for fast ions having large Larmor radius is imperfect.
➔ Radial diffusion of fast ion is enhanced by micro-turbulence.

O-25 S. Zhou et al.

IV

Development of Diagnostics for fusion α-particles in JET DT Experiments

- **Fusion α-particle source diagnostics**

  Neutron and γ-ray emission profiles; Neutron spectrometry

- **Confined α-particle diagnostics**

  γ-ray diagnostics; Neutral Particle Analysers

- **Escaped α-particle diagnostics**

  Scintillator Probe; α-particle collectors

Required quantities to be measured in DT experiments

- Fusion reaction rate: Neutron and γ-ray diagnostics
- Spatial α-particle distribution / redistribution effects: Neutron and γ-ray diagnostics
- α-particle energy distributions: γ-ray and neutron spectrometry, neutral particle analyser
- α-particle slowing down & confinement: γ-ray diagnostics
- α-particle losses:Scintillator Probe, Faraday Cups

Development of Diagnostics for fusion α-particles in JET DT Experiments

Fusion α-particle source diagnostics

Neutron and γ-ray emission profiles; Neutron spectrometr

(P1-12; C. Hellesen)

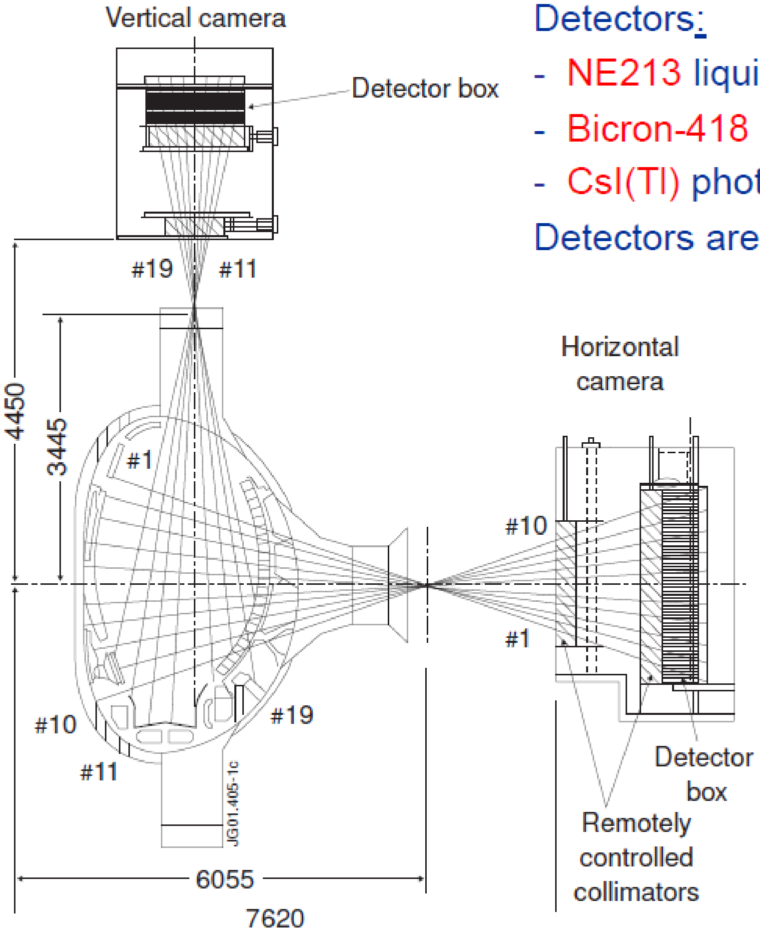

Detectors:

- NE213 liquid scintillators (2.5 & 14 MeV)
- Bicron-418 plastic scintillators (14 MeV)
- CsI(Tl) photo-diodes (hard X-rays and γ-rays)

Detectors are absolutely calibrated

Tracer T Experiments

14-MeV neutron profile measurements in the monotonic current discharges with T-NBI blips

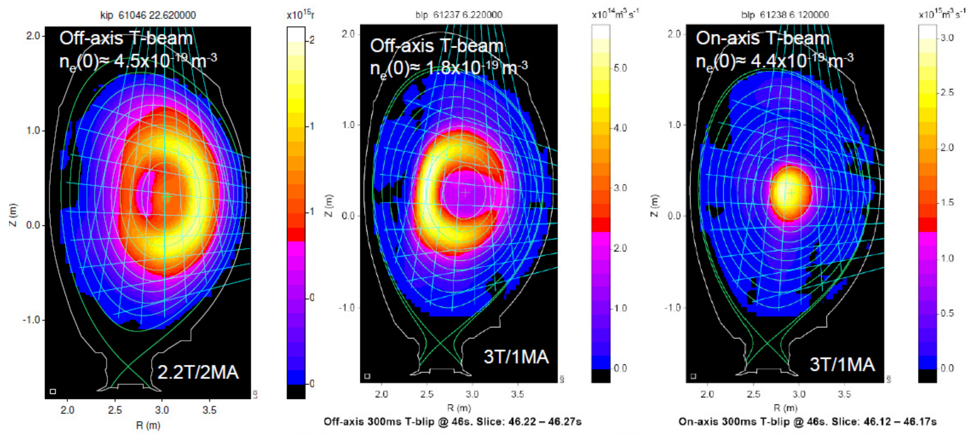

More α-source data in http://users.jet.efda.org/pages/dt-task-force/pages/TTE_AlphaSources_Kiptily/AlphaSources_Table.htm

I-8 V. Kiptily et al

Development of Diagnostics for fusion α-particles in JET DT Experiments

Confined α-particle diagnostics: γ-ray diagnostics

γ-ray spectrometer: $^{9}Be(\alpha,n\gamma)^{12}C$ reaction

$^{9}Be + \alpha \rightarrow {}^{13}C^{*} \xrightarrow{n} {}^{12}C^{*} \xrightarrow{\gamma} {}^{12}C$

BGO, NaI(Tl), $LaBr_3$, HpGe

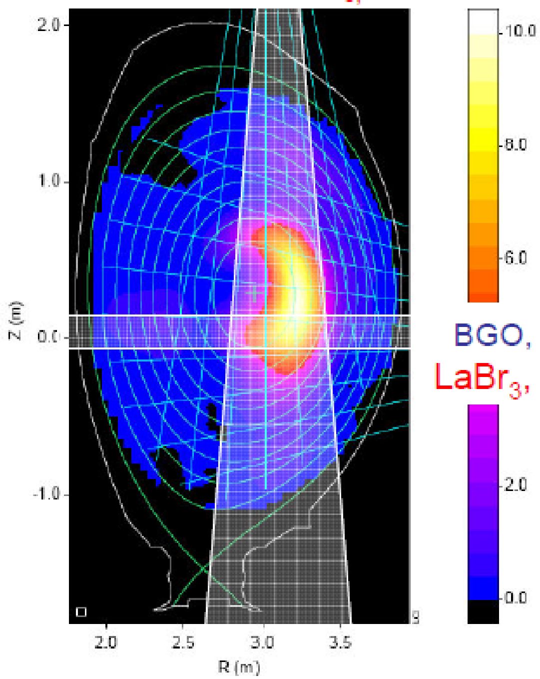

NaI(Tl): energy resolution, $\Delta E/E \approx 8\%$
Slow: decay time ~ 250 ns
Digital Data Acquisition system allows up to 1 MHz PHA

BGO: energy resolution, $\Delta E/E \approx 14\%$
Best detection efficiency!
Slow: decay time ~ 300 ns

New capabilities

$LaBr_3$ (or BrilLanCe): $\Delta E/E \approx 3\%$,
Decay times - < 20 ns
DAQ allows up to 2 MHz PHA

HpGe: $\Delta E/E \approx 0.3\%$ - the Doppler broadening of γ-lines can be measured!
DAQ allows up to 0.5 MHz PHA

Quasi-tangential BGO-spectrometer:
front and rear collimators to improve S/B ratio

A similar diagnostic System was installed On AUG. The γ-ray Generated to a Nuclear raection of Proton has been Dtected. (P2-7: M. Nocente Et al.)

I-8 V. Kiptily et al

Development of Diagnostics for fusion α-particles in JET DT Experiments

Confined α-particle diagnostics: γ-ray diagnostics

γ-ray emission profile: α-particle redistribution measurements

Scheme of the neutron attenuator assembly in the cameras

Approximate attenuation factors

Neutron attenuator	Material	Neutron energy 2.45 MeV	Neutron energy 14.1 MeV
Horizontal	H_2O	10^2	15
Vertical (normal)	H_2O	$10^{2\,(*)}$	15
Vertical (long version)	H_2O	10^4	10^2

(*) Experimentally confirmed on a prototype   V.L. Zoita, MEdC

Vertical Camera can be used for γ-ray emission profile in DT dischages with up to 10^{17} n/s !

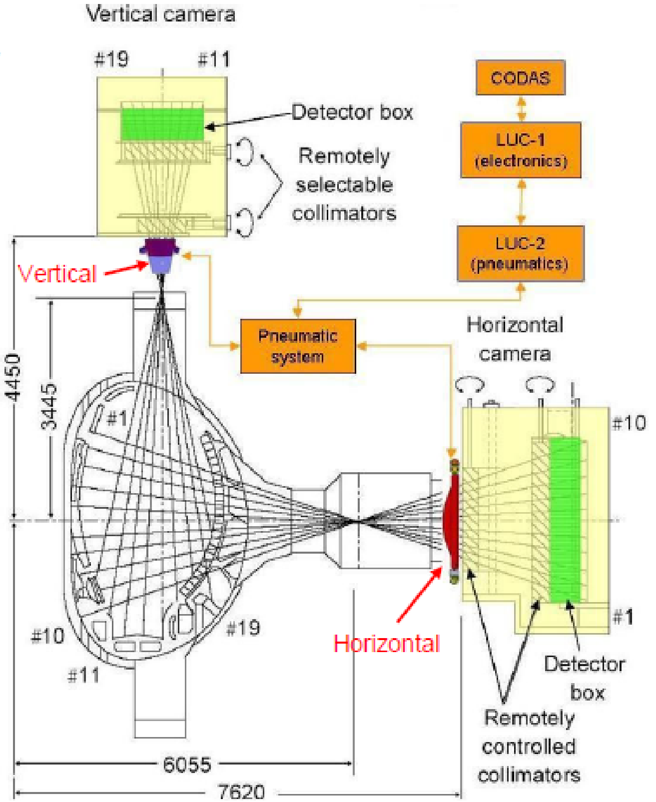

Development of Diagnostics for fusion α-particles in JET DT Experiments

Escaped α-particle diagnostics: Scintillator Probe

I-8 V. Kiptily et al

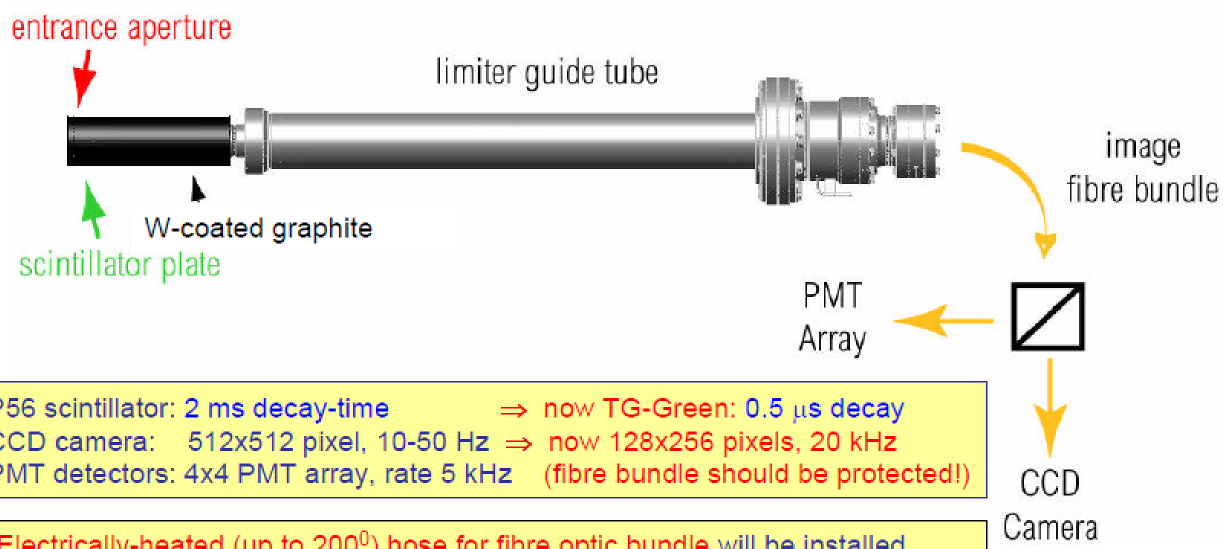

P56 scintillator: 2 ms decay-time ⇒ now TG-Green: 0.5 μs decay
CCD camera: 512x512 pixel, 10-50 Hz ⇒ now 128x256 pixels, 20 kHz
PMT detectors: 4x4 PMT array, rate 5 kHz (fibre bundle should be protected!)

Electrically-heated (up to 200^0) hose for fibre optic bundle will be installed before DT campaign. It is not be degraded by nuclear irradiation up to a total dose of 10^8 rad.

Scintillator probe: first orbit loss measurements

1-MeV tritons and 3-MeV protons

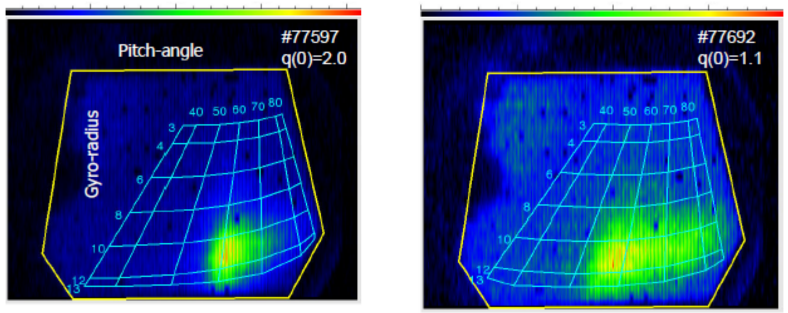

Discharge 2.7T / 1.8 MA

Discharge 2.7T / 2.5 MA

Development of Diagnostics for fusion α-particles in JET DT Experiments

Escaped α-particle diagnostics: Faraday cup Probe with energy discrimination

I-8 V. Kiptily et al

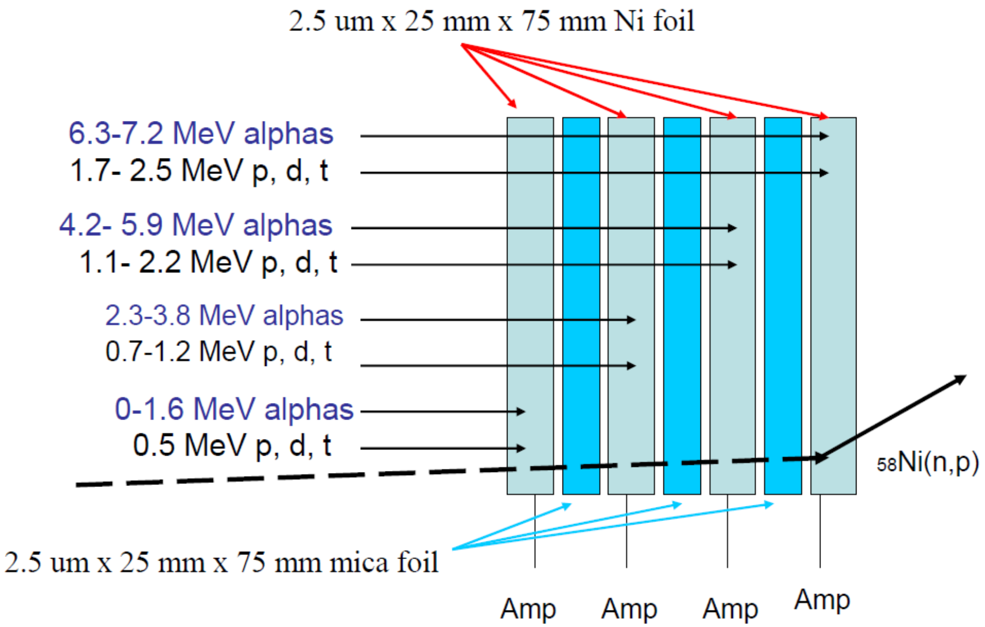

Darrow et al.;Fus. Eng. and Design, **74**, 853, (2005)

Observation (a): Lost alpha particles (or deuterons) with energies up to about 7 MeV (4 MeV) generated during ICRH (up to 6 MW) ^{4}He/d plasmas

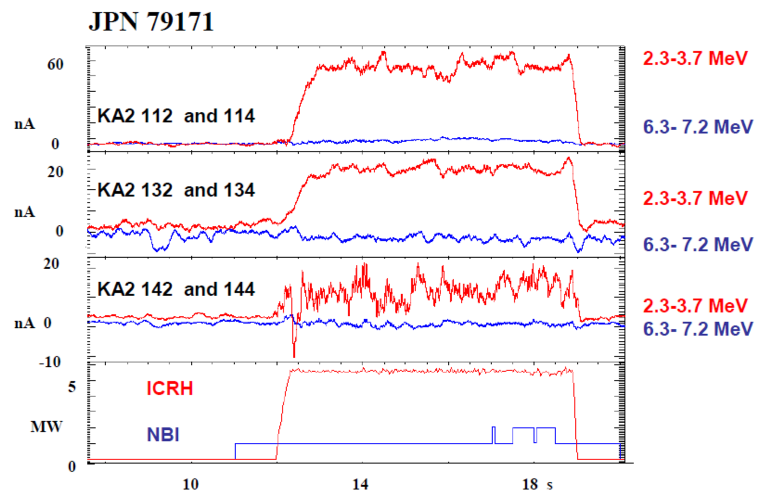

Faraday cup type is also installed inside the vacuum vessel of JET. Energy resolution is done with a detector compsed multiple metal foils. (P1-2: F.E. Cecil et al.)

Diamond Neutral Particle Spectrometer for JET & ITER

EFDA

Aims

- **Charge-exchange atom spectroscopy** with **high temporal resolution** applies to study
- effectiveness of additional heating,
- interaction of plasma instabilities with fast ion component.
- Demanded spectroscopy **temporal resolution ~ 1 ms.**
- Demanded **energy resolution < ~ 10 keV**
- Demanded peak **count rates ~ 10^6-10^7 cps.**

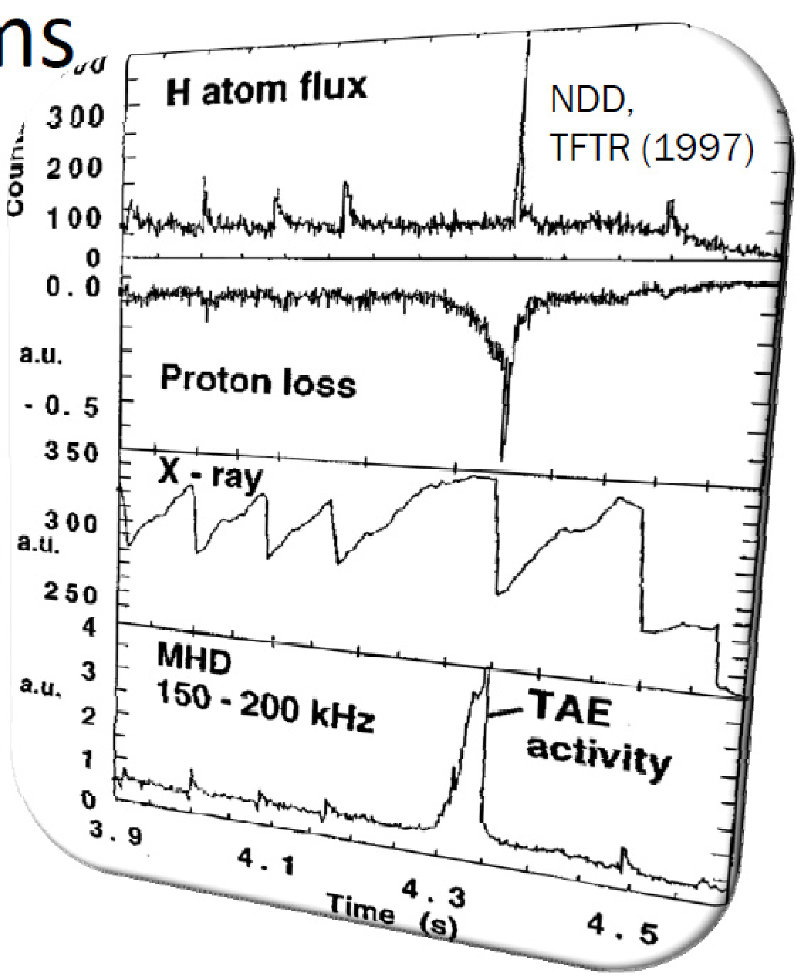

O-22 V.A. Krasilnikov et al

Diamond Neutral Particle Spectrometer for JET & ITER

- **Diamond** has unique **properties** that enable it to be effectively used as a sensitive element in the high-energy particle detectors.
- 5,5 eV - energy band gap
- $>10^{15}$ Ohm*m – electrical resistance
- 10^7 V/cm – breakdown voltage
- $2x10^7$ cm/s - saturated drift velocity
- 10-15 ns - charge collection time

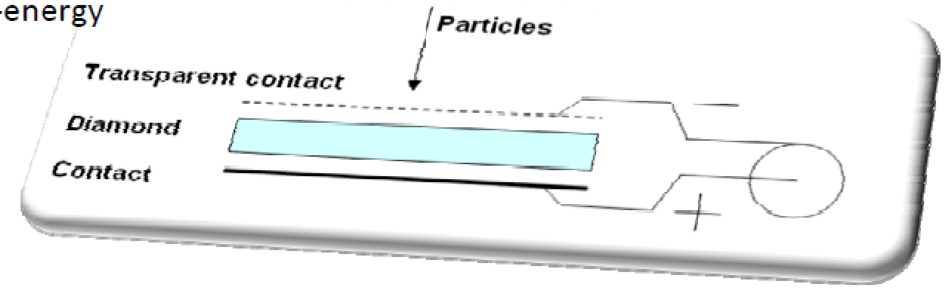

Spectroscopy electronics

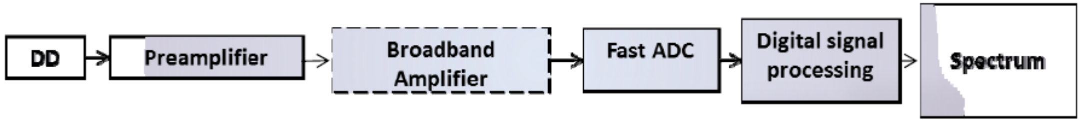

- **The very new spectroscopy amplifiers** and **pulse analyzers** are capable of processing particle fluxes of up to 10^7 cps. They require **extremely low-noise conditions.**
- Specially designed electronics
  - **Preamplifier**
  - **Supply unit**

allows to digitize and process signal with count rates up to 10^6 cps **at relatively high noise levels.**

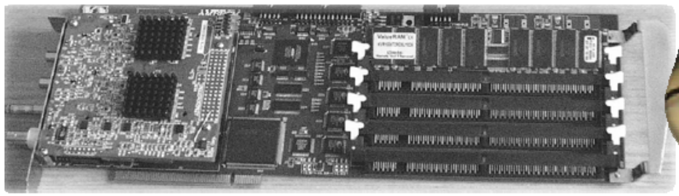

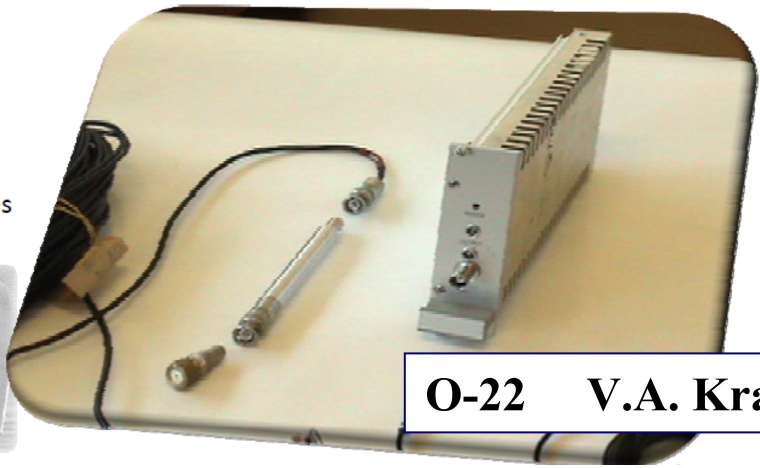

O-22 V.A. Krasilnikov et al

Neutron Emission Profile Monitor for MAST

Most of the fusion neutron production is due to injected neutral deuteron reacting with the thermal deuteron population (beam-thermal) while the beam-beam term accounts for 10 -20 % of the total and the thermal-thermal contribution is negligible.

$$D + D \Rightarrow {}^{3}He\ (0.82\ MeV) + n\ (2.45 MeV),\ Q = 3.27 MeV$$

Detectors:Liquid scintillator coupled to PMT
$2x5x1\ cm^3$ act. V.
14 bit, 256 MB250 MHz sample

^{235}U Fission Chamber

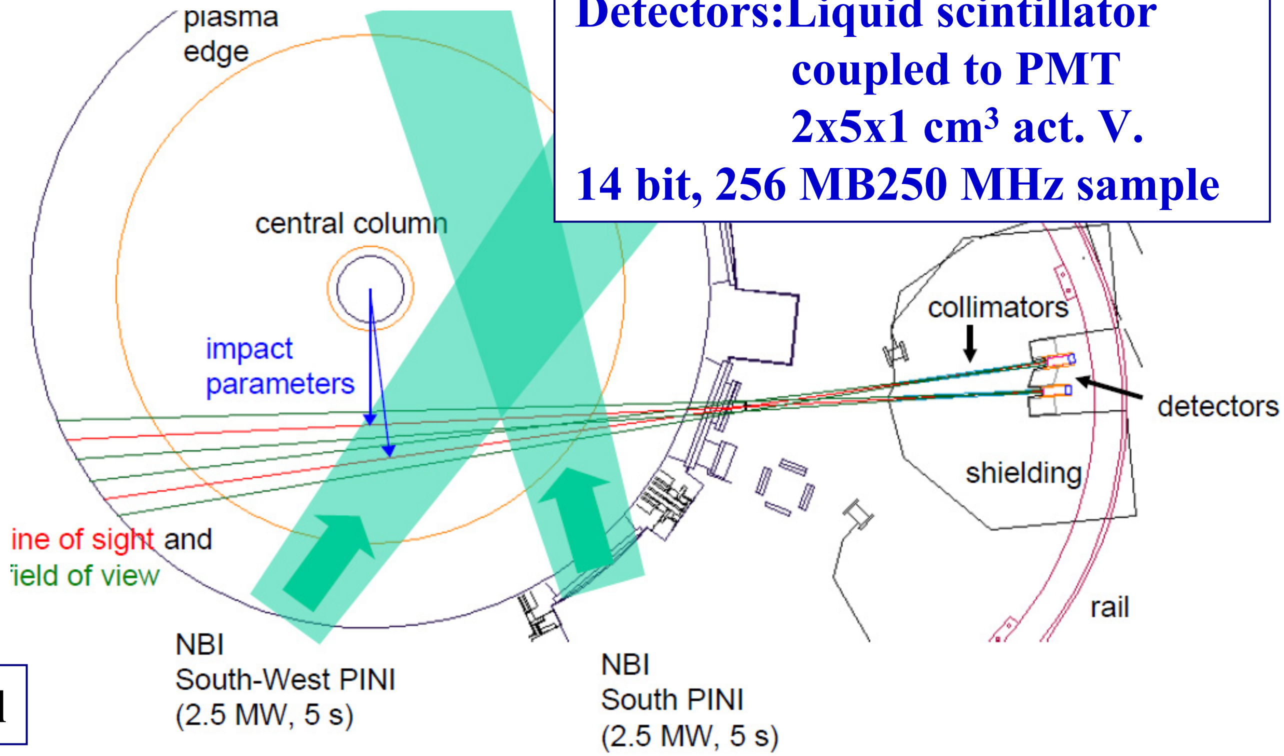

O-23 M. Cecconello et al

Neutron Emission Profile Monitor for MAST

Fishbones

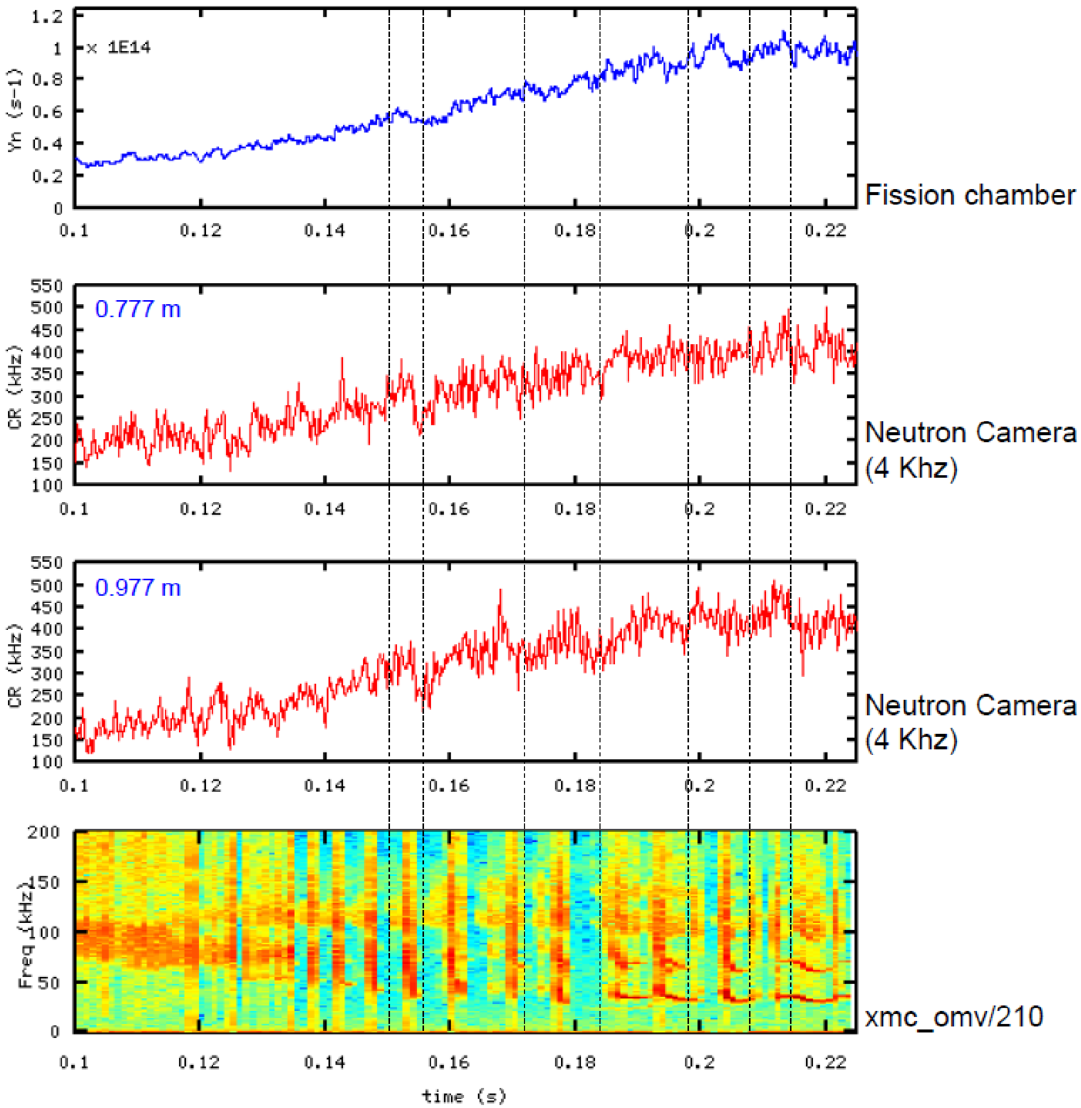

This neutron emisson Profile monitor is Successfully employed In MAST experiments.

O-23 M. Cecconello et al

Development of Fast Ion Charge Exchange Spectroscopy

- **In LHD, a spectroscopic system to measure charge exchange recombination by energetic beam ion up to 190 keV is under development for study of NBI produced energetic ion profile and redistrution of energetic ions due to AEs. This system is similar to those used in DIII-D, AUG and NSTX, but aims at extended energy range up to ~150 keV.**

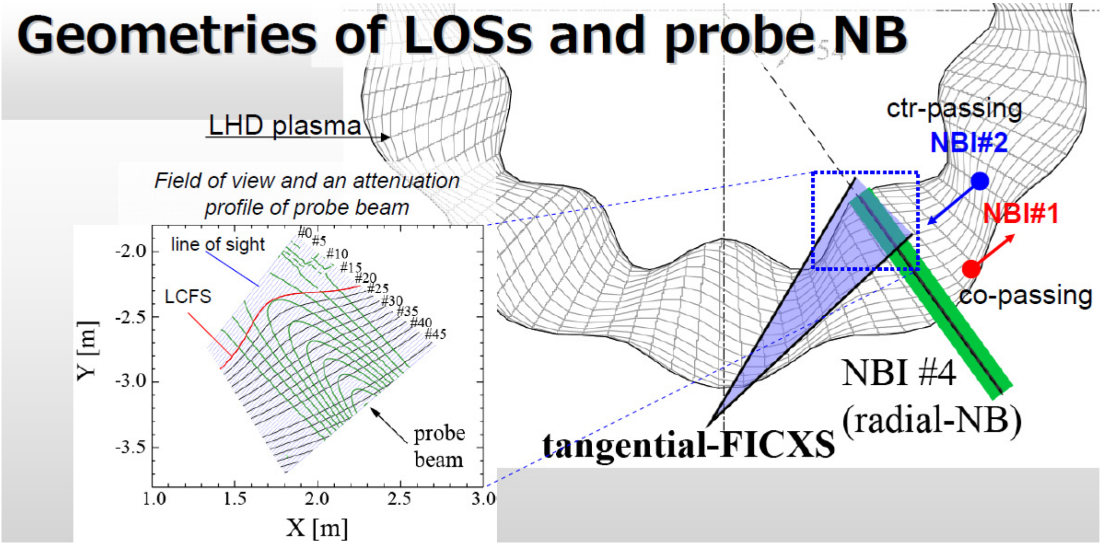

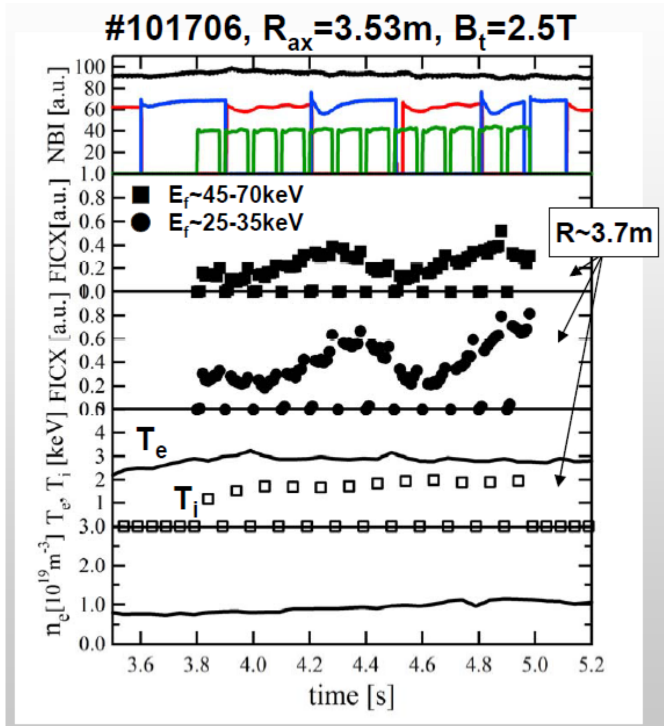

P1-13 T. Ito et al

The initial data have been Obtained, which are Responding to the relevant NBI (#2 NBI: shown in red).

Collective Thomson Scattering System

Geometry of probing and receiving beams for collective Thomson scattering in LHD

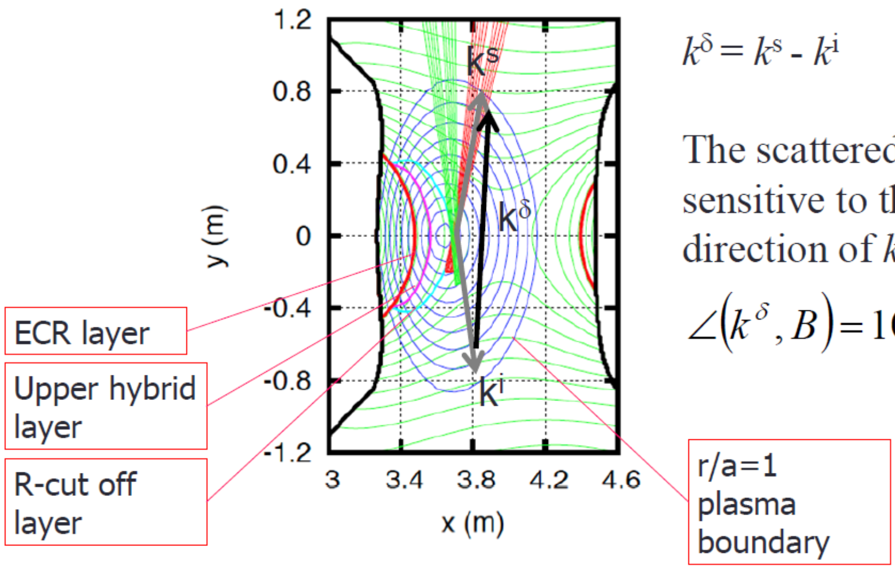

$k^{\delta} = k^{s} - k^{i}$

The scattered signal is sensitive to the direction of k^{δ}

$\angle\left(k^{\delta}, B\right) = 100.4\,\mathrm{deg}.$

Scattering geometry for probing and receiving beams in LHD.
Rax=3.6m, Bt=2.4T

CTS systen is under Development for Fast ion measurements On LHD.

CTS heterodyne receiver system

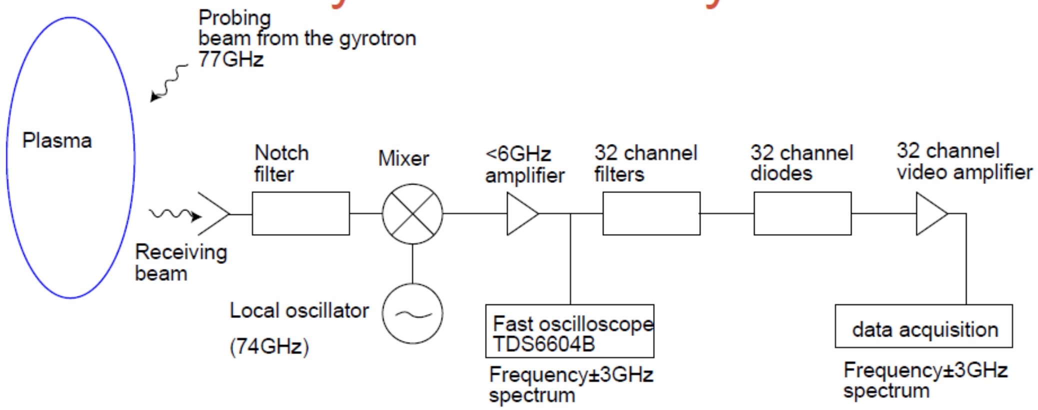

P2-6 M. Nishiura et al

V

Runaway Generation & Disruption

- At plasma densities typical for tokamaks, n ~ 10^{19} – 10^{20} m^{-3} the electric field is small and RE can be produced only during abnormal events such as plasma disruption
- It is known from experience in tokamaks that RE can damage in-vessel component (notorious accident in TFR with burning hole in vacuum vessel)
- RE are dangerous for the plasma facing components because of long range in FW materials and possible deep melting
- Massive RE generation is expected during plasma disruptions in ITER (up to 12 MA of RE current)
- RE must be suppressed in ITER

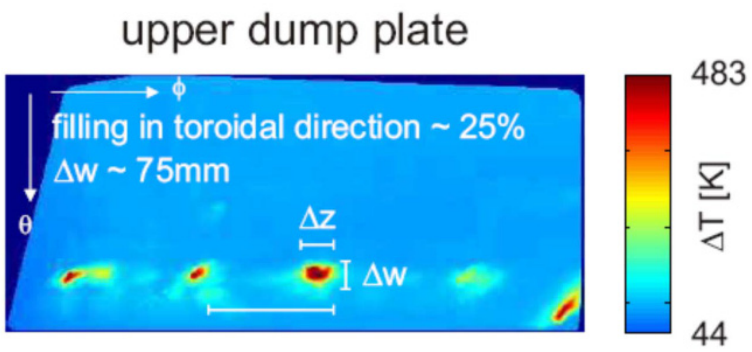

- Due to small ratio V_{perp}/c loss of runaway electrons is extremely localized
- Expected wetted area in ITER is only 0.3-0.6 m^2

I-11 S. Putvinski et al

Runaway Generation & Disruption

Possible strategies

$$\frac{dI_{RA}}{dt} = I_{RA}\left(\gamma\left(\frac{E}{E_c} - 1\right) - \frac{1}{t_{loss}}\right) + S$$

MGI experiments Are conducted in Some large tokamks.

- Disruption
  - Suppress avalanche
    - Collisional $E/E_c < 1$
      - Increase density (Rosenbluth's density)
      - Reduce E
    - RE de-confinement $t_{loss} < \gamma^{-1}(E_c/E)$
  - Magnetic confinement of RE current → In ITER decay of RE current is determined by MGI $t_{CQ\_RE} \sim$ 5-6 s

De-confinement by RMP in ITER is discussing. (O-26: G. Papp et al.)

I-11 S. Putvinski et al

Summary and Future Prospect

- **Large progress in experiments and development of diagnostics has been made for last two years. Further progress is required toward future burning plasma experiments such as ITER, having frequent and effective interactions among experimentalists and theorists.**

- **Energetic particle research area are still in a growing phase and will provide a lot of interesting physics.**